UNIVERSITY OF CALIFORNIA,
IRVINE

Unraveling the Genomic Crosstalk of Host Microbiome in Human and Humanized Preclinical Models of Gulf War Illness

DISSERTATION

submitted in partial satisfaction of the requirements
for the degree of

DOCTOR OF PHILOSOPHY

In Environmental Health Sciences

by

Dipro Bose

Dissertation Committee:
Professor Saurabh Chatterjee, Chair
Professor Stephen Bondy
Professor Ashok Tuteja

2024

DEDICATION

To

my Guru, parents, teachers

and

Gulf War Veterans

"Veterans know better than anyone else the price of freedom, for they've suffered the scars of war. We can offer them no better tribute than to protect what they have won for us." -
(President Ronald Reagan, 1983)

TABLE OF CONTENTS

LIST OF FIGURES

LIST OF TABLES

ACKNOWLEDGEMENTS

I am deeply indebted to my doctoral advisor, Dr. Saurabh Chatterjee whose exceptional support, guidance, and unwavering dedication have been instrumental in shaping me into a researcher. His profound knowledge and encouragement to explore novel research avenues have been invaluable. I am profoundly grateful for his mentorship and providing the laboratory access to state-of-the-art research facilities has contributed to my growth as a doctoral student.

I am grateful to Dr. Stephen Bondy, whose guidance, support, and encouragement have profoundly influenced my perspective and approach toward research. I would also acknowledge Dr. Ashok Tuteja, whose expertise and support have been indispensable for my doctoral research work on Gulf War Illness.

I am deeply appreciative of Punnag Saha, who has been a steadfast pillar of support, akin to family, offering his valuable assistance at every juncture. I am thankful to my present lab colleagues, Subhajit Roy, Ayushi Trivedi, and Madhura More. Their consistent presence and willingness to lend a hand have made all the difference, enriching our shared journey in countless ways. I would also like to thank the seniors of my laboratory for their support and advice.

I take this opportunity to express my heartfelt gratitude to Dr. Ayan Mondal, Dr. Rima Tapader, and Dr. Somdatta Chatterjee, who played a significant role in training me in fundamental research techniques and have consistently offered their wise counsel throughout my journey as a doctoral student.

I am forever indebted to my parents for their boundless care, sacrifices, encouragement and belief in me which have shaped me into the person I am today.

VITA

Dipro Bose

2022-2024 Ph.D. in Environmental Health Sciences, Toxicology Track, University of California, Irvine, CA.

2019-2022 Graduate Research Assistant, Dept. of Environmental Health Sciences, University of South Carolina, Columbia, SC.

2014-2016 M.Tech. in Biotechnology, VIT University, Vellore, India

2009-2013 B.Tech. in Biotechnology, VIT University, Vellore, India

FIELD OF STUDY

Role of microbiome-gut-brain Axis in Gulf War Illness Pathology

Identifying Gut Microbiome Targeted Therapeutic Candidates in Gulf War Illness

PUBLICATIONS

- Bose, D., Saha, P., Roy, S., Trivedi, A., More, M., Klimas, N., Tuteja, A., & Chatterjee, S. (2024). A Double Humanized Mouse Model for Studying Host Gut-Microbiome-Immune Interactions in Gulf War Illness, International journal of molecular sciences (under review).
- Trivedi, A., Bose, D., Saha, P., Roy, S., More, M., Skupsky, J., Klimas, N. G., & Chatterjee, S. (2023). Prolonged Antibiotic Use in a Preclinical Model of Gulf War Chronic Multisymptom-Illness Causes Renal Fibrosis-like Pathology via Increased micro-RNA 21-Induced PTEN Inhibition That Is Correlated with Low Host Lachnospiraceae Abundance. Cells, 13(1), 56. https://doi.org/10.3390/cells13010056
- More, M., Chatterjee, S., Saha, P., Bose, D., Trivedi, A., Roy, S., & Chatterjee, S. (2023). Host microbiome associated low intestinal acetate correlates with progressive NLRP3-dependent hepatic-immunotoxicity in early life microcystin-LR exposure. BMC pharmacology & toxicology, 24(1), 78. https://doi.org/10.1186/s40360-023-00721-7
- Roy, S., Saha, P., Bose, D., Trivedi, A., More, M., Xiao, S., Diehl, A. M., & Chatterjee, S. (2023). Hepatic NLRP3-Derived Hsp70 Binding to TLR4 Mediates MASLD to MASH Progression upon Inhibition of PP2A by Harmful Algal Bloom Toxin Microcystin, a Second Hit. International journal of molecular sciences, 24(22), 16354. https://doi.org/10.3390/ijms242216354
- Bose, D., Stebliankin, V., Cickovski, T., Saha, P., Trivedi, A., Roy, S., More, M., Tuteja, A., Mathee, K., Narasimhan, G., & Chatterjee, S. (2023). Microbiome Dysbiosis Shows Strong Association of Gut-Derived Altered Metabolomic Profile in Gulf War Chronic

Multisymptom Illness Symptom Persistence Following Western Diet Feeding and Development of Obesity. International journal of molecular sciences, 24(4), 4245. https://doi.org/10.3390/ijms24044245

- Saha, P., Upright, M., Bose, D., Roy, S., Trivedi, A., More, M., Scott, G. I., Brooks, B. W., & Chatterjee, S. (2022). Subchronic Oral Cylindrospermopsin Exposure Alters the Host Gut Microbiome and Is Associated with Progressive Hepatic Inflammation, Stellate Cell Activation, and Mild Fibrosis in a Preclinical Study. Toxins, 14(12), 835. https://doi.org/10.3390/toxins14120835
- Saha, P., Bose, D., Stebliankin, V., Cickovski, T., Seth, R. K., Porter, D. E., Brooks, B. W., Mathee, K., Narasimhan, G., Colwell, R., Scott, G. I., & Chatterjee, S. (2022). Prior exposure to microcystin alters host gut resistome and is associated with dysregulated immune homeostasis in translatable mouse models. Scientific reports, 12(1), 11516. https://doi.org/10.1038/s41598-022-15708-3
- Bose, D., Chatterjee, S., Older, E., Seth, R., Janulewicz, P., Saha, P., Mondal, A., Carlson, J. M., Decho, A. W., Sullivan, K., Klimas, N., Lasley, S., Li, J., & Chatterjee, S. (2022). Host gut resistome in Gulf War chronic multisymptom illness correlates with persistent inflammation. Communications biology, 5(1), 552. https://doi.org/10.1038/s42003-022-03494-7
- Mondal, A., Saha, P., Bose, D., Chatterjee, S., Seth, R. K., Xiao, S., Porter, D. E., Brooks, B. W., Scott, G. I., Nagarkatti, M., Nagarkatti, P., & Chatterjee, S. (2021). Environmental Microcystin exposure in underlying NAFLD-induced exacerbation of neuroinflammation, blood-brain barrier dysfunction, and neurodegeneration are NLRP3 and S100B dependent. Toxicology, 461, 152901. https://doi.org/10.1016/j.tox.2021.152901
- Chatterjee, S., Bose, D., & Seth, R. (2021). Host gut microbiome and potential therapeutics in Gulf War Illness: A short review. Life sciences, 280, 119717. https://doi.org/10.1016/j.lfs.2021.119717
- Saha, P., Skidmore, P. T., Holland, L. A., Mondal, A., Bose, D., Seth, R. K., Sullivan, K., Janulewicz, P. A., Horner, R., Klimas, N., Nagarkatti, M., Nagarkatti, P., Lim, E. S., & Chatterjee, S. (2021). Andrographolide Attenuates Gut-Brain-Axis Associated Pathology in Gulf War Illness by Modulating Bacteriome-Virome Associated Inflammation and Microglia-Neuron Proinflammatory Crosstalk. Brain sciences, 11(7), 905. https://doi.org/10.3390/brainsci11070905
- Sarkar, S., Saha, P., Seth, R. K., Mondal, A., Bose, D., Kimono, D., Albadrani, M., Mukherjee, A., Porter, D. E., Scott, G. I., Xiao, S., Brooks, B., Ferry, J., Nagarkatti, M., Nagarkatti, P., & Chatterjee, S. (2020). Higher intestinal and circulatory lactate associated NOX2 activation leads to an ectopic fibrotic pathology following microcystin co-exposure in murine fatty liver disease. Comparative biochemistry and physiology. Toxicology & pharmacology : CBP, 238, 108854. https://doi.org/10.1016/j.cbpc.2020.108854
- Mondal, A., Bose, D., Saha, P., Sarkar, S., Seth, R., Kimono, D., Albadrani, M., Nagarkatti, M., Nagarkatti, P., & Chatterjee, S. (2020). Lipocalin 2 induces neuroinflammation and blood-brain barrier dysfunction through liver-brain axis in murine model of nonalcoholic steatohepatitis. Journal of neuroinflammation, 17(1), 201. https://doi.org/10.1186/s12974-020-01876-4

- Al-Badrani, M., Saha, P., Mondal, A., Seth, R. K., Sarkar, S., Kimono, D., Bose, D., Porter, D. E., Scott, G. I., Brooks, B., Raychoudhury, S., Nagarkatti, M., Nagarkatti, P., & Chatterjee, S. (2020). Early microcystin-LR exposure-linked inflammasome activation in mice causes development of fatty liver disease and insulin resistance. Environmental toxicology and pharmacology, 80, 103457. https://doi.org/10.1016/j.etap.2020.103457
- Bose, D., Saha, P., Mondal, A., Fanelli, B., Seth, R. K., Janulewicz, P., Sullivan, K., Lasley, S., Horner, R., Colwell, R. R., Shetty, A. K., Klimas, N., & Chatterjee, S. (2020). Obesity Worsens Gulf War Illness Symptom Persistence Pathology by Linking Altered Gut Microbiome Species to Long-Term Gastrointestinal, Hepatic, and Neuronal Inflammation in a Mouse Model. Nutrients, 12(9), 2764. https://doi.org/10.3390/nu12092764
- Bose, D., Mondal, A., Saha, P., Kimono, D., Sarkar, S., Seth, R. K., Janulewicz, P., Sullivan, K., Horner, R., Klimas, N., Nagarkatti, M., Nagarkatti, P., & Chatterjee, S. (2020). TLR Antagonism by Sparstolonin B Alters Microbial Signature and Modulates Gastrointestinal and Neuronal Inflammation in Gulf War Illness Preclinical Model. Brain sciences, 10(8), 532. https://doi.org/10.3390/brainsci10080532
- Kimono, D., Bose, D., Seth, R. K., Mondal, A., Saha, P., Janulewicz, P., Sullivan, K., Lasley, S., Horner, R., Klimas, N., & Chatterjee, S. (2020). Host Akkermansia muciniphila Abundance Correlates With Gulf War Illness Symptom Persistence via NLRP3-Mediated Neuroinflammation and Decreased Brain-Derived Neurotrophic Factor. Neuroscience insights, 15, 2633105520942480. https://doi.org/10.1177/2633105520942480
- Seth, R. K., Maqsood, R., Mondal, A., Bose, D., Kimono, D., Holland, L. A., Janulewicz Lloyd, P., Klimas, N., Horner, R. D., Sullivan, K., Lim, E. S., & Chatterjee, S. (2019). Gut DNA Virome Diversity and Its Association with Host Bacteria Regulate Inflammatory Phenotype and Neuronal Immunotoxicity in Experimental Gulf War Illness. Viruses, 11(10), 968. https://doi.org/10.3390/v11100968
- Kimono, D., Sarkar, S., Albadrani, M., Seth, R., Bose, D., Mondal, A., Li, Y., Kar, A. N., Nagarkatti, M., Nagarkatti, P., Sullivan, K., Janulewicz, P., Lasley, S., Horner, R., Klimas, N., & Chatterjee, S. (2019). Dysbiosis-Associated Enteric Glial Cell Immune-Activation and Redox Imbalance Modulate Tight Junction Protein Expression in Gulf War Illness Pathology. Frontiers in physiology, 10, 1229. https://doi.org/10.3389/fphys.2019.01229
- Albadrani, M., Seth, R. K., Sarkar, S., Kimono, D., Mondal, A., Bose, D., Porter, D. E., Scott, G. I., Brooks, B., Raychoudhury, S., Nagarkatti, M., Nagarkatti, P., Jule, Y., Diehl, A. M., & Chatterjee, S. (2019). Exogenous PP2A inhibitor exacerbates the progression of nonalcoholic fatty liver disease via NOX2-dependent activation of miR21. American journal of physiology. Gastrointestinal and liver physiology, 317(4), G408–G428. https://doi.org/10.1152/ajpgi.00061.2019

ABSTRACT OF THE DISSERTATION

Unraveling the Genomic Crosstalk of Host Microbiome in Human and Humanized Preclinical Models of Gulf War Illness

By

Dipro Bose

Doctor of Philosophy in Environmental Health Sciences

University of California, Irvine, 2024

Professor Saurabh Chatterjee, Chair

Understanding the complex pathology of Gulf War Illness (GW), with its multisymptomatic condition, and identifying an efficient treatment has been a longstanding challenge for researchers. Researchers have made significant efforts in conducting mechanistic studies using different combinations of representative Gulf War (GW) chemicals in various experimental animal models in an attempt to create a translatable GWI pre-clinical model. However, there remain confounding factors like paucity of information regarding the actual amount of exposure among the GW Veterans, route, and duration of exposure impede the process.

Our lab has been pioneering GWI research for the past decade. From the very first report about the association of altered gut microbiome in GWI pathology, we have attempted to approach the condition considering the translatable impact of the results on present-day Veterans.

In the first study, the impact of metabolic disorders in underlying GWI conditions has been studied. GW Veterans living in a sedentary lifestyle now have an increased risk of

developing conditions like obesity. The results showed that administration of a Western diet in a mouse model pre-exposed to GW chemicals decreased the abundance of beneficial gut bacteria. A decrease in bacterial diversity is strongly associated with gastrointestinal, hepatic, and systemic inflammation along with increased neurodegeneration. This study further provides cues of pleiotropic marker IL-6 being responsible for GWI pathology via the microbiome-gut-brain axis.

In the second study, the alteration of gut resistome profile due to GW chemical exposure is long-lasting and closely associated with bacterial dysbiosis. In this study, a similar trend in resistome profile has been observed in an experimental murine model and GW Veterans. It was also observed that the altered antibiotic resistance genes were associated with gastrointestinal and systemic inflammation and decreased synaptic plasticity in the brain.

In the third study, a double humanized mouse model have been designed in an approach to have a more translatable GWI murine model. The model has been designed to have both human microbiome and immune system. Exposure to GW chemicals resulted in alteration of gut microbiome and expression of host immune markers which were similar to the results observed in GW Veterans in an earlier study.

INTRODUCTION

Gulf War and Gulf War Illness

In 1990, the first Persian Gulf War took place as a response to the opposition to the invasion of Kuwait by Iraq. The United States (U.S.) along with a coalition of 30 countries deployed an army of 1 million soldiers, among which there were 700,000 U.S. for the liberation of Kuwait under the operation named Operation Desert Shield [1]. This progressed to the combat phase which started in February 1991, which was termed Operation Desert Storm. The coalition forces emerged victorious in the operation and by the end of June 1991 the U.S. troops returned, shortly after which the troops complained to be suffering from a multi-symptomatic condition [2].

Among the 700,000 U.S. troop deployed, nearly 25-32% reported to be suffering from a complex multisymptomatic condition. The symptoms reported fatigue, loss of memory, musculoskeletal pain, cognitive dysfunction, headache, gastrointestinal inflammation, respiratory problems, sleep disturbances and dermatological problems [2]. Due to the vast range of the symptoms and a partial overlap with conditions such as chronic fatigue syndrome and irritable bowel disorder, it was difficult to categorize the condition under any defined pathological conditions. It was initially termed Gulf War Syndrome which was re-named as Gulf War Illness (GWI) [3]. The aging present-day GW Veterans continue to suffer from the symptom persistence of GWI even after three decades of the war.

Case Definitions of Gulf War Illness

There have been several attempts by the National Academy of Sciences to define the multi-symptomatic condition of GWI. Prominent among them were the Haley criteria, the CDC definition and the Kansas criteria [1].

The Haley criteria were based on a survey conducted among the GW Veterans (population size of 249). They reported that the symptoms could be grouped under six main categories like phobia-apraxia, fever-adenopathy, weakness-incontinence, impaired cognition, confusion-ataxia and arthro-myo-neuropathy [4]. This definition lacked in applicability among the vast population of GW Veterans belonging to different divisions.

A research team led by Fukuda, conducted a clinical survey among GW Veterans who had served the Air Force (population size of 3700). According to this study, GW Veteran can be said to be having GWI, if the person reports to be suffering from at least one symptom for six months or more belonging to at least two of the three categories namely symptoms fatigue, musculoskeletal pain, and mood and cognition disorder [5].

The Kansas definition requires that for the Veteran to be suffering from GWI, the person should be having a relatively severe symptom or experiencing two or more symptoms from the following six categories such as fatigue, skin abnormalities, cognitive problem, gastrointestinal problem, musculoskeletal pain, and respiratory symptoms [6].

There is a need to have a uniform and single case definition for GWI cases which would be having a large generalizability among the GW Veterans. However, at present, the Kansas criteria along with CDC criteria are used to determine GWI cases in clinical studies.

Exposures in Gulf War

The GWI condition is attributed to exposure to a large number of toxic chemical compounds in the war theater. It is important to understand that a single chemical compound cannot be identified to be the sole causative agent for the multisymptomatic condition. It is the outcome of two or more of such toxic compounds that have resulted in GWI. The major chemical toxicants reported by the GW Veterans include nerve gas agents like sarin and

cyclosarin, mustard gas, depleted uranium, prophylactic agents like pyridostigmine bromide, pesticides, oil well fires, fuel exposures, and multiple vaccinations [7]. The vast range of the GW toxicants along with elusive nature of toxicity upon combinatorial exposure in GW Veterans makes it difficult to understand the GWI pathology. Lack of information about the amount/dosage of exposure of the individual toxicants along with their route of exposure and period poses a significant challenge especially while modeling pre-clinical animal models to understand the pathology of GWI [8].

It was estimated that around 10,000 troops were exposed to sarin and cyclosarin in the war theater. It was reviewed that though there was evidence of mustard gas exposure, however, further studies were required to estimate the long-term health effects [9].

GW Veterans were exposed to significantly to pesticides and insect repellants including pyrethroids and organophosphates. Studies have reported a direct association between the exposure and severity of symptoms [10].

Pyridostigmine bromide was widely used by military personnel during GW. There was consistent use of anti-nerve gas pills was reported by the GW Veterans. Studies have also reported a dose-response relationship while studying the severity of the symptoms due to its exposure [11].

Studies have reported that depleted uranium was used to increase the defense capacity of heavy armor tanks against enemy attacks. The exposure to depleted uranium among GW Veterans was mostly via inhalation, ingestion, or during accidents like fire incidents [12].

There is recall bias regarding potential health hazards among GW Veterans due to repeated vaccination for meningitis, tetanus, cholera, and typhoid. However, it is predicted that GW Veterans exposed to multiple vaccinations had a strong association with the condition [13].

Treatment strategies of GWI

The multisymptomatic nature of GWI makes it challenging to design mechanistic studies and identify effective therapeutic strategies to ameliorate symptom persistence. To date, no treatment plans are available to cure GWI. However, during the past decade, various clinical trials have been conducted to study the efficacy of potential therapeutic agents. Approaches like cognitive behavior therapy (CBT) and exercise therapy have been tested in GWI Veterans, among them, CBT was found to be effective in decreasing the severity associated with GWI [3]. Compounds like type 2 glucocorticoid receptor blocker mifepristone, antioxidant agent carnosine, steroid drug pregnenolone and coenzyme Q10 (CoQ10) have also been tested in clinical trial studies. Treatment with CoQ10, carnosine and pregnenolone were observed to improve physical function, decrease gastrointestinal inflammation and diarrhea and decrease pain among the GW Veterans who have participated in the respective clinical studies [3].

Asssociation of microbiome-gut-brain axis with Gulf War Illness pathology

The human gut is a major storehouse of microorganisms like bacteria, fungi, viruses, and protozoa right after birth. These form the gut microbiome and are instrumental in maintaining the homeostatic environment in the gut and subsequently the host's health [14]. The gut microbiome plays several important roles which could be divided into three broad categories. Firstly, it helps to maintain the integrity of the intestinal tight junction with the help of tight junction proteins like occludin and claudins as well as the protective mucous layer surrounding the epithelial cells [15]. Next, it regulates the immune function in the gut by inducing the IgA production and elimination of pathogenic bacteria by the production of antibacterial peptides and modulating the immune responses (innate and adaptive) [16].

Further, the gut microbiome also helps in the fermentation of complex carbohydrates providing the host with beneficial metabolites like short-chain fatty acids (SCFA), neuroactive metabolites like serotonin, gamma-aminobutyric acid, tryptophan, and neuropeptides [17]. Various factors can modulate the gut including the environment, age, gender, diet, exposure to various environmental chemicals and toxins, and stress leading to adverse effects on the gastrointestinal as well as the neuronal systems [18]. This crosstalk is termed the microbiome-gut-brain axis [19]. Various pathways connect this bi-directional pathway. The vagus nerve in conjunction with the enteric nervous system and neurotransmitters, constitute the neurological pathways [20]. The secreted SCFAs mainly form the metabolic pathways where these metabolites not only maintain the enterocytes but also can pass the blood-brain barrier (BBB) thereby maintaining neuronal homeostasis in the brain [21]. Finally, cytokines released from the gut, influenced by the microbiome, play a significant role in regulating immune responses, including gastrointestinal inflammation and neuroinflammation, during gut dysbiosis [22].

Our laboratory in collaboration with the Boston Gulf War Illness Consortium was the first to report altered gut bacteriome in deployed GW Veterans compared to the nondeployed Veterans. The decrease in the relative abundances of beneficial gut bacteria was associated with the increased expression of systemic tumor necrosis factor receptor 1 (TNF R-1) [23]. We further observed a similar trend of gut dysbiosis in an acute GWI mouse model, upon exposure to representative GW chemicals permethrin and pyridostigmine bromide which resulted in gastrointestinal inflammation and neuroinflammation [24]. Mechanistically, increased endotoxin levels resulted in intestinal gut barrier disruption which further led to the increase in proinflammatory cytokine expression via toll-like receptor 4 (TLR4)

mediated pathway. Further, TLR4 activation was also observed in the olfactory bulb of the brain which indicated a possible gut-brain axis connection. In another study by Kimono et al, enteric glial cell activation was reported to be associated with bacterial dysbiosis. This further resulted in increased nitrotyrosine expression leading to intestinal tight junction disruption [25].

In another study, we reported gut virome alteration due to exposure to permethrin and pyridostigmine bromide [26]. The gut virome plays a significant role in maintaining the host health homeostasis along with the gut bacteria via the gut-brain axis [27]. A positive association was observed between elevated TLR7 and 9 expressions which recognize viral DNA with the altered virome diversity. Further, BBB disruption, increased activation of microglia, and expression of proinflammatory cytokines were observed indicating a possible link between the gut and brain pathology with virome dysbiosis.

We have shown that gut dysbiosis due to GW chemical exposure continues to persist in mouse models [28]. In this study, increased BBB disruption, followed by increased microglial activation, nitrotyrosine, and proinflammatory cytokine expression, and decreased expression of neuroplasticity marker was associated with the decreased abundance of gut commensal bacteria *Akkermansia muciniphila*.

We have also identified novel gut-microbiome targeted therapeutic candidates which includes neutraceutical Sparstolonin B which is also a TLR4 antagonist, antiviral compounds andrographolide and ribavirin, and bacteria-derived SCFA butyrate in ameliorating increased gut and brain pathology associated with GWI chemical exposure via gut-brain axis. Interestingly, these compounds significantly restored the altered abundance of beneficial gut bacteria [29], [26], [30], [31].

Chapter Overview

The first study investigates whether comorbid conditions like obesity and associated metabolic disorders with underlying GWI exacerbate gastrointestinal inflammation and neuroinflammation. The present-day GW Veterans in their non-combat status are likely to develop metabolic disorders due to sedentary lifestyles, dietary patterns, and post-traumatic stress disorder. I have used a 5-month persistence GWI mouse model and administered a western diet after the initial exposure to representative GW chemicals pyridostigmine bromide and permethrin. I have studied the role of diet-induced obesity with GWI condition in gut dysbiosis and associated intestinal, liver and brain pathology.

In the second study, the role of GW chemicals in altering the host gut resistome closely associated with gut bacteriome has been studied. GW chemicals, especially pesticides are reported to create a selection pressure on the gut bacteriome which results in increased expression of antibiotic resistance genes which could further lead to treatment failures in the aging GW Veterans due to resistance to clinically important antibiotics. I have used a GW persistence mouse model along with samples from GW Veterans with GWI to study the altered gut resistome profile. I have further studied the association between the altered gut resistome and host inflammatory biomarkers. I have also studied the therapeutic potential of fecal microbiota transfer (FMT) in ameliorating increased gastrointestinal and systemic inflammation along with neuroinflammation.

In the third study, a novel strategy of double engraftment of the human immune system along with the human microbiome was used to develop a humanized GWI mouse model. Whole genome shotgun sequencing along with blood immune cytokine ELISA was performed after administration of representative GW chemicals to study the altered gut microbiome,

resistome and expression of systemic immune biomarkers. Another approach of performing fecal microbiota using GWI Veteran sample was used to develop model that closely resembled the microbiome and immune system-associated pathology of a GW Veteran.

CHAPTER 1

Obesity Worsens Gulf War Illness Symptom Persistence Pathology by Linking Altered Gut Microbiome Species to Long-Term Gastrointestinal, Hepatic, and Neuronal Inflammation in a Mouse Model.

Funding: Funding for this project was provided by a DoD-IIRFA grant, W81XWH1810374, and VA merit award, I01 CX001923-01, to Dr. Saurabh Chatterjee.; as well as W81XWH-13-2-0072 to Dr. Kimberly Sullivan. This material is based upon work supported (or supported in part) by the Department of Veterans Affairs, Veterans Health Administration, Office of Research and Development vide Grant No. CX001923-01 to S.C. S.C. is a 5/8th employee with the US Department of Veterans Affairs.

Bose, D., Saha, P., Mondal, A., Fanelli, B., Seth, R. K., Janulewicz, P., Sullivan, K., Lasley, S., Horner, R., Colwell, R. R., Shetty, A. K., Klimas, N., & Chatterjee, S. (2020). **Obesity Worsens Gulf War Illness Symptom Persistence Pathology by Linking Altered Gut Microbiome Species to Long-Term Gastrointestinal, Hepatic, and Neuronal Inflammation in a Mouse Model.** Nutrients, 12(9), 2764. https://doi.org/10.3390/nu12092764.

Underlying obesity conditions exacerbate Gulf War Illness pathology via microbiome-gut liver brain axis in a preclinical mouse model

ABSTRACT

Persistence of Gulf War illness (GWI) pathology among deployed veterans is a clinical challenge even after almost three decades. Recent studies show a higher prevalence of obesity and metabolic disturbances among Gulf War veterans primarily due to the existence of post-traumatic stress disorder (PTSD), chronic fatigue, sedentary lifestyle, and consumption of a high-carbohydrate/high-fat diet. We test the hypothesis that obesity from a Western-style diet alters host gut microbial species and worsens gastrointestinal and neuroinflammatory symptom persistence. We used a 5 month Western diet feeding in mice that received prior Gulf War (GW) chemical exposure to mimic the home phase obese phenotype of the deployed GW veterans. The host microbial profile in the Western diet-fed GWI mice showed a significant decrease in butyrogenic and immune health-restoring bacteria. The altered microbiome was associated with increased levels of IL6 in the serum, Claudin-2, IL6, and IL1β in the distal intestine with concurrent inflammatory lesions in the liver and hyperinsulinemia. Microbial dysbiosis was also associated with frontal cortex levels of increased IL6 and IL1β, activated microglia, decreased levels of brain derived neurotrophic factor (BDNF), and higher accumulation of phosphorylated Tau, an indicator of neuroinflammation-led increased risk of cognitive deficiencies. Mechanistically, serum from Western diet-fed mice with GWI significantly increased microglial activation in transformed microglial cells, increased tyrosyl radicals, and secreted IL6. Collectively, the results suggest that an existing obese phenotype in GWI worsens persistent gastrointestinal

and neuronal inflammation, which may contribute to poor outcomes in restoring cognitive function and resolving fatigue, leading to the deterioration of quality of life.

Keywords: dysbiosis; Western diet; metagenomics; bacterial species; whole genome sequencing; neuroinflammation; peroxynitrite; symptom persistence

INTRODUCTION

Persistence of Gulf War illness (GWI) among deployed veterans is a clinical challenge to diagnose and treat. Though there is strong epidemiological evidence of an association of Gulf War exposures to chronic fatigue, metabolic syndrome, gastrointestinal (GI) disturbances and obesity, the persistence or worsening of the symptoms even long after the war has ended and our troops have returned home remains a challenge for clinicians in numerous health centers nationwide [32]. A recent epidemiological study highlighted that overweight and obesity are highly prevalent among Gulf War and Gulf Era veterans [33]. Persistence of symptoms in ~47% of examined Gulf War (GW) veterans was linked to obesity[34]. There was also a strong association of post-traumatic stress disorder (PTSD) in GW veterans with metabolic syndrome and obesity [34]. The study implied that advancing age and lifestyle factors (Western diet, physical inactivity) are augmenting the development of obesity, metabolic syndrome, and other chronic diseases. It is interesting to note that PTSD can lead to physical inactivity and may increase this risk in aging veterans to develop age-related diseases [34]. Interestingly, a recent preliminary report in mouse models of GWI showed that a high-fat diet leads to dysbiosis, with a different microbiome signature than GWI mice fed a standard chow diet [35]. With the passage of 28 years since the GW, and the GW veterans reaching the age range of 50–60 years, physical inactivity/weight gain would likely

lead to longstanding and exacerbated pathological changes in the brain, liver, and the gastrointestinal (GI) tract. A recent longitudinal study suggests that there is an immediate need to consider the relationship between persistently increasing symptoms and long-term morbidity, especially as veterans age [32]. The carefully designed longitudinal study showed that chronic fatigue (likely from metabolic dysfunction/mitochondrial dysfunction), headaches and pain (as a consequence of inflammation), flatulence or burping (due to GI disturbances), and loss of concentration (owing to neuronal dysfunction) increased or persisted in GW veterans 20 years after their return.

In agreement with the above findings, the preclinical data demonstrated that mice exposed to pyridostigmine bromide and permethrin (PB + PER) exhibited persistent neurobehavioral deficits and neuroinflammation until 22.5 weeks post-exposure [36]. Notably, the adverse health effects of chemicals such as PER and chlorpyrifos associated with GWI also showed an association with obesity and metabolic complications [37]. In a recent study, we have shown that persistence of GWI even after 5 months of exposure largely depends on an altered microbiome and its association with increased damage-associated molecular pattern release from the GI tract, especially the epithelial cells [28]. We have also shown that the enteric glial cell activation resulting from of a sustained microbial dysbiosis in the gut plays a significant role in the release of damage-associated molecular patterns (DAMPs) that further influence an exacerbated neuroimmune response [25]. Interestingly, intestinal inflammation associated with irritable bowel syndrome (IBS), alcoholic steatohepatitis, obesity, non-alcoholic fatty liver disease, or metabolic syndrome has been strongly linked to alterations in the gut microbiome. There are at least 3000 species of bacteria residing in the human gut, and there is a unique prototype of bacterial diversity in every individual [38].

The last decade saw a tremendous increase in our understanding of how gut bacteria participate in health and disease. Significant disorders where gut bacteria have been found to play a role include obesity, metabolic syndrome, and IBS [38].

GWI is also characterized by neuroinflammation and systemic inflammation with elevated levels of pro-inflammatory cytokines, including TNF-α and IL1β [39]. Recent literature shows important connections between microbiome, obesity, and central nervous system disorders with gut microbiome referred to as "second brain" [40]. Interestingly, IBS and obesity have a significant proinflammatory component that includes macrophage activation and triggering of toll-like receptor pathway [41]. Several studies have found strong evidence of a decrease in expression of gut junction proteins, leading to portal endotoxemia [42]. With dysbiosis, obesity, and metabolic syndrome being closely associated, it is not uncommon to find a low systemic inflammation causing significant modulation of gut-immune axis. Since a significant number of veterans presenting persistent GWI symptoms are also obese, it is likely that an underlying inflammatory condition due to obesity or metabolic syndrome contributes to the persistence and exacerbation of symptoms. However, the mechanisms by which obesity or metabolic syndrome leads to persistence of the GWI symptoms remain unclear. Thus, a significant knowledge gap exists about the relationship between GW chemical exposures, weight gain, metabolic syndrome, GI disturbances, and neuroinflammation among GW veterans, especially concerning an altered microbiome. Therefore, the present study investigated the combined effects of GW exposures and the consumption of the Western diet. Such a study is germane to a significant percentage of veterans with GWI because veterans have aged since the exposure to GW chemicals in the 1990s, are inactive physically (owing to incidences of PTSD, disabilities, and chronic fatigue)

and likely to consume a standard American Diet (i.e., the Western diet, rich in fat and carbohydrates) [43]. The study addresses the paradigm that obesity potentiates persistence of GW chemical exposure-induced GI disturbances marked by alterations in tight junction protein levels, site-specific inflammation, metabolic syndrome, and neuroinflammation. Using an established mouse model of chronic GWI where animals received a Western diet for 5 months after GW chemical exposure, and shotgun metagenomics, we show that the alterations of species-specific microbiome persisted and worsened with obesity. The persistent microbiome alterations were strongly associated with GI inflammation, higher serum levels of proinflammatory levels of IL6, and insulin, which caused liver inflammation. Western diet-induced obesity was also associated with microglial activation that led to persistent neuroinflammation—a pathology correlated with altered microbiome.

MATERIALS AND METHODS

Materials

Pyridostigmine bromide (PB) and permethrin (Per) were purchased from Sigma-Aldrich (St. Louis, MO, USA). Primary antibodies including anti-Claudin-2, anti-Occludin, anti-CD68, anti-α-Smooth Muscle Actin (α-SMA), anti-transmembrane protein 119 (TMEM119), anti-3-nitrotyrosine (3-NT) and anti-phosphorylated Tau (p-Tau) were purchased from Abcam (Cambridge, MA, USA). Anti-3-nitrotyrosine, anti-IL1β, anti-IL6, anti-brain-derived neurotrophic factor (BDNF), anti-CD40, and anti-β-actin primary antibodies were purchased from Santacruz Biotechnology (Dallas, TX, USA). Anti-insulin receptor substrate 1 (IRS1) primary antibody was purchased from Cell Signaling Technology (Danvers, MA, USA). Anti-glial fibrillary acidic protein (GFAP) and anti-S100β primary antibodies were purchased

from Proteintech (Rosemont, IL, USA). Species-specific biotinylated secondary antibodies and streptavidin-HRP (Vectastain Elite ABC kit) were purchased from Vector Laboratories (Burlingame, CA, USA). Fluorescence-conjugated (Alexa Fluor) secondary antibodies and ProLong Diamond antifade mounting media with 4′,6-diamidino-2-phenylindole (DAPI) were purchased from Thermofisher Scientific (Grand Island, NY, USA). All other chemicals used in this study were purchased from Sigma unless otherwise specified. Animal tissues were sent to AML laboratories (Baltimore, MD, USA) and Instrument Resources Facility, University of South Carolina School of medicine (Columbia, SC, USA), for paraffin embedding and sectioning. Microbiome analysis was performed at Cosmos ID (Rockville, MD, USA).

Animals

C57BL/6J adult wild-type male mice (10 weeks) were purchased from the Jackson Laboratories (Bar Harbor, ME, United States) and used in this study. Mice were implemented in accordance with National Institutes of Health (NIH) NIH guidelines for human care and use of laboratory animals and local Institutional Animal Care and Use Committee (IACUC) standards. The animal handling procedures were approved by University of South Carolina, Columbia, SC, United States. Upon arrival, all mice were housed at 22–24 °C with a 12 h light/12 h dark cycle and ad libitum access of food and water. According to our experimental design, all mice were fed either with normal chow diet from Teklad (Madison, WI, USA) or Western diet from Research Diets (New Brunswick, NJ, USA). On completion of animal experiments, all mice were sacrificed. Organs including liver and distal part of small intestine were collected and fixed in 10% neutral buffered formaldehyde, whereas frontal cortex was collected and fixed in Bouin's solution (Sigma Aldrich St. Louis, MO, USA). Preparation of

serum samples was performed using fresh mice blood collected by cardiac puncture immediately after anesthesia of mice. Fecal pellets were obtained from the colon and preserved for microbiome analysis.

Mouse Model of Gulf War Illness (GWI)

Mice were exposed to GW chemicals (PB + PER) as described in our previous studies [28]. After 1 week of acclimatization, all mice were randomly distributed into four treatment groups. The first and third groups of mice were given only vehicle (0.6% dimethyl sulfoxide (DMSO) for two weeks and denoted as CHOW (n = 6) and WD (n = 6), respectively. The second and fourth group of mice were treated with a combination of GW chemicals PB (2 mg/kg body weight and diluted in PBS) and Per (200 mg/kg body weight, diluted in DMSO and PBS) tri-weekly for two weeks by oral gavage and denoted as CHOW+GWI (n = 6) and WD+GWI (n = 6), respectively. All the mice groups were fed with chow diet during the initial two weeks of GW chemical exposure. Following GW chemical exposure for 2 weeks, both the WD and WD+GWI mice groups were shifted to Western diet continuously for 20 weeks, whereas both the CHOW and CHOW+GWI mice groups were continued with normal chow diet. The Western diet (Research Diets, Cat#12079B) used for this study has 17% kcal protein, 40% kcal fat, and 43% kcal carbohydrate distribution. Fecal pellets from these mice were sent for microbiome analysis. Blood, distal small intestine segments, liver tissue and frontal cortex tissue segments were collected following sacrifice 5 months post-GW chemical exposure. Enzyme-Linked Immunosorbent Assay (ELISA) was performed from serum of 4–5 mice samples per group.

Microbiome Analysis

Fecal pellets from each experimental mouse were collected in a sterile environment and snap frozen in liquid nitrogen for microbiome analysis at CosmosID (Rockville, MD, USA). Briefly, total DNA isolation and purification were performed using the ZymoBIOMICS Miniprep kit. Library preparation and quantification were performed using Qubit dsDNA HS assay (ThermoFisher, Waltham, MA, USA) and qualified on a 2100 bioanalyzer instrument (Agilent, Santa Clara, CA, USA) to show a distribution with a peak in the expected range. Further, whole-genome shotgun sequencing (WGS) was performed using the next-generation sequencing (NGS) platform and according to the vendor-optimized protocol. The unassembled sequencing reads for each sample were analyzed by the CosmosID bioinformatics platform. The Diverging bar charts were generated using the phylum- and species-level relative abundance matrices from the taxonomic analysis. All values were converted to their Log2 distance from the organism's average across all groups. Linear Discriminant Analysis Effect Size (LEfSe) figures were generated using the LefSe tool from the Huttenhower lab, based on phylum- and species-level relative abundance matrices from taxonomic analysis [38]. LefSe is calculated with a Kruskal–Wallis alpha value of 0.05, a Wilcoxon alpha value of 0.05, and a logarithmic Linear Discriminant Ananlysis (LDA) score threshold of 2.0. In the LefSe figures, red bars to the right convey that the organism in that group is more abundant in the "WD+GWI" group than the "CHOW+GWI" group. Green bars to the left convey that the organism is more abundant in the "CHOW+GWI" group. Stacked bar figures were generated from the phylum- and species-level relative abundance matrices from the taxonomic analysis. Stacked bar figures for each group were generated using the R package ggplot2. Heat maps were creating using the NMF R package, based on the relative abundance information from the taxonomic analysis. A hierarchically clustered heat map is

provided. Alpha diversity boxplots were calculated from the species-level abundance score matrices from the taxonomic analysis. Chao, Simpson, and Shannon alpha diversity metrics were calculated in R using the R package Vegan. Beta Diversity Principal Coordinate Analyses were calculated from the species-level relative abundance matrices from the taxonomic analysis. Bray–Curtis diversity was calculated in R using the R package Vegan with the function vegdist. Beta diversity PCoA tables were generated using Vegan's function PCoA. PERMANOVA tests for each distance matrix were generated using Vegan's function Adonis2.

Mouse Microglial Cell Culture and Treatment

Immortalized mouse microglial cells SIM-A9 were purchased from ATCC (ATCC® CRL-3265), subcultured and grown on Dulbecco's Modified Eagle Medium/F12 (DMEM/F12), 10% fetal bovine serum (FBS) and heat-inactivated 5% horse serum. The cells were incubated at 37 °C using a humidified CO2 incubator (5% CO2 concentration).

Approximately 0.05 × 106 number of cells were seeded onto a 24-well tissue culture plate and growth was permitted to reach 70% confluency before the experiment. Serum starvation was achieved using DMEM/F12 media, supplemented with 1% FBS for at least 18 h. Following sera starvation, cells were treated with serum (25 µL/mL) obtained from the CHOW, CHOW+GWI, WD, and WD+GWI mice groups, respectively, or PBS (VEH), or LPS (1 µg/mL) for 24 h. Cells were harvested for in vitro immunofluorescence experiments and supernatants were collected for measuring IL6 by enzyme-linked immunosorbent assay (ELISA) and cellular cytotoxicity assay.

Immunohistochemistry

Deparaffinization of paraffin-embedded small intestine, liver, and brain tissue sections was performed following the standard laboratory procedure. Briefly, tissues were immersed successively in 100% xylene, 1:1 solution of xylene and ethanol, 100% ethanol, 95% ethanol, 70% ethanol, 50% ethanol, and deionized water for 3 min each. Following deparaffinization, antigen epitope retrieval was performed using the epitope retrieval solution and steamer (IHC-World, Woodstock, MD, USA). Endogenous peroxidase activity was blocked using 3% H2O2 solution for 20 min, followed by serum blocking (5% goat serum) for 1 h. After serum blocking, primary antibodies for IL1β, IL6, CD68, α-SMA, and BDNF were diluted (1:300) in blocking buffer and applied on the tissue sections. All sections were kept at 4 °C for overnight incubation in a humidified chamber. After overnight incubation, the tissue sections were washed with 1X PBS-T (PBS + 0.05% Tween 20) 3 times. Biotinylated secondary antibodies (species specific) were probed at 1:250 dilution, followed by incubation with streptavidin conjugated with horseradish peroxidase at 1:500 dilution. Finally, the chromogenic substrate solution of 3,3-diaminobenzidine (DAB) (Sigma-Aldrich) was applied on the sections and counterstaining was performed using Mayer's hematoxylin (Sigma-Aldrich). Mounting of all tissue sections was performed using Simpo mount (GBI Laboratories, Mukilteo, WA, USA). Reactivity of the applied antibodies in the sections was observed under 10X and 20X objectives and images were captured using an Olympus BX43 microscope (Olympus, Center Valley, PA, USA). Morphometric data analyses were performed using CellSens Software from Olympus America (Center Valley, PA, USA).

Immunofluorescence Staining

Deparaffinization and epitope retrieval procedures of paraffin-embedded small intestine and brain tissue sections were performed as described previously. Following the epitope retrieval process, the tissue sections were permeabilized using PBS-T (PBS + 0.1% Triton X-100) solution for 1 h. Blocking was performed using 5% goat serum and the sections were incubated with primary antibodies of anti-Occludin, anti-Claudin-2, anti-GFAP, anti-S100β, anti-CD40, and anti-TMEM119 (at 1:300 dilution) and kept at 4 °C overnight. Anti-IgG secondary antibodies (species specific) conjugated with Alexa Fluor 488 or 633 (Invitrogen) were used at 1:250 dilutions. Tissue sections were mounted using ProLong Gold antifade reagent with DAPI (Life Technologies, Carlsbad, CA, USA). Images were taken under 40× (for in vivo experiments) and 60× magnifications (for in vitro experiments) with an Olympus BX63 microscope.

Western Blot

Western blot was performed using the proteins extracted from liver and frontal cortex of mice tissues. Protein samples were extracted using RIPA lysis buffer containing protease and phosphatase inhibitors, followed by estimation of the extracted tissue proteins by the BCA assay kit (Thermo Fisher Scientific, Rockford, IL, USA). Approximately 30 µg of proteins extracted from each sample, were added to a mixture containing 1X NuPAGE™ LDS Sample Buffer (Thermo Fisher Scientific, Rockford, IL, USA) and 10% β-mercaptoethanol, and then boiled for 5 min for denaturation purposes. The protein samples were subjected to standard SDS-PAGE using Novex 4–12% bis-tris gradient gel and nitrocellulose membrane transfer of resolved protein bands was performed using the Trans-Blot Turbo transfer system (Bio-rad, Hercules, CA, USA). Following Ponceau S staining, membrane blocking was performed with

5% bovine serum albumin (BSA) for 1 h. Primary antibodies including anti-IRS-1, anti-p-Tau, and anti-β-actin were diluted (1:1000) and probed overnight at 4 °C. Compatible horseradish peroxidase-conjugated species-specific secondary antibodies were used to tag the primary antibody. For the development of the blot, Pierce ECL Western blotting substrate (Thermo Fisher Scientific, Waltham, MA, USA) was used. Finally, the blots were captured by G: Box Chemi XX6 and densitometry analysis was performed using Image J software.

Serum ELISA

Serum collected from the CHOW, CHOW+GWI, WD, and WD+GWI mouse groups was used to quantify IL6 and insulin concentration using commercially available ELISA kits from Thermo Fisher Scientific (Waltham, MA, USA) and Crystal Chem (Elk Grove Village, IL, USA). IL6 ELISA was also performed using supernatant collected from mouse microglial SIM-A9 cells. The ELISA procedures were performed according to the manufacturer's protocol.

Cell Cytotoxicity Assay

Cell cytotoxicity was determined using 100 µL of supernatant from the sera-treated SIM A9 cells by the LDH-Cytotoxicity Colorimetric Assay Kit (BioVision, Milpitas, CA, USA) following the manufacturer's protocol. The cytotoxicity was calculated using the formula (supplied with the kit): Cytotoxicity (%) = (Test Sample − Low Control)/(High Control − Low Control) × 100. Low control was cells in DMEM/F12 media with 1% serum and high control was cells in DMEM/F12 media with 1% serum along with 1% Triton X-100.

Statistical Analyses

All experiments were performed with 5–6 mice per group and each individual mouse was treated as a single sample. The statistical analysis was carried out by unpaired t-test (two-tailed tests with equal variance) and one-way analysis of variance (ANOVA) for assessing the difference between multiple groups. For all analyses, $p \leq 0.05$ was considered statistically significant, and data were presented as the mean ± SEM. Statistical significance was measured by Bonferroni–Dunn post-hoc analysis for all intergroup comparisons.

RESULTS

Shotgun Metagenomics Show Alteration of Species Composition and Abundance in Western Diet-Fed Mice with GWI and Obesity

Shotgun metagenomic analysis of fecal contents was performed using next-generation sequencing to discern whether Western diet-induced obesity caused an altered species profile in the host of GWI mice. Results showed a marked observed difference in the species profiles and relative abundance among the Chow, Chow+GWI, WD, and WD+GWI groups (Figure 1.1A). Species diversity, richness, and abundance were also studied. Results show that several species and clusters were differentially altered between groups (Figure 1.1B). Detailed analysis of species diversity, richness, and abundance (via LEfSe analysis) showed that at $p = 0.01$, the species *Lactococcus lactis* and *Streptococcus thermophilus* were significantly increased in the WD+GWI group when compared to the Chow+GWI group (Figure 1.2B). However, at $p = 0.05$, the species *Akkermansia muciniphila* and *Staphylococcus xylosus* were also significantly increased in the WD+GWI group when compared to the CHOW+GWI group (Supplementary Figure 1.1). Sixteen bacterial species, including *Lachnospiraceae species, Clostridium, and Enterorhabdus*, dominated the abundance in the

Chow+GWI group over and above the WD+GWI group (Figure 1.2A). Results also showed that the relative abundance of *Lactococcus lactis, Akkermansia muciniphila*, and *Lachnospiraceae bacterium 28-4* showed an observed difference in the WD+GWI group over and above the Chow+GWI group (Supplementary Figure 1.1). Shannon diversity analysis, which is used to describe species evenness and richness using abundance scores, showed a marked difference in the WD+GWI group when compared to the Chow+GWI group though the results were not significant at the $p < 0.05$ level. Interestingly, Shannon diversity indices were significantly different between the Chow and WD groups (Figure 1.2C). Beta diversity shows the difference in microbial species-level composition in an environment or treatment group and can be represented by Bray–Curtis distance. PERMANOVA testing showed that the Bray–Curtis beta diversity of WD+GWI compared to the Chow+GWI group was significantly different (Figure 1.2D). To show whether bacterial species that are known to exert a beneficial association to gut and neuronal health are present, analyses of the most abundant, seven such species were performed (Figure 1.2E,F). Results showed that butyrogenic bacteria, bacteria which contributes to good immune health, such as *Lachnospiraceae Bacterium A2, COE-1, 3-1, 10-1, Eubacterium species*, *Ruminococcacae, Enterohabdus sp*, and *Hungatella*, decreased significantly in the WD+GWI group when compared to the Chow+GWI group. However, *Dorea* sp, a bacterial species known to be associated with bloating, constipation and bad gut health, was significantly decreased in the WD+GWI group when compared to the Chow+GWI group (Figure 1.2E). The direct species comparison of individual bacteria among these two groups suggested strongly that a prolonged Western diet feeding and the resultant underlying obesity decrease bacterial species that are known to improve gut, neuronal and immune health (Figure 1.2E,F).

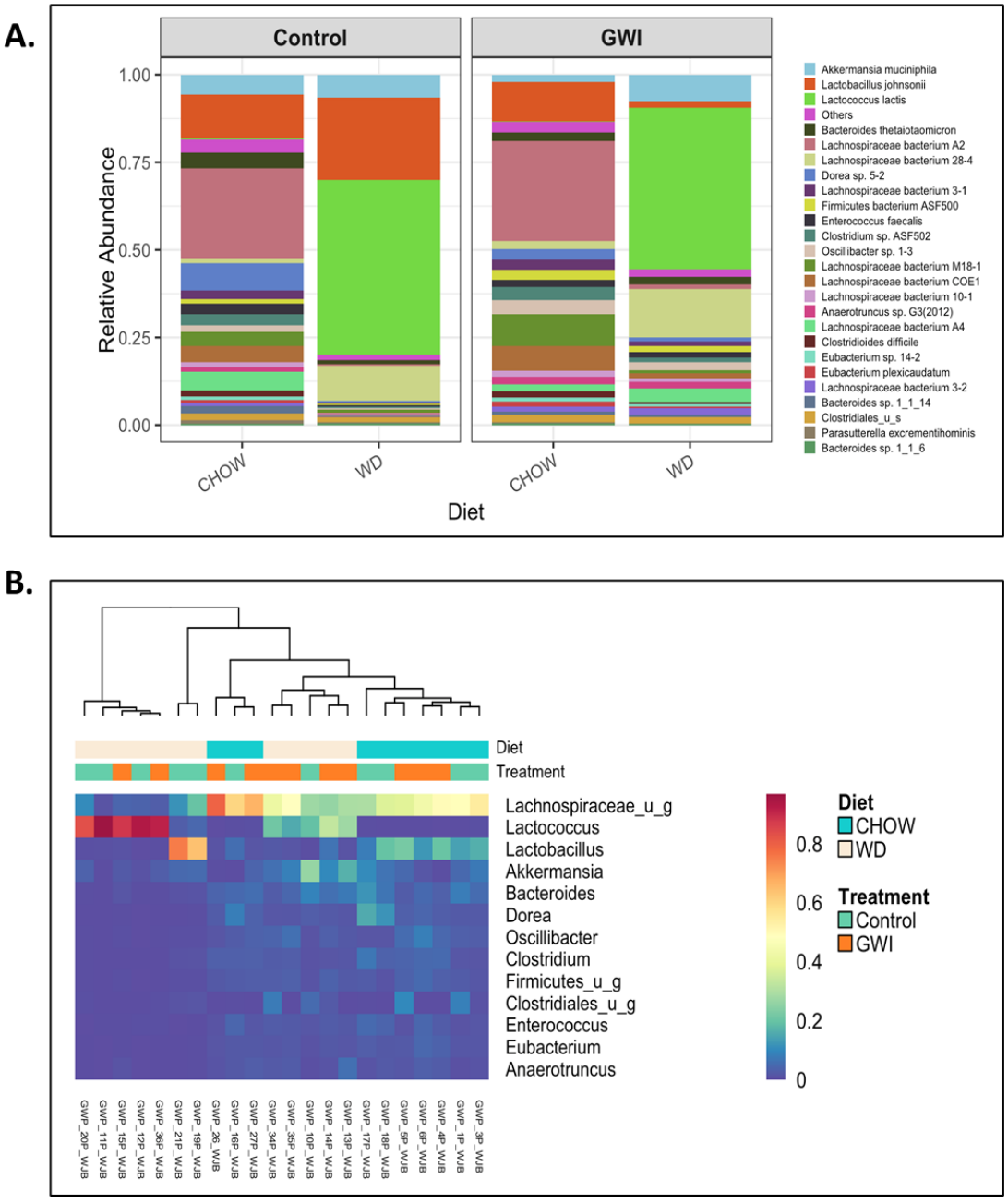

Figure 1.1. Obesity induces microbial dysbiosis in Gulf War illness (GWI) persistence. (A). A stacked bar graph presented the relative abundance of species in both the control and GWI groups. The left box (control) includes both the lean (CHOW) and obesity (WD) control groups. However, the right box (GWI) includes both GWI persistence in the lean mice (CHOW+GWI) and in the obese mice (WD+GWI) groups. **(B).** Relative abundance heatmap and hierarchical clustering at species levels in all study groups.

A.

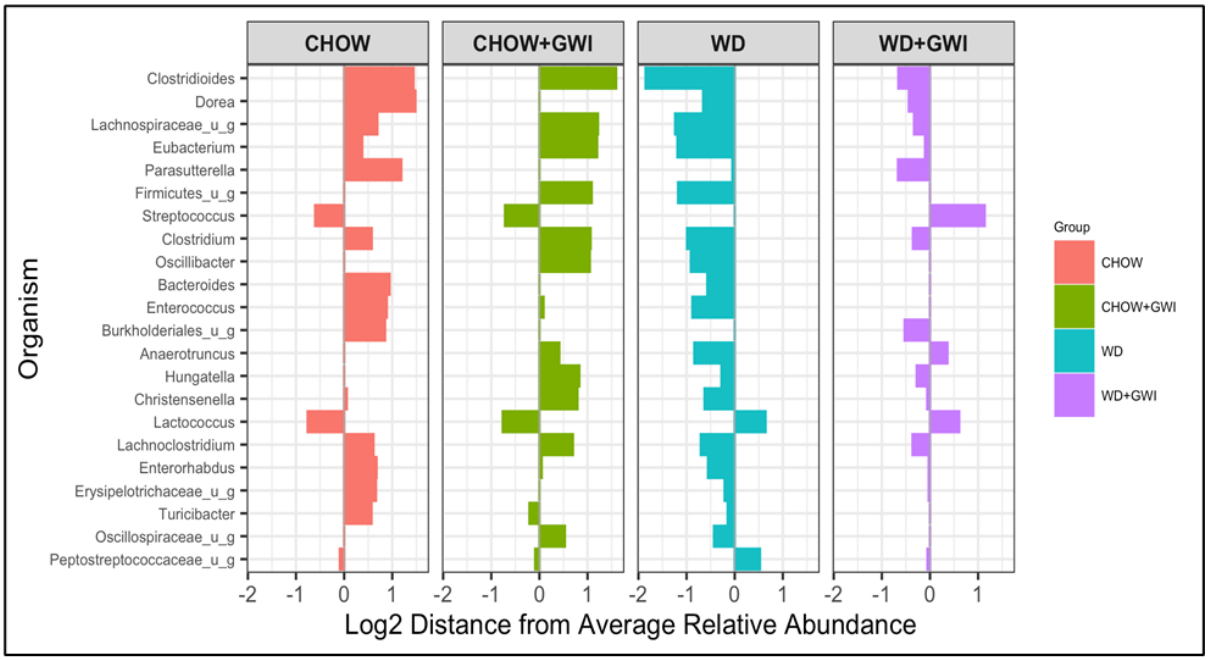
CHOW
CHOW+GWI
WD
WD+GWI
Organism
Clostridioides
Dorea
Lachnospiraceae_u_g
Eubacterium
Parasutterella
Firmicutes_u_g
Streptococcus
Clostridium
Oscillibacter
Bacteroides
Enterococcus
Burkholderiales_u_g
Anaerotruncus
Hungatella
Christensenella
Lactococcus
Lachnoclostridium
Enterorhabdus
Erysipelotrichaceae_u_g
Turicibacter
Oscillospiraceae_u_g
Peptostreptococcaceae_u_g
-2 -1 0 1
Log2 Distance from Average Relative Abundance
Group
CHOW
CHOW+GWI
WD
WD+GWI

B.

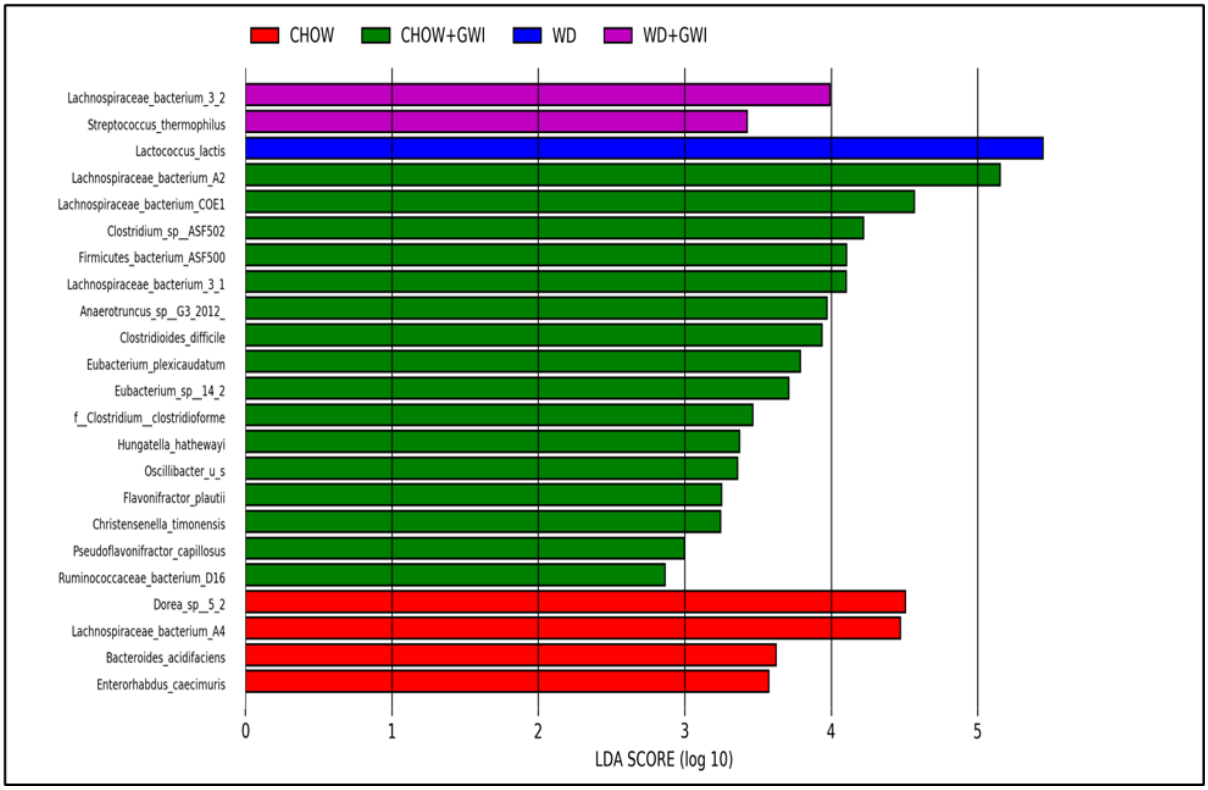
CHOW
CHOW+GWI
WD
WD+GWI
Lachnospiraceae_bacterium_3_2
Streptococcus_thermophilus
Lactococcus_lactis
Lachnospiraceae_bacterium_A2
Lachnospiraceae_bacterium_COE1
Clostridium_sp__ASF502
Firmicutes_bacterium_ASF500
Lachnospiraceae_bacterium_3_1
Anaerotruncus_sp__G3_2012_
Clostridioides_difficile
Eubacterium_plexicaudatum
Eubacterium_sp__14_2
f__Clostridium__clostridioforme
Hungatella_hathewayi
Oscillibacter_u_s
Flavonifractor_plautii
Christensenella_timonensis
Pseudoflavonifractor_capillosus
Ruminococcaceae_bacterium_D16
Dorea_sp__5_2
Lachnospiraceae_bacterium_A4
Bacteroides_acidifaciens
Enterorhabdus_caecimuris
0 1 2 3 4 5
LDA SCORE (log 10)

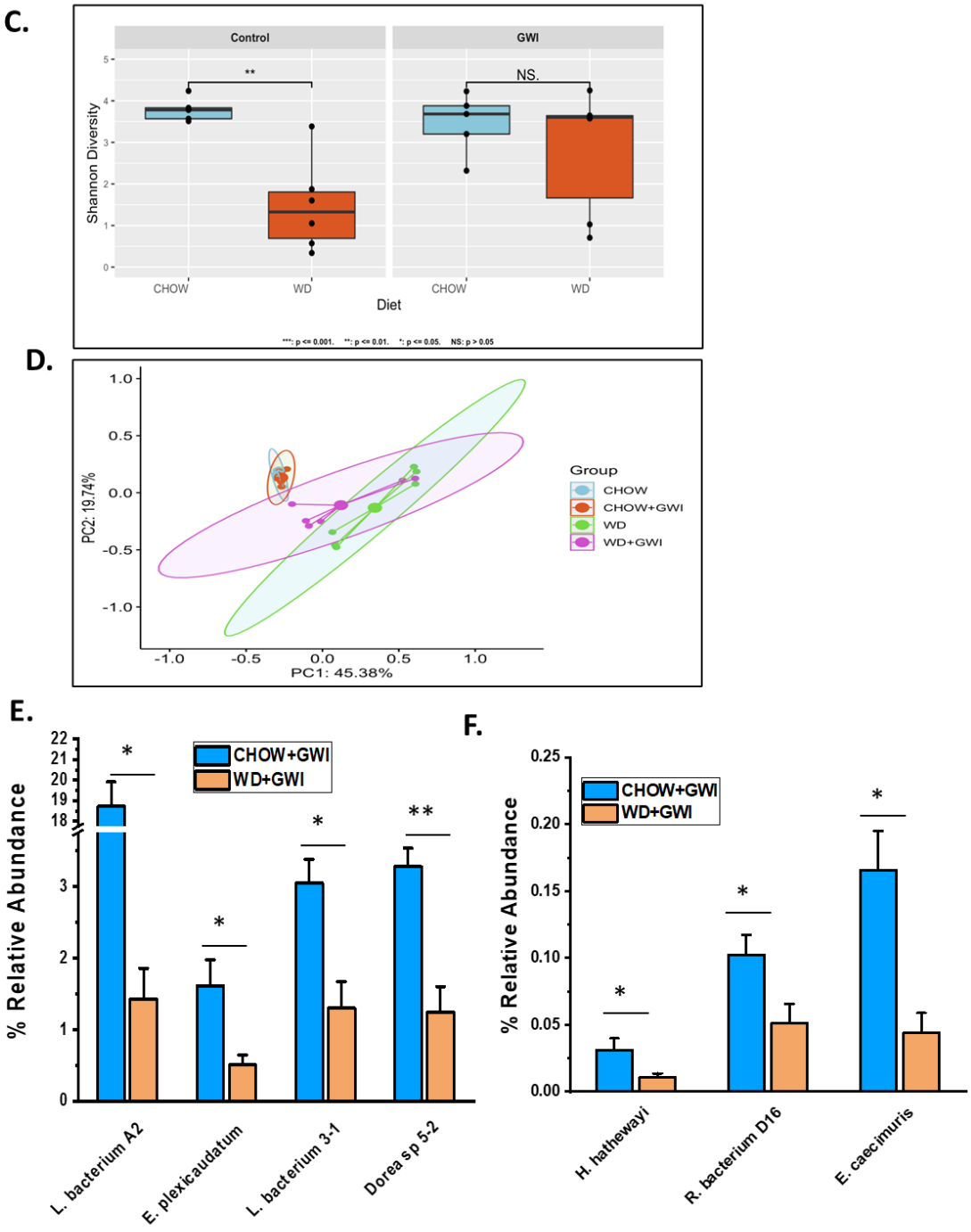

Figure 1.2. Obesity induces microbial dysbiosis at the species level in Gulf War illness (GWI) persistence. (A). Diverging bar (centroid) graph showing organisms' log2 relative abundance at species levels in the CHOW (lean), CHOW+GWI (persistence Gulf War illness), WD (obese) and WD+GWI (persistence Gulf War illness underlying obesity) groups. **(B)**. Differential species abundance (LEfSe analysis) among all study groups (CHOW, CHOW+GWI, WD and WD+GWI) is calculated using three methods: the Kruskal–Wallis sum-

rank test, the Wilcoxin rank-sum test, and Linear Discriminant Analysis (LDA). $p \leq 0.01$ for Kruskal–Wallis and Wilcoxon tests; LDA score ≥ 2.0 or ≤ −2.0. **(C)**. Box plot showing α diversity (Shannon) in all experimental groups. The left box (control) includes both lean (CHOW) and obesity (WD) control groups. However, the right box (GWI) includes both GWI persistence in the lean mice (CHOW+GWI) and in the obese mice (WD+GWI) groups. **(D)**. Bray–Curtis β diversity plot with 95% confidence ellipse in all experimental groups including both the lean (CHOW) and obesity (WD) control groups, and both GWI persistence in the lean mice (CHOW+GWI) and in the obese mice (WD+GWI) groups. **(E,F)**. Bar graphs showing the percent relative abundance of beneficial bacterial species. Data were presented as the mean of percent relative abundance with SEM. t-test analyses were performed. * denotes a significant level at $p < 0.05$ and ** denotes a significant level at $p < 0.001$, NS = not significant.

Western Diet-Fed Mice with GWI Show Increased Serum Levels of Proinflammatory Cytokine IL6 and Hyperinsulinemia

To show whether WD feeding and underlying obesity worsened serum levels of IL6, a reliable indicator of GWI pathology, serum ELISA was performed in mice. Results showed that IL6 levels were significantly increased in the WD+GWI group compared with the Chow+GWI group (Figure 1.3A). Notably, alpha diversity representing species abundance was strongly correlated (Pearson's R) with increased IL6 levels in the blood of the WD+GWI group when compared to the chow+GWI group, suggesting a probable role of the microbiome diversity observed in WD+GWI mice in elevated serum IL6 (Figure 1.3C) ($r = 0.6$). Aging, an underlying obesity phenotype, and chronicity of GWI pathology, can often lead to increased insulin levels in the blood, signifying underlying metabolic disease. Insulin levels in WD+GWI mice showed a significant increase in its levels when compared to the Chow+GWI group (Figure 1.3B), and microbiome dysbiosis represented by alpha diversity was strongly associated with the insulin level increase in the blood of the WD+GWI group (Figure 1.3D). The results suggested that proinflammatory levels of IL6 and

hyperinsulinemia were higher in underlying obesity with microbial dysbiosis represented by alpha diversity and might be a probable cause of such pathology.

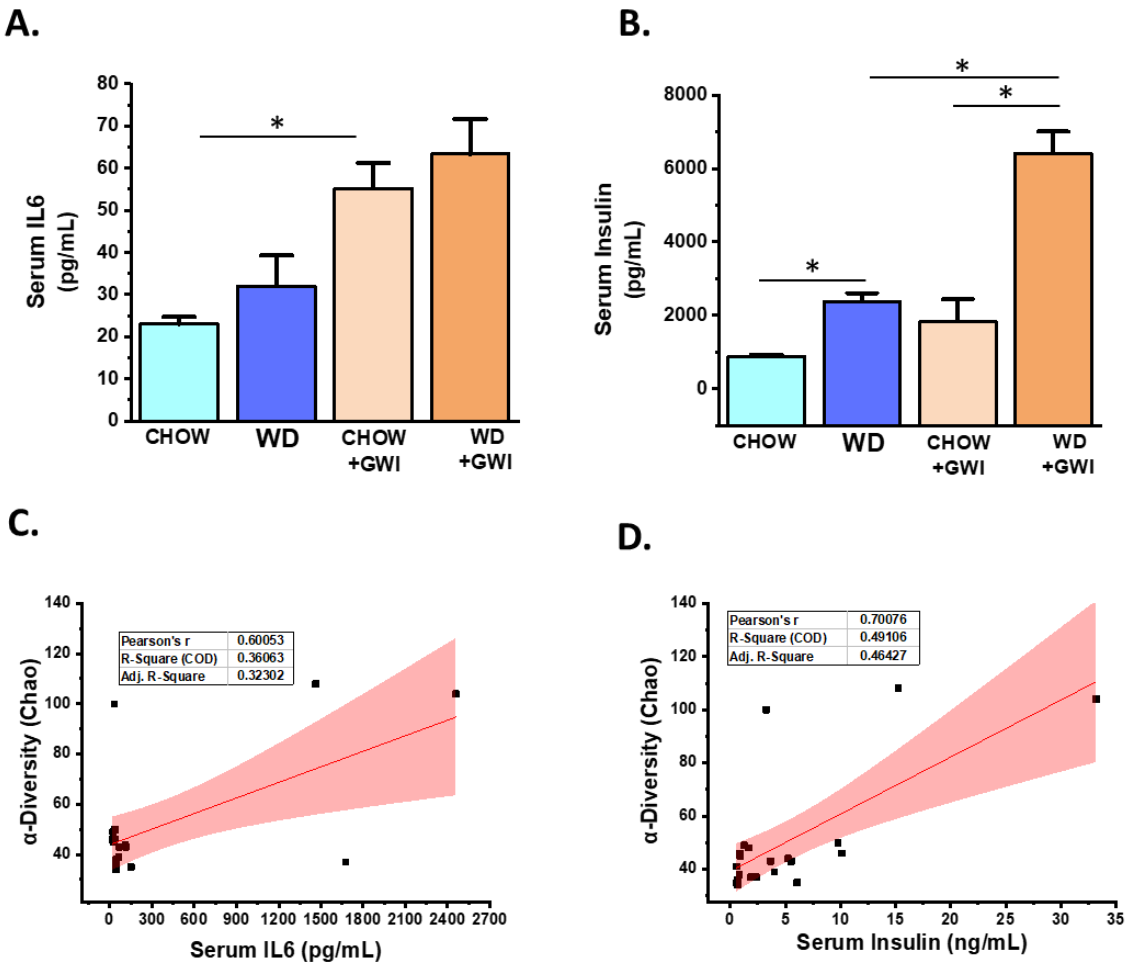

Figure 1.3. Obesity-induced microbial dysbiosis is associated with systemic IL6 levels and insulin resistance Gulf War illness (GWI) persistence. (A). Bar graph showing serum IL6 level (pg/mL) in all the CHOW (lean), CHOW+GWI (persistence Gulf War illness), WD (obese) and WD+GWI (persistence Gulf War illness underlying obesity) groups, and **(B)**. Serum insulin level (pg/mL) in all groups—CHOW, WD, CHOW+GWI, and WD+GWI. Data in A and B were presented as the mean and SEM. t-test analyses were performed. * denotes a significant level at $p < 0.05$. (C,D). Correlation plot of microbiome α diversity index (chao) by serum IL6 **(C)**, and by serum insulin **(D)**. Results of multivariate analyses for association with serum ELISA measurements are shown. Pearson's linear regression is shown in red with 95% confidence bands. IL6, Interleukin 6.

Western Diet-Fed Mice with GWI Show Altered Tight Junction Protein Expression and Enteric Glial Cell Activation, Thus Worsening GWI Intestinal Pathology

We determined whether underlying obesity caused an alteration of tight junction proteins in the distant ileum by Claudin-2 and Occludin immunofluorescence analysis. Results showed that GWI mice that were fed with the Western diet showed significantly increased levels of Claudin-2 when compared to chow-fed mice (Chow+GWI) (Figure 1.4A,D) ($p < 0.01$). The WD+GWI group also showed significantly decreased levels of Occludin when compared to the Chow+GWI group (Figure 1.4B,E) ($p < 0.01$). Activation of enteric glial cells has been shown to be aiding in the proinflammatory events in the intestine and contribute to GWI intestinal pathology [25]. Activation of these cells, as shown by the co-localization of GFAP/S100B, was significantly increased in the WD+GWI group when compared to the Chow+GWI group (Figure 1.4C,F) ($p < 0.01$). The co-localization events are shown by yellow pointed arrows. To show whether the microbial diversity was associated with the intestinal changes in pathology, a correlation analysis was carried out. Results showed that microbial diversity was strongly correlated with an increase in Claudin 2 levels in the WD+GWI group ($r = 0.7$) (Figure 1.4G). However, both Occludin levels and activation of enteric glial cells were not correlated with microbial species diversity and abundance in the WD+GWI group (Figure 1.4H,I). The results suggested that the underlying obesity following Western diet feeding was responsible for altered expression of tight junction protein, especially Claudin-2 and Occludin and concomitant activation of enteric glial cells, but microbiome diversity was only able to influence Claudin-2 protein levels in the obesity phenotype.

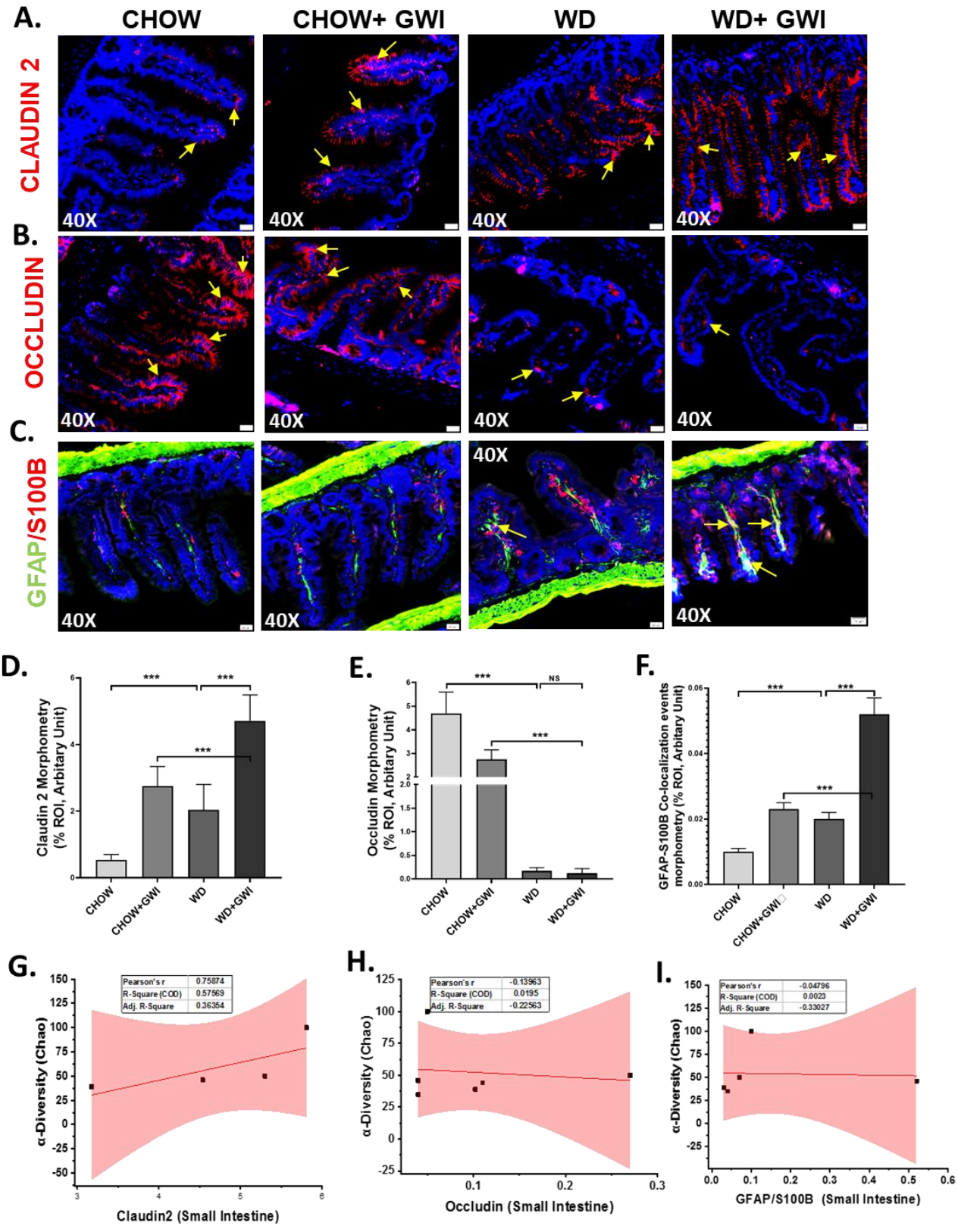
A.
CHOW
CHOW+ GWI
WD
WD+ GWI
CLAUDIN 2
40X
B.
OCCLUDIN
C.
GFAP/S100B
D.
Claudin 2 Morphometry (% ROI, Arbitary Unit)
CHOW
CHOW+GWI
WD
WD+GWI
E.
Occludin Morphometry (% ROI, Arbitary Unit)
NS
F.
GFAP-S100B Co-localization events morphometry (% ROI, Arbitary Unit)
G.
Pearson's r 0.75874
R-Square (COD) 0.57569
Adj. R-Square 0.36354
α-Diversity (Chao)
Claudin2 (Small Intestine)
H.
Pearson's r -0.13963
R-Square (COD) 0.0195
Adj. R-Square -0.22563
Occludin (Small Intestine)
I.
Pearson's r -0.04796
R-Square (COD) 0.0023
Adj. R-Square -0.33027
GFAP/S100B (Small Intestine)

Figure 1.4. Tight junction protein levels, enteric glial cell activation, and their correlation with microbial species diversity in Gulf War Illness (GWI) following an obesogenic diet feeding. (A–C). Immunoreactivity of Claudin 2 (red) in **(A)**, Occludin (red) in **(B)** and co-localization of GFAP/S100B (yellow) in **(C)** as shown by immunofluorescence microscopy in intestinal tissue sections from CHOW (lean), CHOW+GWI (persistence Gulf War illness), WD (obese) and WD+GWI (persistence Gulf War illness in underlying obesity) mice. Immunoreactivity of Claudin 2, Occludin, and co-localization of GFAP/S100B was indicated as yellow arrows. All images were taken at 40× magnification (50 μm). (**D–F)**. Bar graphs showing immunoreactivity of Claudin 2 in **(D)**, Occludin in **(E)** and GFAP/S100B co-localization **(F)**. Results were displayed as the mean ± SD of ROI% of three different areas (n = 6). Significance was tested by unpaired t-test; *** $p < 0.001$, NS = non-significant. (G–I). Correlation plot of α diversity (Chao) of bacterial species index by immunoreactivity obtained from immunofluorescence of Claudin 2 as **(G)**, Occludin as **(H)**, and co-localized GFAP/S100B as **(I)** of the WD+GWI mouse group. Pearson's linear regression is shown in red with 95% confidence bands. GFAP, Glial fibrillary acid protein; S100B, S100 calcium binding protein B.

Western Diet-Fed Mice with GWI Show Altered Tissue Proinflammatory Mediators IL1β and IL6, Thus Worsening GWI Intestinal Pathology

To show whether the underlying obesity worsens the release of proinflammatory cytokines from the intestinal segments, immunoreactivities of IL1β and IL6 were studied using immunohistochemistry. Results showed that IL1β tissue levels were increased significantly in the WD+GWI group when compared to the Chow + GWI group (Figure 1.5A,C) ($p < 0.01$), while IL6 tissue levels also followed a similar pattern when compared similarly (Figure 1.5B,D) ($p < 0.01$). Notably, both IL1β and IL6 tissue levels were positively correlated with microbiome diversity in the gut (Figure 1.5E,F) ($r = 0.68$; 0.78). The results suggested that the underlying obesity following Western diet feeding worsened the GWI intestinal inflammation, as shown by increased levels of IL1β and IL6. Further, the microbiome diversity evident from abundance scores positively correlated with the increased levels of the above proinflammatory mediators.

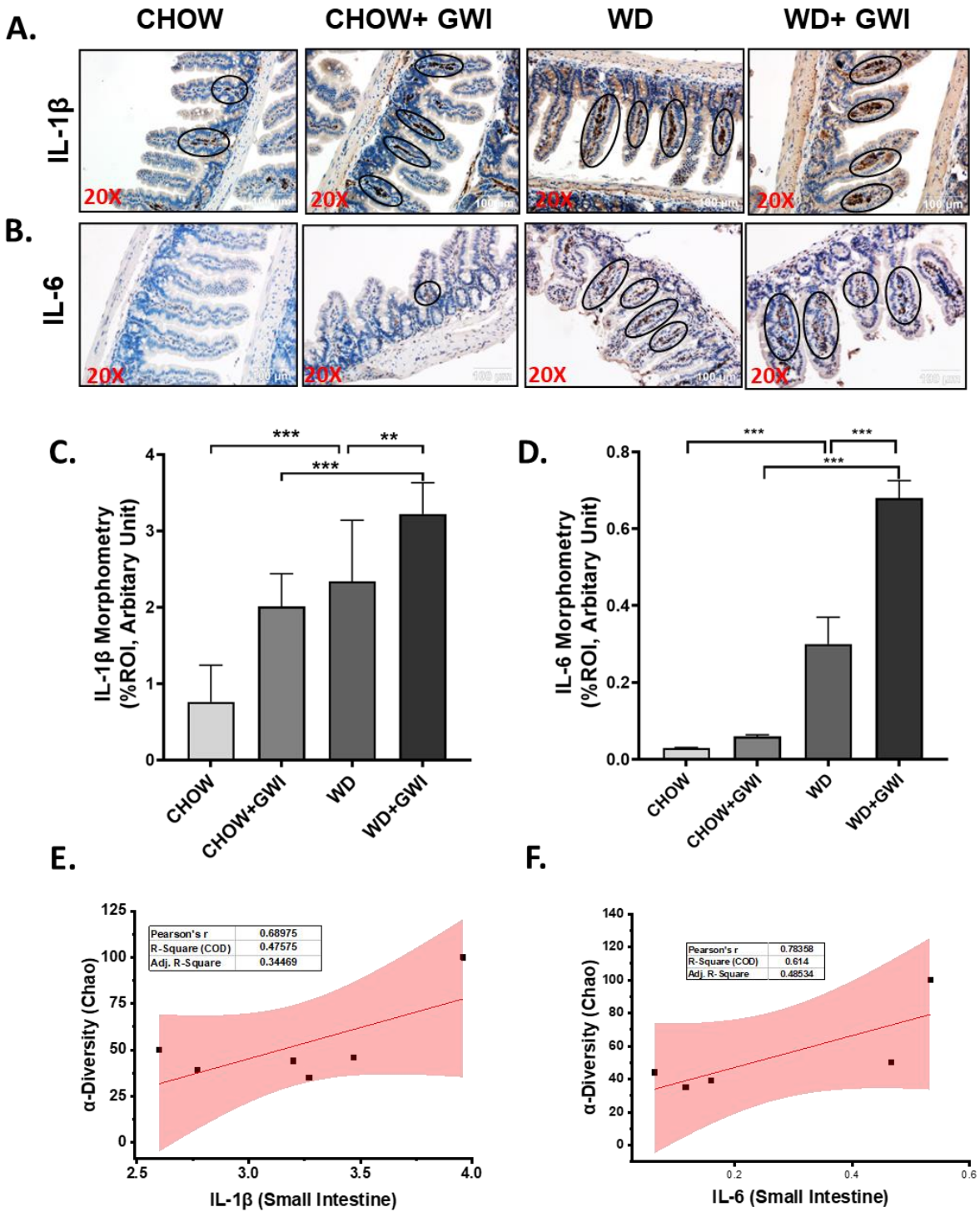

Figure 1.5. Gastrointestinal inflammation and its correlation with microbial species diversity in Gulf War illness (GWI) following obesogenic diet feeding. (A,B). Immunoreactivity of inflammatory markers IL1β **(A)** and IL6 **(B)** proteins was shown by immunohistochemistry in intestinal tissue sections from the CHOW (lean), CHOW+GWI (persistence Gulf War illness), WD (obese) and WD+GWI (persistence Gulf War illness

underlying obesity) mice groups. Immunoreactivity was indicated by black circles. Images were taken at 20× magnification (scale 100 μm). **(C,D)**. Bar graph showing immunoreactivity of IL1β as **(C)**, and IL6 as **(D)**. Results were displayed as the mean ± SD of ROI% of 3 different areas (n = 6). Significance was tested by unpaired t-test; ** $p < 0.01$, and *** $p < 0.001$. **(E,F).** Correlation plot of α diversity (Chao) of bacterial species index by immunoreactivity obtained from immunohistochemistry of IL1β as **(E)** and IL6 as **(F)** of the WD+GWI mouse group. Pearson's linear regression is shown in red with 95% confidence bands. IL1β, Interleukin 1 beta; IL6, Interleukin 6.

Western Diet-Fed Mice with GWI Show Altered Hepatic Kupffer Cell Activation and Profibrotic Phenotype, Thus Worsening GWI Hepatic Pathology

GWI patients hardly report liver abnormalities in the clinics owing to the silent nature of liver pathology especially related to fatty liver or its most progressive inflammatory form though obstructive liver disease cases have been documented [44]. We have shown previously that underlying liver inflammation is prevalent in mice models with the absence of any liver inflammatory foci and fibrotic pathology, a situation similar to early non-alcoholic fatty liver disease [29]. We determined whether a Western diet feeding would worsen liver pathology in GWI mice by examining CD68 (a Kupffer cell activation marker), and a-SMA (a myofibroblast phenotype marker) immunoreactivity. Results showed that CD68 levels were significantly increased in the livers of the WD+GWI group when compared to the Chow+GWI group (Figure 1.6A,C) ($p < 0.01$). Results also showed that α-SMA levels were significantly increased in the livers of the WD+GWI group when compared to the Chow+GWI group (Figure 1.6B,E) ($p < 0.01$). Notably, hepatic levels of insulin receptor substrate 1 (IRS-1), an important mediator in insulin resistance, were significantly decreased in the WD+GWI group when compared to the Chow+GWI group, suggesting that Western diet feeding worsened insulin resistance (Figure 1.6G,H). The data for IRS-1 also corroborated the increased hyperinsulinemia in the WD+GWI group observed earlier. The

increased diversity of the microbial species in the WD+GWI group correlated positively with increased CD68 and α-SMA (Figure 1.6D,F) (r = 0.74 and 0.9, respectively), suggesting that increased hepatic inflammation and stellate cell activation for a probable profibrotic phenotype is strongly associated with increased species diversity. However, there was a negative correlation between increased species diversity and IRS-1 protein levels, suggesting that microbiome changes may be aiding in the observed insulin resistance (Figure 1.6I) (r= −0.6).

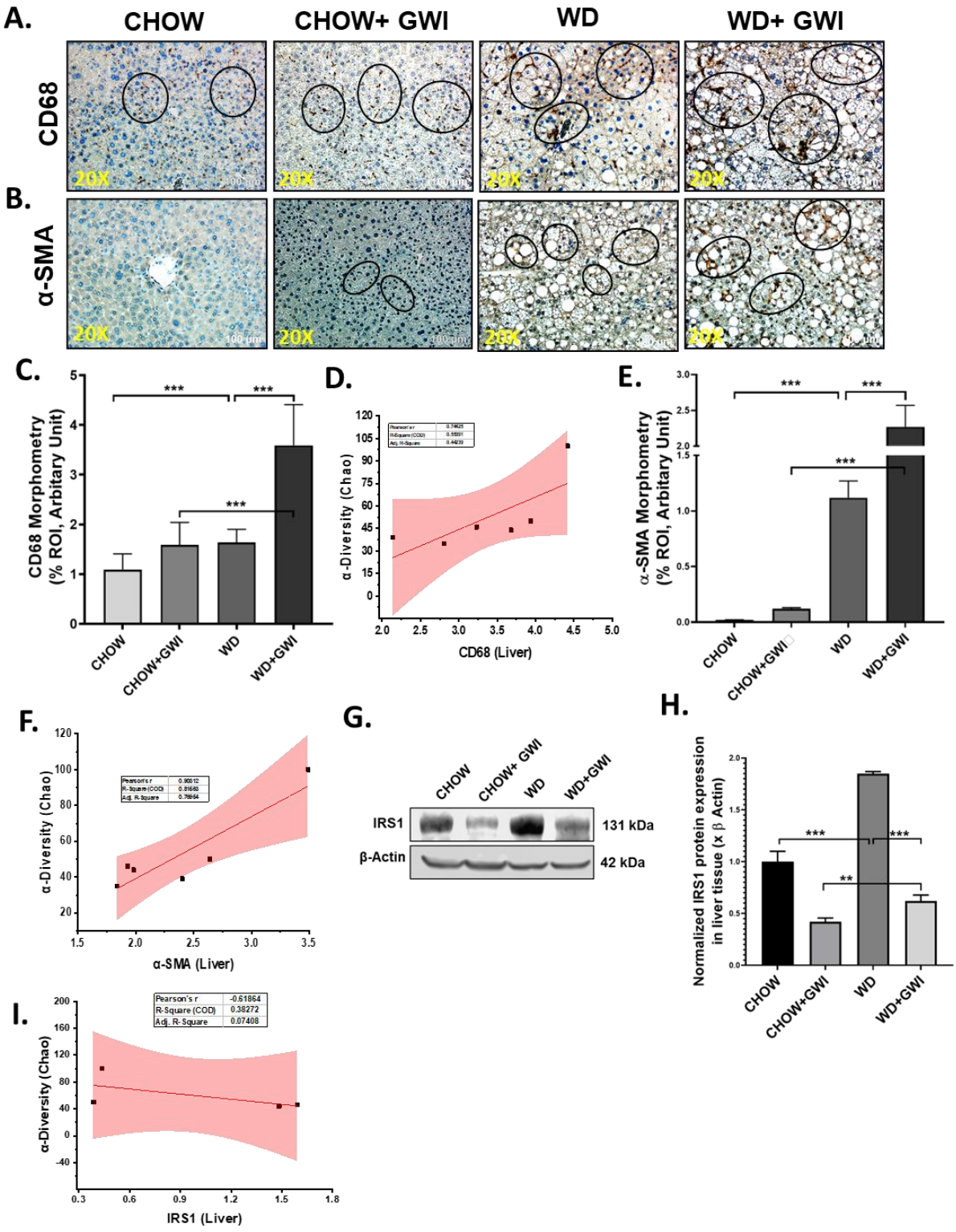

Figure 1.6. Kupffer cell and stellate cell activation in the liver and their correlation with microbial species diversity in Gulf War Illness (GWI) following obesogenic diet feeding. (A,B). Immunoreactivity Kupffer cell activation marker CD 68 **(A)** and stellate cell

activation marker α-SMA **(B)** proteins were shown by immunohistochemistry in liver sections from the CHOW (lean), CHOW+GWI (persistence Gulf War illness), WD (obese) and WD+GWI (persistence Gulf War illness underlying obesity) mice groups. Immunoreactivity was indicated by black circles. Images were taken at 20× magnification (scale 100 μm). **(C,E)**. Bar graph showing immunoreactivity of CD 68 as **(C)**, and α-SMA as **(E)**. Results were displayed as the mean ± SD of ROI% of three different areas (n = 6). Significance was tested by unpaired t-test; ** $p < 0.01$, and *** $p < 0.001$. **(G)**. Immunoblot analyses of IRS-1 from liver tissue lysates of the CHOW, CHOW+GWI, WD, and WD+GWI mouse groups. **(H)**. Densitometric analyses of IRS-1 immunoreactivity displayed as the mean ± SD (n = 3), normalized against β-actin, and plotted as a bar graph. **(D,F,I)** Correlation plot of α diversity (Chao) of bacterial species index by immunoreactivity obtained from immunohistochemistry of CD 68 as **(D)** and α-SMA as **(F)** and immunoblot of IRS-1 **(I)** of the WD+GWI mouse group. Pearson's linear regression is shown in red with 95% confidence bands. CD68, Cluster of Differentiation 68; α-SMA, alpha-smooth muscle actin; IRS1, insulin receptor substrate 1.

Western Diet-Fed Mice with GWI Show Heightened Neuroimmune Activation, Thus Worsening GWI Neuronal Pathology

Gulf War illness is perceived as a neuroimmune disease [39]. Chemical exposures during the war theater have been considered as significant effectors of neuronal pathology. Further, the neuronal pathology persists even 28 years after the war ended. We have shown previously that microbial dysbiosis connects neuroinflammation via mediators of the persistent dysbiosis. We ascertained whether the underlying obesity due to Western diet feeding would worsen persistence of neuroinflammation and related pathology through immunohistochemistry for proinflammatory mediators in the frontal cortex. Results showed that IL6 and IL1β tissue levels in the frontal cortex increased significantly in the WD+GWI group when compared to the Chow+GWI group (Figure 1.7A–D) ($p < 0.01$). Microglia, the brain-specific macrophages with an active role in neuroinflammation, have been shown to play a significant role in GWI pathology. Results showed that levels of CD40 co-localization events with microglial marker TMEM119 were significantly increased in the WD+GWI group

when compared to the Chow+GWI group (Figure 1.8A,B) ($p < 0.01$). To ascertain whether the dysbiosis shown earlier at the species level correlated with the observed neuroinflammation both for the proinflammatory cytokines and microglial activation, a Pearson's R was calculated for each of these comparison parameters. Results showed that levels of frontal cortex IL6 and IL1β were correlated with alpha diversity of the microbiome species in the same group (WD+GWI) (Figure 1.7E,F) ($r = 0.73$ for IL6) while the same positive correlation was observed for microglial activation (Figure 1.8C) ($r = 0.89$). The results suggested that obesity worsened neuronal inflammation and microglial activation, and the microbial species diversity was strongly associated with the brain inflammatory pathology.

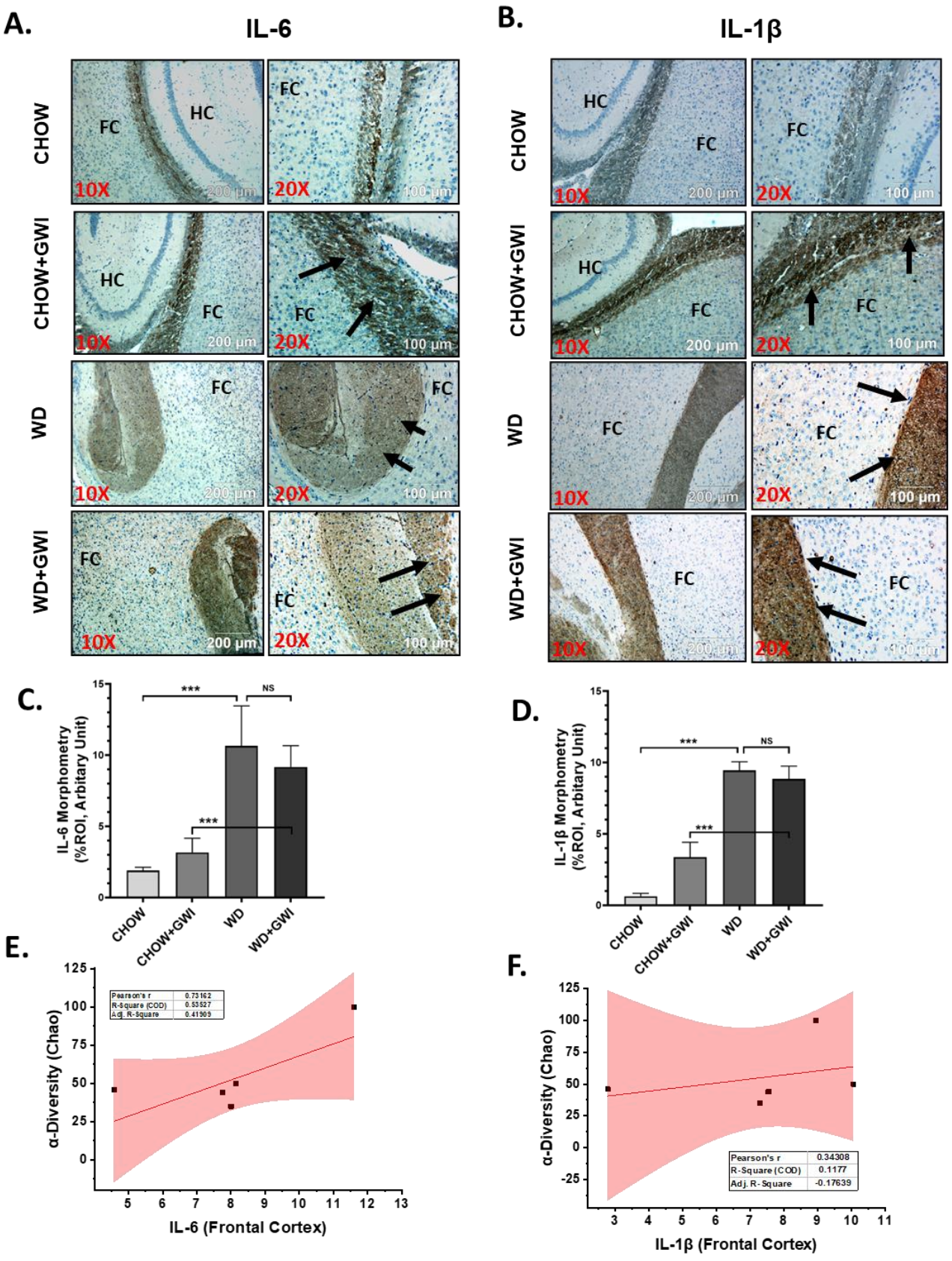
A.
IL-6
B.
IL-1β
CHOW
CHOW+GWI
WD
WD+GWI
HC
FC
10X
20X
200 µm
100 µm
C.
IL-6 Morphometry (%ROI, Arbitary Unit)
***
NS
CHOW
CHOW+GWI
WD
WD+GWI
D.
IL-1β Morphometry (%ROI, Arbitary Unit)
E.
α-Diversity (Chao)
IL-6 (Frontal Cortex)
Pearson's r 0.73162
R-Square (COD) 0.53527
Adj. R-Square 0.41909
F.
IL-1β (Frontal Cortex)
Pearson's r 0.34308
R-Square (COD) 0.1177
Adj. R-Square -0.17639

Figure 1.7. Neuroinflammation and its correlation with microbial species diversity in Gulf War Illness (GWI) following obesogenic diet feeding. (A) and **(B)** Immunoreactivity of neuroinflammatory markers IL6 **(A)** and IL1β **(B)** proteins was shown by immunohistochemistry in brain slices (the focused area is cerebral cortex) from the CHOW (lean), CHOW+GWI (persistence Gulf War illness), WD (obese) and WD+GWI (persistence Gulf War Illness underlying obesity) mice groups. Immunoreactivity was indicated by black arrows. Images were taken at 10× and 20× magnification. The frontal cortex is marked as FC, and HC is the hippocampus. **(C,D).** Bar graph showing immunoreactivity of IL6 as **(C)**, and IL1β as **(D)** Results were displayed as the mean ± SD of ROI% of three different areas (n = 6). Significance was tested by unpaired t-test; *** $p < 0.001$; NS = non-significant. **(E,F)**. Correlation plot of α diversity (Chao) of bacterial species index by immunoreactivity obtained from immunohistochemistry of IL6 as **(E)** and IL1β as (F) of the WD+GWI mouse group. Pearson's linear regression is shown in red with 95% confidence bands. IL1β, Interleukin 1 beta; IL6, Interleukin 6.

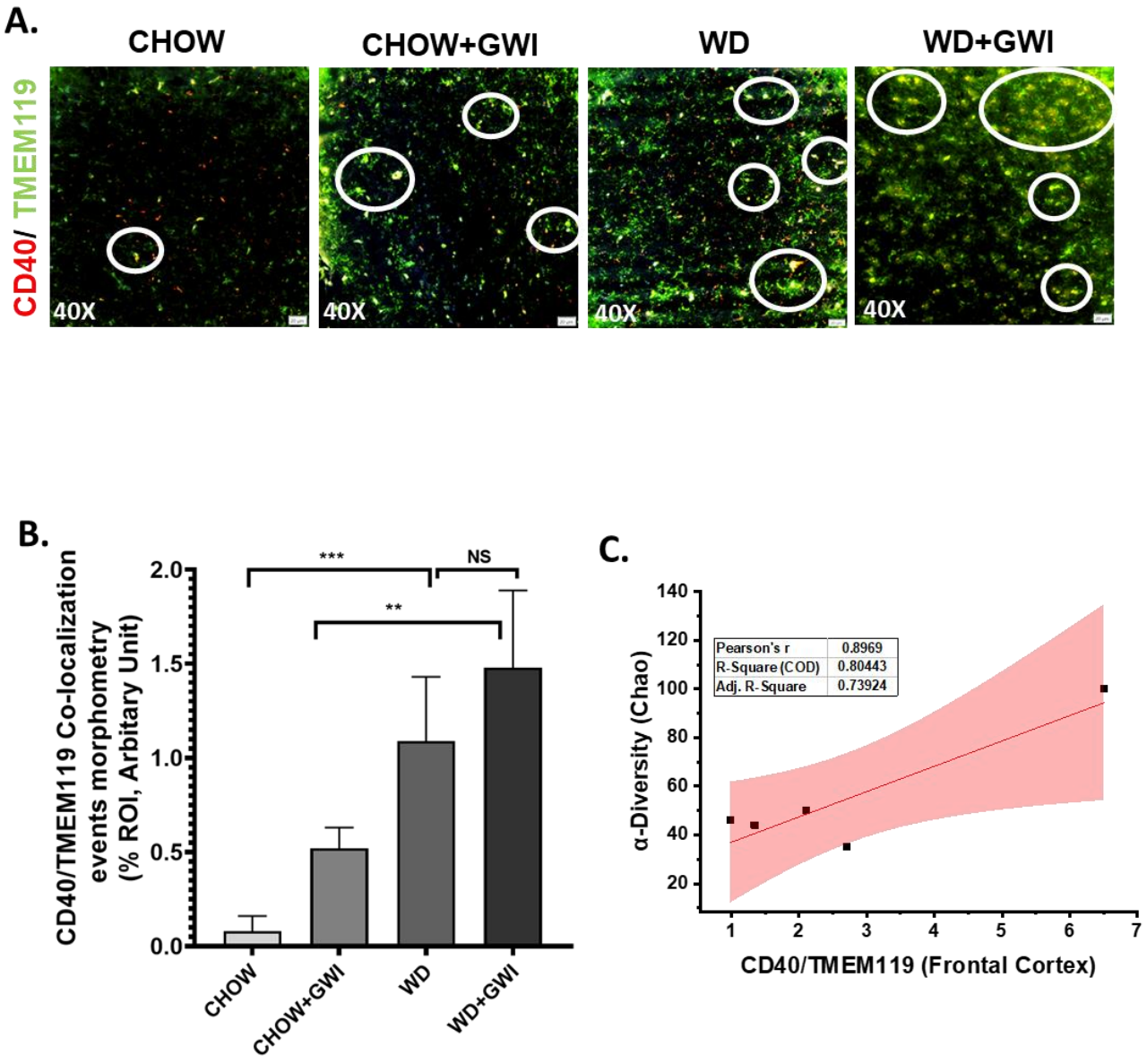

Figure 1.8. Microglial activation in the frontal cortex and its correlation with microbial species diversity in Gulf War illness (GWI) following an obesogenic diet feeding. (A). Co-localization of TMEM119/CD40 (yellow), as shown by immunofluorescence microscopy in frontal cortex sections from the CHOW (lean), CHOW+GWI (persistence Gulf War illness), WD (obese) and WD+GWI (persistence Gulf War illness underlying obesity) mice groups. Immunoreactivity was indicated by white circles. All images were taken at 40× magnification (50 µm). **(B)** Bar graph showing immunoreactivity of TMEM119/CD40 co-localization. Results were displayed as the mean ± SD of ROI% of three different areas (n = 6). Significance was tested by unpaired t-test; ** $p < 0.01$, and *** $p < 0.001$; NS = non-significant. **(C).** Correlation plot of α diversity (Chao) of bacterial species index by immunoreactivity obtained from immunofluorescence of co-localized TMEM119/CD40 of the WD+GWI mouse group. Pearson's linear regression is shown in red with 95% confidence bands. CD40, Cluster of Differentiation 40; TMEM119, Transmembrane protein 119.

Western Diet-Fed Mice with GWI Show Decreased Tissue Specific Content of Neurotrophic Factor BDNF and a Concomitant Rise in Tau Phosphorylation, Thus Worsening the Risk of GWI Neurocognitive Deficiencies

GWI symptom persistence in patients often reflects cognitive and memory deficits. Notably, neuroinflammation and microglial activation have been shown to cause decreased BDNF release, which has a notable role in neurogenesis and synaptic plasticity. Further, the accumulation of phosphorylated Tau protein exhibits a strong correlation with memory and recognition problems. We uncovered whether the underlying obesity decreased the tissue content of BDNF and increased phosphorylated Tau in the frontal cortex by immunohistochemistry on brain slices. Results showed that BDNF levels were significantly decreased in the frontal cortex of the WD+GWI group when compared to the Chow+GWI group (Figure 1.9A,B) ($p < 0.05$). Phosphorylated Tau assessment by immunoblot showed a significant increase in the protein levels in the frontal cortex of the WD+GWI group when compared to the Chow+GWI group (Figure 1.9D,E) ($p < 0.05$). Notably, microbial species diversity as assessed by alpha diversity was negatively correlated with levels of BDNF (Figure 1.9C) ($r = 0.65$) and positively correlated with levels of phosphorylated Tau protein (Figure 1.9F, $r = 0.6$). The results above suggested that the underlying obesity due to Western diet feeding for a prolonged time decreases neurotrophic mediator BDNF while increasing accumulation of phosphor Tau protein, a mediator for defects in memory and Alzheimer-like pathology.

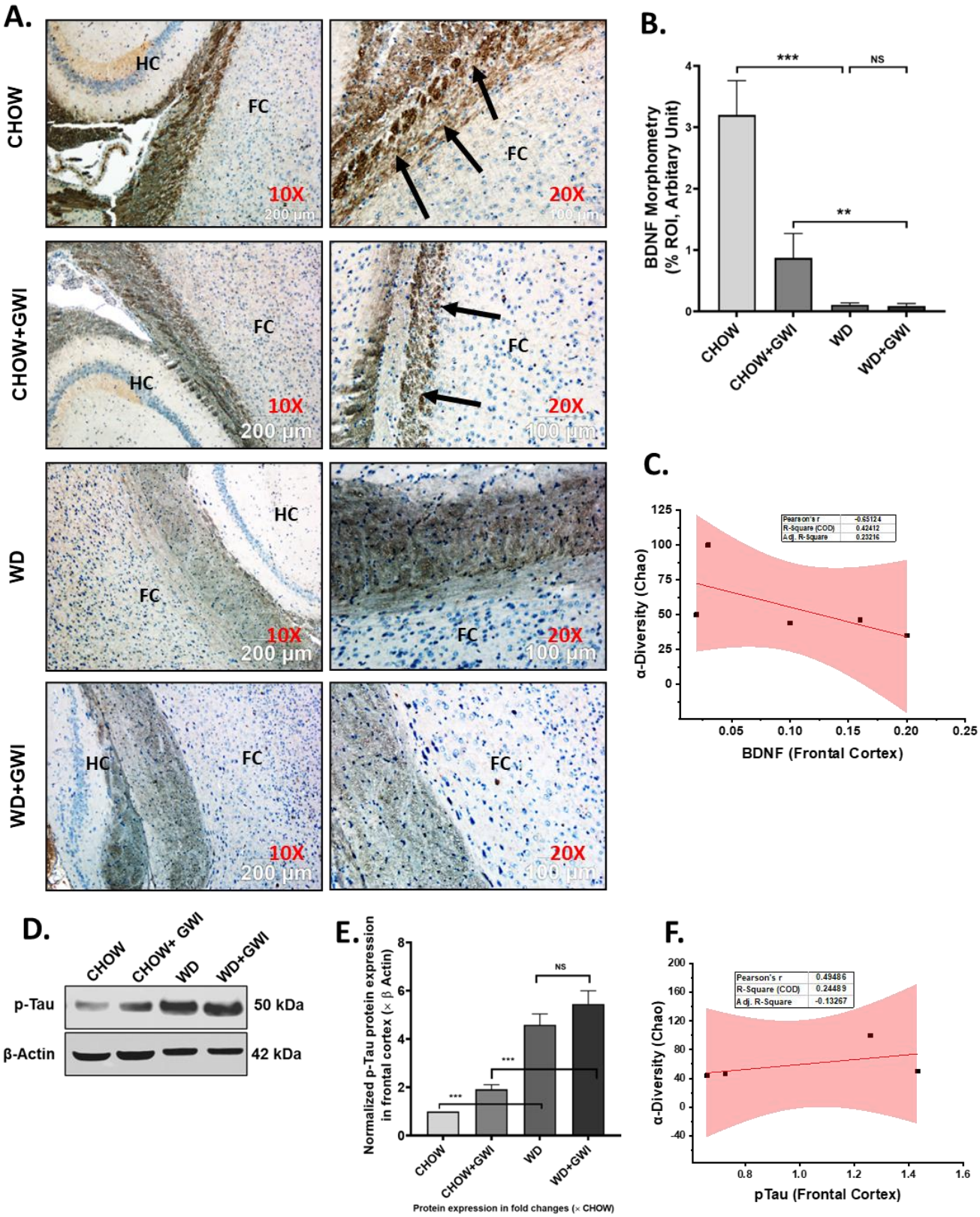
A.
CHOW
CHOW+GWI
WD
WD+GWI
HC
FC
10X
200 µm
20X
100 µm
B.
BDNF Morphometry (% ROI, Arbitary Unit)
***
NS
**
CHOW
CHOW+GWI
WD
WD+GWI
C.
Pearson's r -0.65124
R-Square (COD) 0.42412
Adj. R-Square 0.23216
α-Diversity (Chao)
BDNF (Frontal Cortex)
D.
CHOW
CHOW+ GWI
WD
WD+GWI
p-Tau
50 kDa
β-Actin
42 kDa
E.
Normalized p-Tau protein expression in frontal cortex (× β Actin)
Protein expression in fold changes (× CHOW)
F.
Pearson's r 0.49486
R-Square (COD) 0.24489
Adj. R-Square -0.13267
α-Diversity (Chao)
pTau (Frontal Cortex)

Figure 1.9. BDNF and accumulation of p-Tau and its correlation with microbial species diversity in Gulf War Illness (GWI) following an obesogenic diet feeding. (A). Immunoreactivity of neurotrophic marker BDNF protein was shown by immunohistochemistry in brain slices (the focused area is cerebral cortex) from the CHOW (lean), CHOW+GWI (persistence Gulf War illness), WD (obese) and WD+GWI (persistence Gulf War illness underlying obesity) mice groups. Immunoreactivity was indicated by black arrows. Images were taken at 10× and 20× magnification. The frontal cortex is marked as FC and the hippocampus as HC. **(B)**. Bar graph showing immunoreactivity of BDNF. Results were displayed as the mean ± SD of ROI% of three different areas (n = 6). Significance was tested by unpaired t-test; ** $p < 0.01$, and *** $p < 0.001$; NS = non-significant. **(D)**. Immunoblot analyses of p-Tau from frontal cortex tissue lysates of the CHOW, CHOW+GWI, WD, and WD+GWI mouse groups. **(E)**. Densitometric analyses of p-Tau immunoreactivity displayed as the mean ± SD (n = 3), normalized against β-actin and plotted as a bar graph. **(C,F).** Correlation plot of α diversity (Chao) of bacterial species index by immunoreactivity obtained from immunohistochemistry of BDNF **(C)** and immunoblot of p-Tau **(F)** of the WD+GWI mouse group. Pearson's linear regression is shown in red with 95% confidence bands. BDNF, Brain-derived neurotrophic factor; p-Tau, phosphorylated Tau.

Mouse Serum from Mice with GWI and Underlying Obesity with an Altered Microbiome Activate Microglial Cells, Cause M1 Polarization and Induce Oxidative Stress and Cytotoxicity

The data described above clearly show an association with microbiome dysbiosis in mice that are obese and have GWI but does not causally link the dysbiosis-induced systemic inflammation to changes in microglia. We determined whether the GWI and obesity-induced microbiome dysbiosis would release the circulatory mediators of microglial activation through an ex vivo/in vitro approach. SIM-A9 cells were incubated with mouse serum from the Chow, Chow+GWI, WD, and WD+GWI groups. An LPS-treated group was used as a positive control. Results showed that there was a significant increase in co-localization events of CD40 and TMEM119 in SIM-A9 cells-incubated with serum from the WD+GWI group when compared to the Chow or WD or Chow+GWI groups (Figure 1.10A,C) ($p < 0.05$). Tyrosyl radical formation, as indicated by 3-nitrotyrosine, significantly increased in the

WD+Chow group when compared to the Chow or WD or Chow+GWI groups (Figure 1.10B,D) ($p < 0.05$). We examined whether the serum from mice with GWI and obesity would induce M1 polarization of microglia and release proinflammatory cytokine IL6, a crucial mediator in worsening GWI-associated neuroinflammation, by screening supernatants for the cytokine concentration using ELISA. Results showed that there was a significant increase in secreted IL6 in the supernatant of cells incubated with the WD+GWI group when compared to either the Chow or GWI alone or Chow+GWI groups (Figure 1.10E) ($p < 0.01$). The same group showed marked cytotoxicity as assessed by LDH release (Figure 1.10F). The results suggested that mouse serum from the WD-GWI group might harbor damage-associated molecular patterns, preferably HMGB1 or IL6, that may be instrumental in the activation of microglia shown in Figure 1.9.

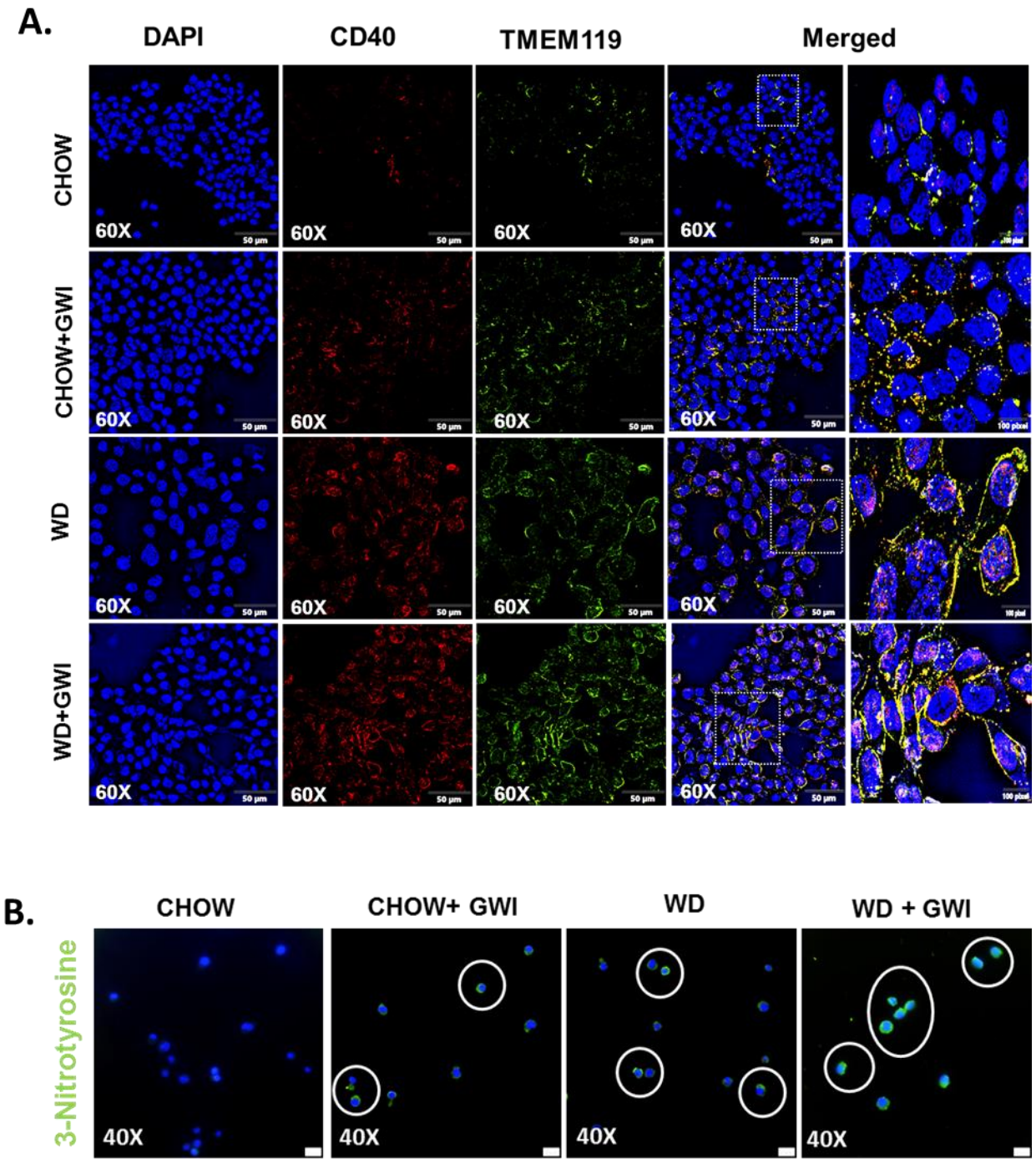
A.
DAPI
CD40
TMEM119
Merged
CHOW
CHOW+GWI
WD
WD+GWI
60X
50 µm
B.
CHOW
CHOW+ GWI
WD
WD + GWI
3-Nitrotyrosine
40X

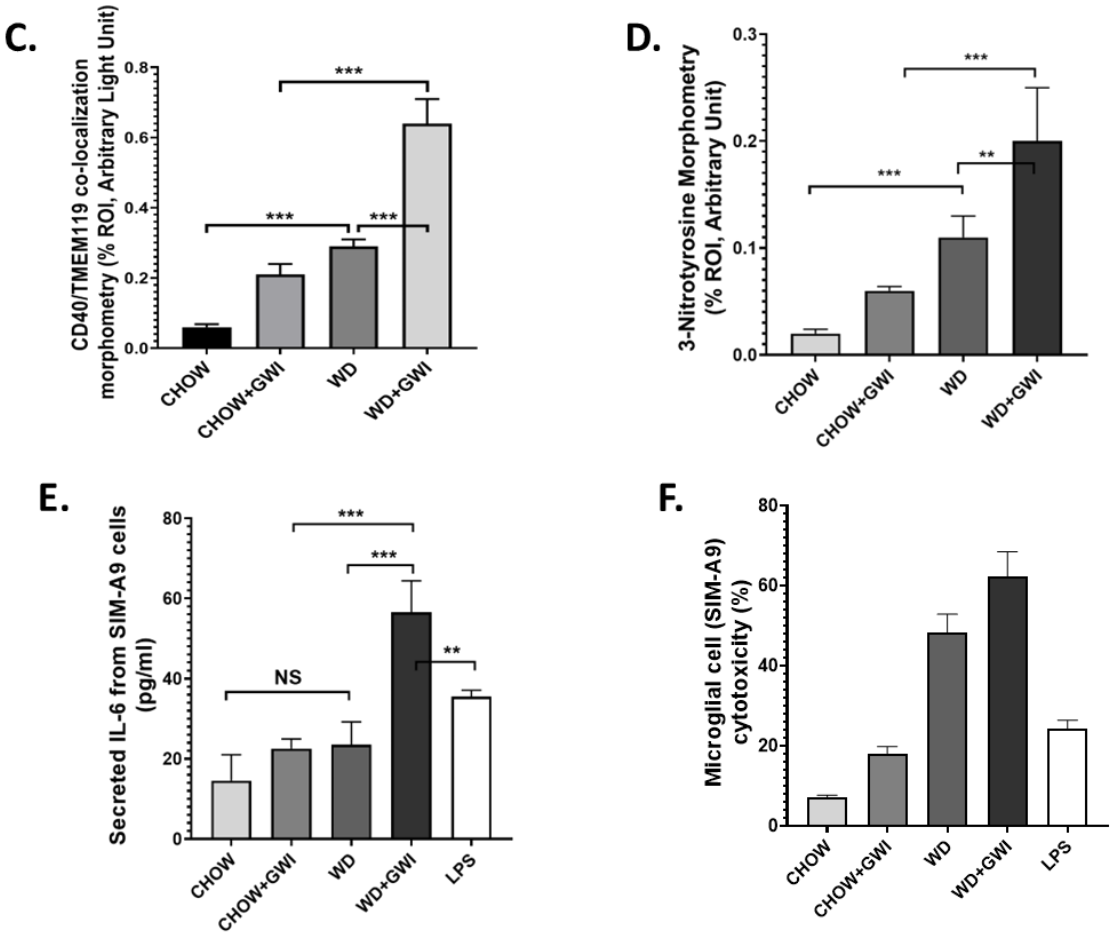

Figure 1.10. Obese mice serum induces microglial activation, tyrosine nitration, and IL6 release in mouse SIM-A9 cells. (A). Co-localization of CD40/TMEM119 (yellow) as shown by immunofluorescence microscopy in mouse microglial cells SIM-A9 treated with serum from CHOW (lean), CHOW+GWI (persistence Gulf War illness), WD (obese), and WD+GWI (persistence Gulf War illness underlying obesity). Nucleus was stained with DAPI. Images were taken at 60× magnification and a magnified image of the merged channels is presented at the right side. **(B)**. Immunoreactivity of 3-nitrotyrosine as shown by immunofluorescence microscopy in mouse microglial cells SIM-A9 treated with serum from CHOW, CHOW+GWI, WD, and WD+GWI. Immunoreactivity was indicated as white circles. Nucleus was stained with DAPI. Images were taken at 40× magnification. **(C,D).** Bar graph showing immunoreactivity of CD40/TMEM119 co-localization **(C)** and 3-nitrotyrosin **(D)**. Results were displayed as the mean ± SD of ROI% of three different areas (n = 3). Significance was tested by unpaired t-test; ** $p < 0.01$, and *** $p < 0.001$; NS = non-significant. **(E)**. IL6 concentration (pg/mL) in supernatants from SIM-A9 cells treated with serum from CHOW, CHOW+GWI, WD, WD+GWI mice groups and with lipopolysaccharide (LPS) (1 µg/mL) were displayed by bar graph. Data were calculated and expressed as the mean ± SD; significance was calculated by paired t-test between the groups; ** $p < 0.01$, and *** $p < 0.001$. **(F)**. Bar graph depicting percentage cytotoxicity by lactate dehydrogenase assay using supernatant of SIM-A9 cells treated with serum from CHOW, CHOW+GWI, WD, WD+GWI mice groups or

with LPS (1 μg/mL), Data were calculated and expressed as the mean ± SD (n = 3). CD40, Cluster of Differentiation 40; TMEM119, Transmembrane protein 119; Il-6, Interleukin 6; DAPI, 4′,6-diamidino-2-phenylindole.

DISCUSSION

The present study describes the obesity-induced worsening of GWI-associated inflammation in the gastrointestinal tract, hepatic inflammatory changes that are a precursor to metabolic disturbances and neuroinflammation that may form the basis of cognitive decline and memory loss. The mouse model of chronic GWI was adopted from a published study by Zakirova Z et al. [45] to mimic exposures experienced by GW veterans who returned to a non-combat role after deployment and live in the United States [1]. In addition, like the rest of the continental US, veterans have adapted to a sedentary lifestyle or were physically incapacitated due to an injury suffered during the deployment [34]. This study used a Western diet (43% carbohydrate, 44% fat) that is a staple dietary pattern in the US and other Western societies [46]. Such a diet induces obesity and primarily mimics the present-day US dietary habit [47]. The Western diet remains a better model than a high-fat diet (60% kcal fat/low carb)-induced obesity for our studies since it models our veterans and is not merely mimicking a high-fat diet-induced morbidly obese condition with implications in the liver and other cardiovascular complications [48]. Our results show that obesity-induced by a Western diet for 20 weeks (~equivalent to 15.5 years in GW veterans) [49] resulted in a unique microbiome signature that caused a significant decrease in the butyrogenic bacterial species. Notably, the microbiome species changed in richness, diversity, and abundance, which was strongly correlated with gastrointestinal and hepatic alterations, and neuroinflammation.

To date, the current study is the most comprehensive microbial analysis in the GWI mouse model. The present study expands our earlier acute phase study that showed the microbiome dysbiosis via a V3–V4 16s sequencing [24]. With a rapidly evolving technology to evaluate microbiome dysbiosis, it is important that better and more sophisticated techniques must be applied to unearth the microbiome puzzle that may have lasting answers to the cause and the treatment of GWI. We used the shotgun metagenomics method for microbiome analysis at the species level using the next-generation sequencing platform, a sophisticated and better alternative to our earlier approach. A recent study reported the high-fat and low-carbohydrate diet (45% kcal fat)-induced microbiome changes in GWI, but the study was entirely based on 16s RNA sequencing. Though 16S rRNA gene sequencing is highly useful regarding bacterial classification, it may be noted that it has low phylogenetic power at the species level and a weak discriminatory power for some genera. Further, DNA-related studies are necessary to provide absolute resolution to these taxonomic problems [50].

Akkermansia muciniphila, a widely studied species known to have a beneficial effect in gastrointestinal disorders, was significantly decreased in Chow+GWI, and the decrease was strongly associated with gut abnormalities and inflammation [28]. In contrast, we observed a marked increase in abundance of *Akkermansia muciniphila* in the WD+GWI group (Supplementary Figure 1.1) when compared to the Chow+GWI group, suggesting that mucin degradation by this species was an adaptive response by the intestinal microenvironment to ensure that a proper defense can be launched following a possible rapid loss of membrane integrity in the WD+GWI group (increased Claudin-2 levels and decreased Occludin) though more detailed studies need to be performed to back the above hypothesis [28] (Figure

1.4A,B). It may be noted that *Akkermansia* species have been associated with intestinal membrane integrity. However, the mechanisms of such a response are unclear at this time, and more species-level studies with higher n values need to be carried out to understand the commensalism of other species. The above argument is backed by our data related to the abundance of another beneficial microbe, *Lactococcus lactis. Lactococcus lactis* was found to be abundant in the WD+GWI group when compared to the Chow+GWI group. Interestingly, *Lactobacillus lactis* has been shown to release antioxidant defense enzyme superoxide dismutase and can be a strong player in the host anti-inflammatory response [51]. Together with *Akkermansia,* species such as Lactobacillus lactis may be aiding the host intestinal microenvironment to launch an effective and robust wound healing response following the chronic obesity-induced worsening of GWI intestinal inflammation (Figure 1.2B and Supplementary Figure 1.1). These findings are relevant for planning a future effective probiotic therapy where a combination of *Lactobacillus lactis* and *Akkermansia sp*. may be used in our GWI veterans.

We have shown before that butyrate-producing bacteria and bacterial species that promote gut health are significantly decreased in GWI. Similar results were also observed in the present study, where several butyrogenic bacteria and other prominent beneficial microbes were significantly decreased in the WD+GWI group (Figure 1.2E,F). Further, butyrate generated as a metabolic product of these bacteria has been shown to possess a robust anti-inflammatory effect largely by its ability to trigger an adaptive immune response involving T regulatory cells [52]. We used LEfSe analysis to determine specific bacteria taxa that were differentially abundant and partially depleted in the WD+GWI group. We identified *Hungatella sp, Eubacterium sp, Lachnospiraceae bact 3.1*, *Ruminococcaceae bact D16*,

Lachnospiraceae bact A2, Blautia, and Enterohabdus cecimuris as the most differentially depleted genera associated with GWI-led worsening of symptoms in an underlying obesity condition (Figure 1.2B, Supplementary Figure S1.1). Notably, *Dorea* sp. decreased as well in the WD+GWI group, suggesting an adaptive response probably similar to the type of response we observed with *Akkermansia sp*. The results assume immense significance, since chronicity of GWI symptoms and their subsequent worsening might be due to the partial depletion of these beneficial microbes. However, gnotobiotic studies using the individual strains or a combination of these strains in the future will be valuable to authenticate these results.

Chronicity of GWI manifests in mild to severe gastrointestinal disturbances in the subsection of patients. We have shown that GI inflammation persists in the mouse model. The levels of proinflammatory events such as increased proinflammatory mediators like IL6, IL1β, inflammasome activation with concomitant alterations of tight junction proteins are strongly associated with persistent dysbiosis even 5 months after the GW chemical exposure that mimics war theater [28]. Our results of a further worsening of the GI inflammatory surge and events that contribute to a leaky gut in underlying obesity suggest that a Western dietary behavior and sedentary lifestyle (mice in the present model were not subject to exercise) can aggravate GI disturbances. Interestingly, one of our earlier studies showed an underlying liver inflammation but failed to show a liver disease phenotype that manifests in a significant elevation of liver enzymes or marked steatosis [29]. The underlying obesity due to prolonged Western diet consumption significantly elevated liver injury, as shown by increased Kupffer cell and stellate cell activation, markers of ensuing steatohepatitis, and or metabolic syndrome. The results and our assumptions about a possible metabolic syndrome were also

backed by significant hyperinsulinemia and a decrease in insulin receptor substrate 1 level in the liver (Figure 1.6). Significantly enough, all the results associated with a diseased liver were strongly associated with an altered microbiome species diversity (Figure 5 and Figure 6).

Gulf War illness veterans show a consistent decrement of brain function that includes cognitive and memory deficits [1]. Many of the symptoms reported by veterans with GWI are indicative of central nervous system (CNS) dysfunction, and indeed this has been corroborated by structural and functional neuroimaging and biomarker studies [1]. The decrements in brain function, such as memory and learning deficits, plague the veterans even today and highlight the need for proper diagnostic pathology and treatment. Most studies that model persistence of GWI symptoms do not consider the various comorbidities accompanying brain dysfunction in veterans. For example, a GWI veteran in the age range of 50–55 years and consuming a Western diet has limited mobility due to combat-related injuries, and may suffer from increased weight gain, hypertension, type II diabetes and a host of other chronic diseases. Thus, it is essential to study the weight gain-associated comorbidities and their role in worsening the neuronal disturbances. Our results of increased frontal cortex levels of IL6 and IL1β and their strong association with an altered species diversity show that obesity-induced unique microbiome signature might exacerbate the proinflammatory microenvironment in the brain. Interestingly, we have shown that IL6 remains elevated in serum and the brain following GW chemical exposure. IL6 and IL1β have been shown to contribute to major depression, dementia, and neurodegenerative disease phenotypes by [53]. Our results of a gut–brain connection to neuroinflammation strongly support the argument of increased focus on the mechanisms that may lead to these

phenotypes, especially the role of microglial activation following stimulation by circulatory IL1β and IL6 [54]. Microglial activation in our mouse model showed a significant increase in the WD+GWI group when compared to the Chow+GWI group, suggesting that obesity-associated microbial dysbiosis and increased serum IL6 levels might contribute to such activation and possibly connect to neurodegenerative phenotype (Figure 1.8). Our results of exacerbation of neuroinflammation following Western diet-induced obesity are corroborated by other experimental studies where microglial activation is seen as an important event [64]. Microglial activation and subsequent amplification of inflammation in the brain is associated with regulation by neurotrophic factors such as BDNF [55]. Furthermore, obesity is associated with decreased levels of BDNF. Further, the accumulation of phosphorylated tau is indicative of neurodegenerative changes [56]. The underlying obesity in the GWI mouse model resulted in a significant decrease in BDNF and a parallel increase in phosphorylated tau protein, indicating a neurodegenerative phenotype associated with microbial dysbiosis (Figure 1.9). Interestingly, microglial activation also leads to a neurodegenerative phenotype and is extensively reviewed [57]. To strengthen our conclusion of such an association between dysbiosis, increased microglial activation and neurodegeneration, we incubated a transformed microglial cell line with serum from WD+GWI that had significant species diversity and a unique phenotype of increased bacterial species known to increase inflammation. Increased secretion of IL6, peroxynitrite generation, and increased cytotoxicity in these cells show a linear relationship between Western diet consumption, microbial dysbiosis, and neuroinflammation via a microglial activation pathway. Having shown that GWI mice with dysbiosis have an elevated circulatory IL6, it is not surprising that an even higher serum IL6 (Figure 1.3) in the WD+GWI group

caused an M1 polarization (secreted IL6) to seeded microglial cells (Figure 1.10) [58]. The ex vivo/in vitro data also form the basis of a likely mechanism of microglia-induced neuroinflammation and neuronal dysfunction in the WD+GWI group. We also found a robust association between obesity in a GWI model and dysbiosis that is in line with a recent study in a Gulf War illness mouse model that showed dysbiosis following high-fat diet feeding [35]. Such a scenario is likely in GWI veterans because they are aging and have limited physical activity. Moreover, studies on the effects of mouse serum from the experimental in vivo groups exhibiting gut dysbiosis on microglia partially proved a relationship between gut dysbiosis and neuroinflammation. Our present study also advances our understanding about a likely scenario in veterans with an overweight or obese phenotype. Notably, one strength of our study lies in possible mechanistic links of an obese phenotype to persistence of GWI symptoms such as GI disturbances, liver abnormalities and neuronal pathology 28 years after the war ended. Nonetheless, a detailed mechanistic study using either an antibiotic-induced gut sterility control group or germ-free mice will be necessary to confirm the mechanisms mentioned above. Limitations include a moderate sample size of 5–6 mice per group and future studies should build on the preliminary findings of this study to focus on specific mechanistic underpinnings in each organ system with a large sample size. Further, GWI is a multisymptom disorder and dysbiosis-linked associations in pathology seen in mouse models only reflect a trend in disease progression rather than a causality. Improved rodent preclinical models may see benefits in finding definitive pathology and drug pathways. In summary, the results of this study suggest that the underlying obesity due to a Western diet contributes to persistence of gastrointestinal and hepatobiliary alterations and neuroinflammation over the longer term. Such effects are likely the result of a sustained

microbial species-level diversity. Targeted probiotic approaches in combination with anti-inflammatory nutraceuticals might help to prevent a poor outcome in obesity-associated worsening of GWI symptoms that we observe in GW veterans today. Additionally, the results have implications for understanding the inflammation processes in chronic illnesses and the aging process.

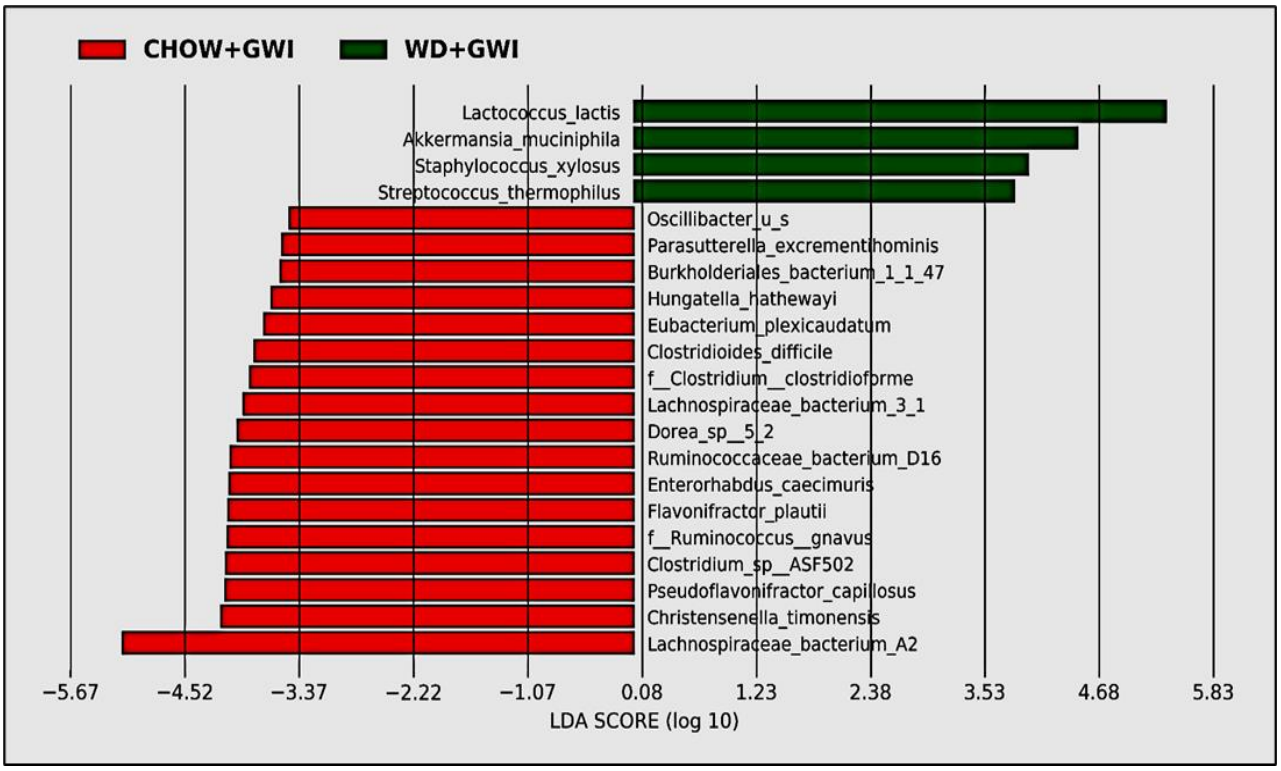

Supplementary Figure 1.1: Differential abundance (LEfSe analysis) plot. Differential abundance (LEfSe analysis) plot of significant OTU at species level between CHOW+GWI (GWI persistence in lean mice) and WD+GWI (GWI persistence in obese mice) groups. The LEfSe analysis is calculated using three methods: Kruskal-Wallis sum-rank test, Wilcoxon rank-sum test, and Linear Discriminant Analysis. Analysis meet $p \leq 0.05$ for Kruskal-Wallis and Wilcoxon tests and have an LDA score ≥ 2.0 or ≤ -2.0.

CHAPTER 2

Host gut resistome in Gulf War chronic multisymptom illness correlates with persistent inflammation

Funding: This study was supported by DoD-IIRFA Grant W81XWH1810374 to Dr.Saurabh Chatterjee, W81XWH-13-2-0072 to Dr. Kimberly Sullivan. and VA Merit Award I01CX001923-01 to Dr. Saurabh Chatterjee. Partially supported by a National Science Foundation EPSCoR Program OIA-1655740 to Dr. Jie Li. This work was supported in part by a Merit Review Award I01CX001923-01 from the United States (U.S.) Department of Veterans Affairs Clinical Sciences Research and Development Service. Disclaimer: The contents do not represent the views of the U.S. Department of Veterans Affairs or the United States Government.

Bose, D., Chatterjee, S., Older, E., Seth, R., Janulewicz, P., Saha, P., Mondal, A., Carlson, J. M., Decho, A. W., Sullivan, K., Klimas, N., Lasley, S., Li, J., & Chatterjee, S. (2022). Host gut resistome in Gulf War chronic multisymptom illness correlates with persistent inflammation. Communications biology, 5(1), 552. https://doi.org/10.1038/s42003-022-03494-7.

UNDERSTANDING THE ASSOCIATION BETWEEN ALTERED HOST GUT RESISTOME AND CHRONIC PATHOLOGY IN GULF WAR ILLNESS

ABSTRACT

Chronic multisymptom illness (CMI) affects a subsection of elderly and war Veterans and is associated with systemic inflammation. Here, using a mouse model of CMI and a group of Gulf War (GW) Veterans' with CMI we show the presence of an altered host resistome. Results show that antibiotic resistance genes (ARGs) are significantly altered in the CMI group in both mice and GW Veterans when compared to control. Fecal samples from GW Veterans with persistent CMI show a significant increase of resistance to a wide class of antibiotics and exhibited an array of mobile genetic elements (MGEs) distinct from normal healthy controls. The altered resistome and gene signature is correlated with mouse serum IL-6 levels. Altered resistome in mice also is correlated strongly with intestinal inflammation, decreased synaptic plasticity, reversible with fecal microbiota transplant (FMT). The results reported might help in understanding the risks to treating hospital acquired infections in this population.

Keywords: resistome, gut, antibiotic resistance gene, mobile genetic elements, whole genome shotgun sequencing

INTRODUCTION

Antibiotic resistance has emerged as a threat to public health on the local and global scale [59]. Resistance to antibiotics is conferred on bacteria by ARGs. All of the ARGs collectively form a resistome, and usually are carried by the opportunistic pathogens humans may encounter, thus increasing the risk of acquired infections that are difficult to treat with currently approved antibiotics [60]. The evolution of drug resistance in such pathogens is driven by chromosomal mutation and the acquisition of ARGs. Since most of the ARGs are linked to MGEs, they can transfer easily through horizontal gene transfer (HGT) among different clones, taxa and habitats [61].

The human gut harbors multiple commensal microorganisms and forms a good reservoir of ARGs. The gut environment predisposes ARG transfer, sometimes leading to emergence and spread of specific bacterial clones carrying genes of resistance and/or virulence. The most frequently reported genes are those directed against tetracycline, β-lactams, aminoglycosides, and glycopeptides. Tetracycline and glycopeptide resistant genes are most common in fecal samples of human [62]. On the other hand, human microbiota is also influenced by environmental factors like exposure to chemicals (pesticide, biocide) along with antibiotics that can alter the microbial composition and affect colonization resistance to pathogens. The selection pressure due to the exposure to such chemicals have resulted in emergence and increase of ARGs in both environment as well as gut microbiome [63]. A report from Sun et al., shows that changes in living environment can alter the human gut microbiota and resistome [62]. Another similar study by Gao et al. suggested that exposure

to Triclosan resulted in gut microbiome and resistome alteration that persisted over a prolonged exposure [64].

Numerous studies have reported that elderly and war Veterans often suffer from multiple syndromes with inflammatory phenotypes and are more susceptible to resistance against a large number of antibiotics [65]. Veterans have been reported to be resistant to amoxicillin, β-lactams, fluoroquinolones, methicillin and most importantly the carbapenem group of antibiotics [66]. In our present study, we aimed to analyze the ARG and MGE patterns in a Gulf War Illness (GWI) mouse model as well as in a cohort of GW Veterans. GWI is a complex multisymptom illness often closely associated with chronic multisymptom illnesses but now classified exclusively as GWI. The above referred condition are reported by a section Veterans who returned from Operation Desert Shield/Desert Storm in 1990–1991. Symptoms reported by the GW Veterans include fatigue, headache, cognitive dysfunction, musculoskeletal pain, respiratory and gastrointestinal dysfunctions more often characterized by a persistent systemic inflammation with higher IL-6, TNF-R1 and IL-1β blood levels. These symptoms have been linked to chemical exposures experienced during the war [1].

Several studies in preclinical mouse models of GWI have reported that exposure to chemicals such as insecticides and anti-nerve gas agents resulted in gut microbial dysbiosis. There has been a decrease in the relative abundance of several beneficial bacteria. Recently, a study in GWI Veterans also reported similar alteration of gut microbiom [24]. With reported studies on microbial dysbiosis patterns in the preclinical animal models as well as the GW Veterans well established, and with studies suggesting the potential of environmental chemicals in

increasing antibacterial resistance, we hypothesized that exposure to environmental pesticides and pyridostigmine bromide (PB) may also lead to an alteration of ARGs and MGEs expression, an important constituent of the gut resistome. In the present study we used both GW Veteran stool samples and fecal pellets from a GWI persistence mouse model administered with representative GW chemicals to study the alteration in gut resistome. We also studied the possible associations between gut resistome and GWI proinflammatory pathology by using a prolonged fecal microbiota transfer regimen that aimed to recolonize the mouse gut with microbiota from a healthy donor.

MATERIALS AND METHODS

Per and PB were purchased from Sigma-Aldrich. Primary antibodies anti-interleukin-1β (IL-1β), anti-brain derived neurotrophic factor (BDNF) were purchased from Santacruz Biotechnology (Dallas, TX, USA). Species specific biotinylated secondary antibodies and streptavidin-HRP (Vectastain ABC Kit) were purchased from Vector laboratories (Burlingame, CA, USA). All other chemicals used in the present study were purchased from Sigma unless specified. Animal tissues were sent for paraffin embedding and sectioning to AML Laboratories (St. Augustine, FL, USA). Fecal samples from experimental mice groups and GW Veterans were sent to COSMOSID (Germantown, MD, USA) for whole-genome sequencing.

Mouse model of Gulf War Illness.

After 1 week of acclimatization, the mice were randomly distributed into three groups. The first group received vehicle (0.6% dimethyl sulfoxide) for 2 weeks and were denoted Control (n = 11). The second and third mice groups denoted GWI (n = 11) and GWI_FMT (n = 6) were

treated with Per [200 mg/kg body dissolved in DMSO and phosphate buffer saline(PBS)] and PB (2 mg/kg dissolved in PBS) by oral gavage tri-weekly for 15 days. After the 2 weeks of GW chemical exposure, GWI group mice were allowed to persist for 20 weeks. Fecal microbiota transplant was administered in GWI_FMT after GW chemical exposure. 100 mg of fecal pellets were collected from healthy C57BL/6 J mice of same age group as the GWI_FMT mice. The pellets were homogenized in 1 ml of PBS and centrifuged at 3000 × g for 5 min. 100 µl of supernatant was dosed in each mouse on alternate days of a week for 20 weeks [67](Fig. 2.1a).

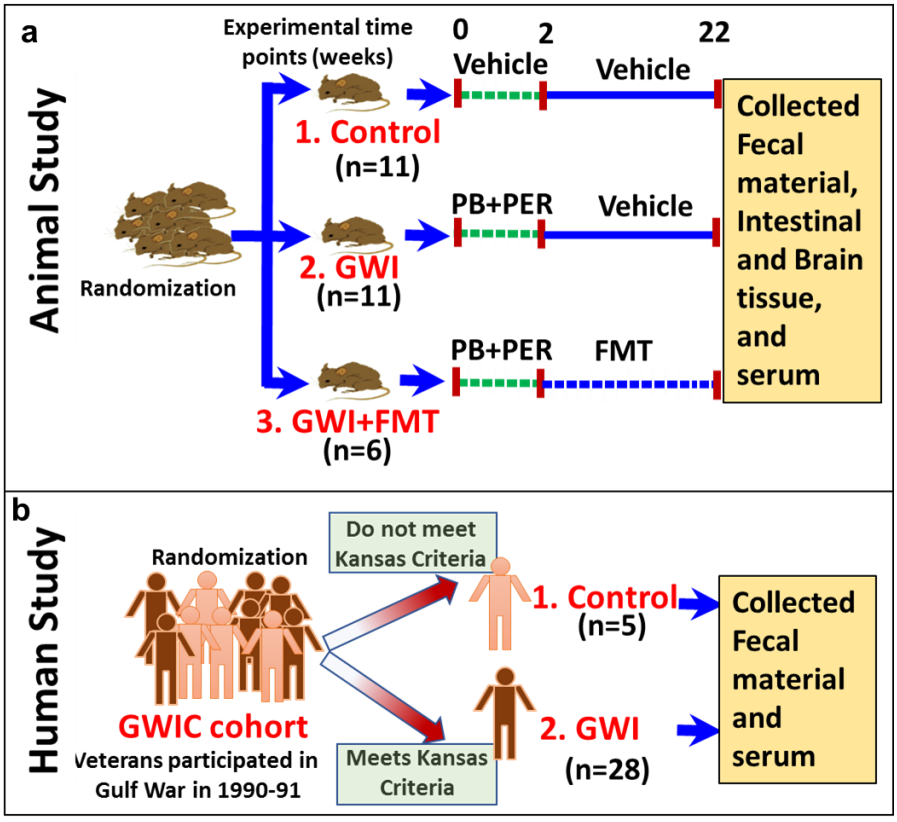

Figure 2.1. a Experimental mouse model of Gulf War Illness (GWI). b Study design of Veteran participants in Boston Gulf War Illness Consortium (GWIC) based on Kansas GWI criteria.

Human subjects: GW Veterans with GWI and controls

The Boston Gulf War Illness Consortium (GWIC) performs preclinical and clinical studies to understand the pathophysiology behind the complex symptoms in GW Veterans to aid in designing of possible therapeutic strategies. Veterans were included as participants in GWIC studies based on requirement that they had to be deployed in the GW i.e., from August 1990 to July 1991. The GWIC used the Kansas GWI criteria as the case definition which requires the Veterans to have symptoms in 3 out of 6 broadly defined group of symptoms (neurological, pain, gastrointestinal, skin, respiratory, fatigue) to meet criteria of CMI in GW Veterans known as Gulf War Illness (GWI) [6]. GW Veterans who do not meet Kansas criteria are deemed the control group.

The Veterans who participated in the GWIC, underwent multiple tests including neuropsychological assessments, health surveys, biological specimen collection, and brain imaging. The present study was conducted as a GWIC call-back study in which we aimed to reassess 150 of the GWIC participants. For this study, data from the first 33 recruited subjects from the microbiome call-back study has been analyzed. The recruitment of participants was via telephone on completion of GWIC study protocol. After filling out a brief questionnaire regarding screening, the participants were sent a stool collection kit which was then shipped back to the study investigators (Fig. 2.1b).

Collection of demographical, deployment exposure, and health symptom information from GWIC participants

The full GWIC protocol has been previously published in Steele et al., 2021 . Briefly, the GWIC participants had to answer to surveys regarding demographics and health condition which

included Multi-dimensional Fatigue Inventory (MFI-20), Pittsburg Sleep Quality Index and McGill Pain Inventory [68]. The Structured Neurotoxicant Assessment Checklist (SNAC) and Kansas Gulf War and health Questionnaire and Kansas Gulf War Experiences surveys were given to obtain details about self-reported exposures. The survey regarding health condition provided the details if the participants had an ascertained diagnosis of the medical conditions reported by them [69]. As part of the call-back study, the Veterans also filled out questionnaires about their current and recent gut health and use of antibiotics or probiotics.

Collection of stool samples from participants

The GWIC participants of the microbiome study were mailed a Second Genome stool collection kit (Second Genome, San Francisco, CA, USA). The kit was a self-collecting kit which contained a bar-coded vial with stabilizing solution for long term preservation of nucleic acids in stool during transportation and storage. Once received from the subjects, the stool samples were stored at −20 °C and upon collection of significant sample numbers, they were sent for WGS by COSMOSID. The protocol was approved by Institutional Review Board at Boston University School of Public Health (proposal no. GW170068) on 4/15/2021. Sample collection from GWIC participants were done following all ethical guidelines and informed consent was also obtained.

DNA extraction and whole-genome shotgun sequencing

Briefly, the total DNA from mouse and human samples were isolated and purified using ZymoBIOMICS Miniprep kit. DNA was quantified using Qubit dsDNA HS assay (Thermofisher, Waltham, MA, USA). Illumina Nextera XT library preparation kit was used with modifications for preparing DNA libraries. Illumina HiSeq 4000 and Illumina NextSeq 550 platform was

used to perform WGS for mice and human samples respectively, following protocol optimized by vendor. 2x150bp of read length and an average insert size of 1400 bp were used for sequencing. DNA libraries were prepared using the Nextera XT DNA Library Preparation Kit (Illumina) with Nextera Index Kit (Illumina) for mice and IDT Unique Dual Indexes for human samples, with total DNA input of 1 ng. Genomic DNA was fragmented using a proportional amount of Illumina Nextera XT fragmentation enzyme. Combinatory dual indexes were added to each sample followed by 12 cycles of PCR to construct libraries. DNA libraries were purified using AMpure magnetic Beads (Beckman Coulter) and eluted in QIAGEN EB buffer. DNA libraries were quantified using Qubit 4 fluorometer and Qubit™ dsDNA HS Assay Kit. Upon data arrival, raw data were backed up to Amazon AWS and run through fastqc and a multiqc report was generated83 The multiqc report was checked to ensure read depth thresholds were met, and that there were no abnormalities with read quality, duplication rates, or adapter content. Taxonomic results were checked on the COSMOSID-Hub Microbiome platform to ensure there were contamination or barcoding issues.

We obtained a total of 536.92 million (M) sequencing reads with per sample averages of 9.33 M reads in the Control samples, 8.49 M reads in the GWI samples, 10.12 M reads in the GWI_FMT samples, 11.32 M reads in the Hum_Control samples, and 11.17 M reads in the Hum_GWI samples.

Metagenomic analysis and assembly

MetaPhlAn v3.0.784 was used to profile the taxonomic composition of each sample with default parameters. The resulting relative abundance tables were then merged with the

provided python tool, “merge_metaphlan_tables.py”. A custom python script was used to filter the data to contain only species level identifications and prepare the operational taxonomic unit (OTU) table for statistical analysis. The metaWRAP v1.3.285 pipeline was used to process and assemble raw sequencing reads from each sample. First, the “read_qc” module was used with default parameters to trim sequencing adapters and bases with low PHRED scores. To decontaminate the data, reads mapping to the human reference genome GRCh38.p12 (RefSeq Acc: GCF_000001405.38) and the mouse reference genome GRCm38.p6 (RefSeq Acc: GCF_000001635.26) were removed by the metaWRAP “read_qc” module. After decontamination and quality control, we recovered a total of 532.43 million (M) sequencing reads with per sample averages of 9.22 M reads in the Control samples, 8.24 M reads in the GWI samples, 9.96 M reads in the GWI_FMT samples, 11.28 M reads in the Hum_Control samples, and 11.13 M reads in the Hum_GWI samples. Decontaminated reads were used for de novo assembly using metaSPAdes86 as contained in the metaWRAP “assembly” module with default parameters. Resulting contigs were binned by the “binning” module which uses three binning methods, metaBAT2 v2.12.187, MaxBin2 v2.2.688, and CONCOCT v1.0.089 to produce three sets of bins. The “bin_refinement” module was used to refine these three bin sets to produce a single set of best bins. Finally, the single bin set was used by the “bin_reassembly” module which extracts the reads mapping to each bin and uses them for a second round of de novo assembly to improve the completion and reduce the contamination of the bins.

Antimicrobial resistance gene family and MGE identification

Contigs produced through metaWRAP were used for open reading frame (ORF) finding using MetaProdigal v2.6.390 with parameters "-c -p meta". ORFs were then clustered with CD-HIT v4.8.191,92 with parameters "-c 0.95 -s 0.90" corresponding to 95% sequence identity threshold over 90% of the shorter ORF length. Next, ORFs were mapped to the Comprehensive Antibiotic Resistance Database (CARD) v3.1.093 and a recently published custom Mobile Genetic Element (MGE) database composed of 278 distinct genes and over 2000 unique gene sequences using the tool "nhmmer" from the HMMER v3.3.194 software with parameters "-E 0.001 -incE 0.001" corresponding to an e-value threshold of 0.001 for matches [64]. A custom python script was used to filter multiple hits to select the single best hit for each ORF. Finally, Microsoft Excel was used to generate count data for ARGs and MGEs.

Laboratory methods

Immunohistochemistry

The fixed mouse small intestine and frontal cortex tissues were paraffin embedded and 5 μm thick sections were done for immunohistochemistry. Deparaffinization were performed following previous protocol. Antigen retrieval was performed using epitope retrieval solution and steamer (IHC world, Woodstock, MD, USA). Three percent hydrogen peroxide was used for blocking endogenous peroxidase activity for 20 mins. Serum blocking was performed using 10% goat serum for 1 h. Tissue sections were incubated with primary antibodies for IL-1β and BDNF at 1:200 dilution for overnight in humified chamber at 4 °C. After incubation, the tissue sections were washed three times with PBS containing 0.05% Tween 20 solution. Tissues were probed with species specific biotinylated antibodies (1:200 dilution) followed by incubation with horse radish conjugated streptavidin (1:500 dilution).

3,3'-diaminobenzidine was used as chromogenic substrate solution and counterstaining was performed using Mayer's hematoxylin. The stained tissues sections were mounted using Aqua Mount (Lerner Laboratories, Kalamazoo, MI, USA). The images were acquired using Olympus BX63 microscope (Olympus, Center Valley, PA, USA). Morphometry was performed using Cellsens Software from Olympus America (Center Valley, PA, USA).

Quantitative RT-PCR

Quantitative RT-PCR (qRT-PCR) was performed to measure ARG expression in DNA extracted from mouse and human stool samples. Gene specific primers were designed using Primer3 (version 0.4.0) and IDT, purchased from Sigma (St. Louis, MO, USA) (Supplementary Table 2.1). SYBR Green Supermix (BioRad, Hercules, CA, USA) was used in CFX96 thermal cycler (BioRad, Hercules, CA, USA). The samples (both mouse and human) were run in triplicates for each gene. Ct or threshold cycle values of all ARG genes were normalized with 16 S as internal control. $2-\Delta\Delta ct$ method was used to calculate the relative fold change of the ARGs.

ELISA

Serum IL-6 level was estimated using serum collected from the mice groups using commercially available kit from Proteintech (Rosemont, IL, USA). Serum IL-6 of Veteran participants in this study was measured using commercially available ELISA kit from Abcam (Boston, MA, USA). The ELISA was performed according to the manufacturer's protocol.

Statistical analysis and reproducibility

Analyses were performed using R v3.6.3 (1). ARG, MGE, and OTU count data were normalized based on library size using the "estimateSizeFactors" function from the "DESeq2" package95 with the parameters "type = poscounts". Normalized count data were then log transformed with the base R function "log2". Permutational analysis of variance (PERMANOVA) was calculated using the "adonis" function from the package "vegan" (2) with Bray-Curtis dissimilarity and 9999 permutations. Welch two-sample t-test was implemented using the base R function "t-test" with the parameters "conf.level = 0.95, alternative = two.sided" indicating 95% confidence level and two-tailed testing. PCA ordinations of ARG and Taxonomy abundance data were performed using the "rda" function from "vegan". Procrustes analysis was performed using PCA ordinations with the function "protest" from "vegan" with 9999 permutations. Principle coordinate analysis (PCoA) was performed with the "pcoa" function from the "ape" package with Bray-Curtis dissimilarity. Statistical analysis for q-RTPCR, immunohistochemistry and ELISA was done using Prism (Graphpad, San Diego, CA). One-way ANOVA was used for comparing between the three mice groups and Welch's t-test was used for comparison between the Veteran groups for statistical analysis of immunohistochemistry and ELISA. Chao1 α-diversity was calculated using the "chao1" function from the "fossil" package. Correlation analyses between α-diversity and selected biomarkers were performed using Pearson's correlation implemented by the base R function "cor". All visualizations were rendered using the "ggplot2" package unless otherwise described. For all analyses, $p < 0.05$ was considered statistically significant, and data are represented as mean ± standard error of mean or mean± standard deviation. Each figure and data set has been provided with individual P-values for better clarity.

RESULTS

Characterization of antimicrobial resistance in mouse fecal samples

We performed whole-genome shotgun sequencing, metagenomic assembly, and functional gene annotation on fecal samples collected from three groups (Control, GWI, and GWI_FMT) to construct ARG profiles associated with the GWI mice model and the FMT treatment. We detected 455 unique ARGs across all groups with 538 ± 16 (mean ± standard error) total ARGs in Control, 514 ± 15 total ARGs in GWI, and 567 ± 19 total ARGs in GWI_FMT. Performing PERMANOVA revealed a significant deviation in the ARG profiles across sample groups ($p = 0.0001$, $R2 = 34\%$). This indicated that the resistome profile of each sample group were distinct from each other. To get a clearer picture of the specific changes in the resistome, we performed differential abundance analysis of the ARGs to identify significantly changed genes (DESeq2, negative binomial generalized linear models (GLMs), Wald's test, $p < 0.05$). Comparing these selected ARGs between sample groups, we observed a significant decrease in their sum relative abundances from Control to GWI ($p = 0.02021$, Welch two-sample t-test) and a significant increase when comparing GWI to GWI_FMT group ($p = 0.00005425$, Welch two-sample t-test, Fig. 2.2a).

Looking to connect ARG changes with gut microbiome composition, we performed procrustes rotation of the principal component analyses (PCAs) of the resistome and microbiome profiles which showed a significant correlation ($p = 0.0001$, PROTEST, $M2 = 0.4302$, Fig. 2.2b), confirming that resistome changes were in fact linked to microbial dysbiosis. Further, principal coordinate analysis of ARG profiles showed clustering of profiles according to sample group with the first two axes accounting for 49% of the variance

in the ARG profiles. The GWI_FMT group formed an independent cluster from both GWI and Control groups (ape, pcoa, PCoA1 accounting for 34% of variance in ARG profile, Fig. 2.2c).

We also examined the profiles of MGEs constituting the mobilome in each sample group. We detected 77 unique MGEs evenly distributed across all groups with 77 ± 3 total MGEs in Control, 74 ± 2 total MGEs in GWI, and 81 ± 3 total MGEs in GWI_FMT. PERMANOVA showed significant differences in the mobilomes with respect to sample group, supporting the observed deviations in resistome profile which we previously linked to changes in the microbiome composition ($p = 0.0001$, $R2 = 24\%$). We selected differentially abundant MGEs (DESeq2, negative binomial GLMs, Wald's test, $p < 0.05$), compared their sum relative abundances as previously described for ARGs. The changes observed in the sum relative abundances between Control to GWI ($p = 0.4717$, Welch two-sample t-test) and between GWI and GWI_FMT ($p = 0.1119$, Welch two-sample t-test, Fig. 2.2d) were not statistically significant. Hence, on administration of representative GW chemicals in GWI mice model, we did not see an increase in the relative abundance of ARGs and the changes observed in the relative abundances of MGEs were not significant.

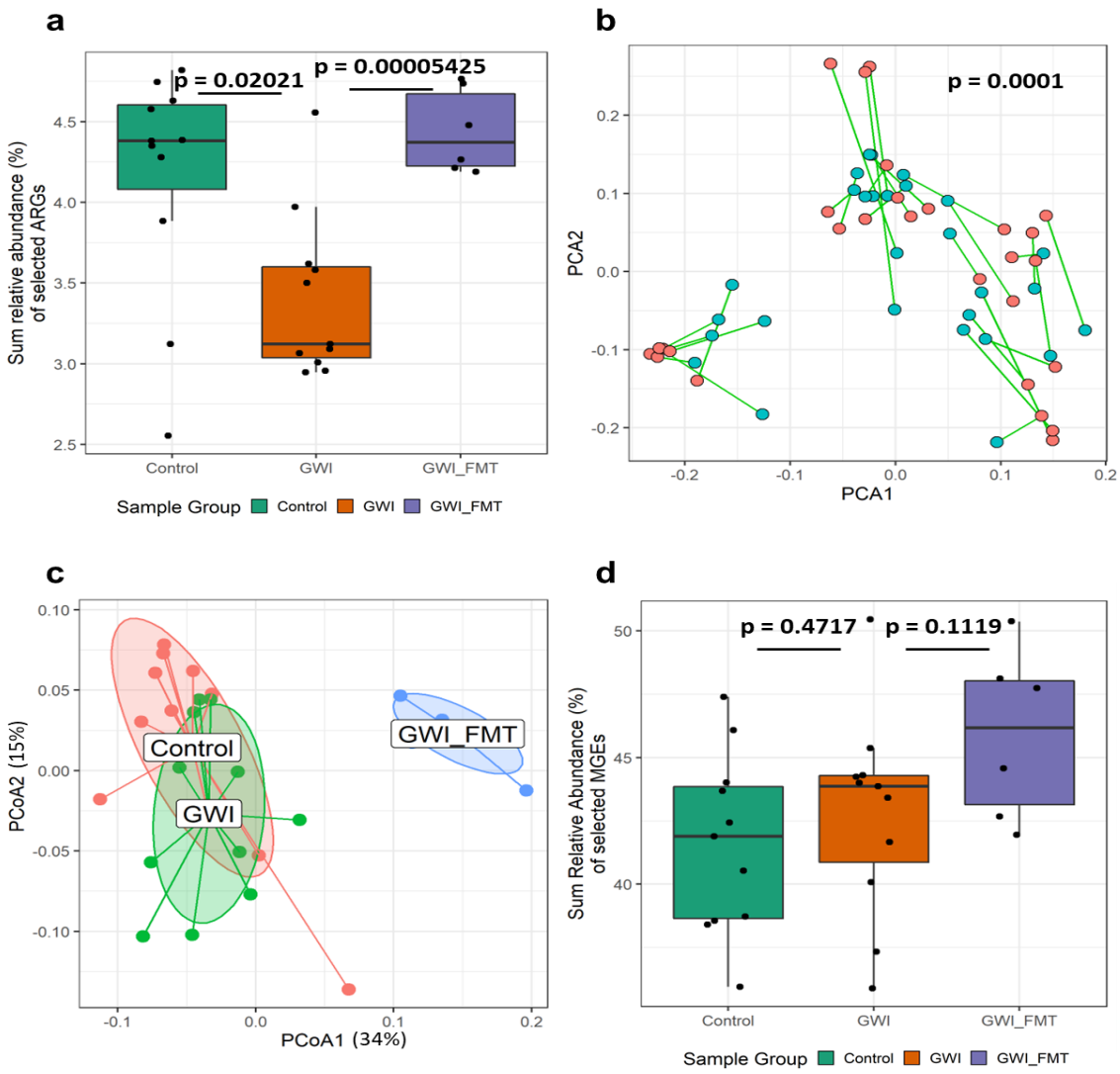

Figure 2.2. Distribution of ARGs and MGEs in persistence GWI mouse models. a Box plots showing sum relative abundance (%) of selected antibiotic resistance genes (ARGs) in Control (adult C57BL/6 J mice administered with vehicle, n = 11 biologically independent samples), GWI (adult C57BL/6 J mice administered with GW chemicals, n = 11 biologically independent samples) and GWI_FMT (adult C57BL/6 J mice group exposed to GW chemicals followed by Fecal Microbiota Transfer (FMT) treatment, n = 6 biologically independent samples). Median values of 4.38% in Control, 3.12% in GWI, and 4.37% in GWI_FMT indicated by solid black lines. b Procrustes rotation analysis comparing resistome (blue) and microbiome (red) changes using PCA ordinations, (X-axis: PCA1, Y-axis: PCA2, PROTEST, M2 = 0.4302, p = 0.0001). c PCoA of Bray-Curtis dissimilarity between ARG and Taxa profiles across sample groups. Principal coordinate axes PCoA1 (34%) and PCoA2 (15%) are calculated to explain 49% of variance detected. Lines connect points from the center of gravity of each sample group. d Box plots showing sum relative abundance (%) of selected mobile genetic elements (MGEs) Control, GWI and GWI_FMT. Boxes in the box plots indicate interquartile range. Error bars in the box plots extend to the most extreme values within 1.5 times the interquartile range. Outlier data points are represented by black dots drawn

outside of the box plot. p-values were determined using PROTEST or Welch's t-test where $p < 0.05$ was considered statistically significant.

Distribution of ARGs and MGEs across the different groups in GWI mouse model

We detected multiple ARGs imparting resistance to antimicrobial classes which have been marked as highly important and critically important by the World Health Organization (WHO) (AGISAR, 2018). In our analysis, glycopeptide resistance genes were the most abundant ARG observed across all three mice groups (not statistically significant). Using differential abundance analysis, we identified the individual ARGs which were significantly altered (DESeq2, negative binomial GLMs, Wald's test, $p < 0.05$). Among these ARGs, *vanXYN* (ARO: 3002969), and *adeS* (ARO: 3000549) were significantly increased in the GWI group compared to the Control group (DESeq2, negative binomial GLMs, Wald's test, $p < 0.05$, Fig. 2.3a). This result is suggestive of a potential effect of GW chemicals on the individual ARGs. FMT treatment decreased the abundance of *vanXYN* and *adeS* genes as observed in the GWI_FMT group over the GWI group, however it was not statistically significant. Interestingly, there were 6 unique ARGs which were only present in the mouse GWI group.

When comparing the resistant drug classes across the three groups, it was observed that glycopeptide antibiotics followed by aminoglycosides, peptide, phenicol, and diaminopyrimidine antibiotics were among the resistant drug classes that were detected in the 3 experimental mice groups ($p = 0.0001$, PERMANOVA, $R2 = 33\%$, Fig. 2.3b). Based on their mechanisms of resistance, antibiotic efflux, antibiotic target alteration, antibiotic target protection, and antibiotic inactivation mechanisms were among the antibiotic resistance

mechanisms that were detected in the 3 experimental mice groups ($p = 0.0001$, PERMANOVA, $R2 = 31\%$, Fig. 2.3c).

ARGs have a high propensity to mobilize from one bacterium to another through the MGEs by horizontal gene transfer9. We thus investigated the presence of different MGEs and MGE types among the three mice groups. We observed that relative abundances of *ISCR8, ISCrsp1*, and *Tn916-orf6* increased (not statistically significant) in the GWI group compared to Control but significantly decrease in the GWI_FMT group (DESeq2, negative binomial GLMs, Wald's test, $p < 0.05$, Fig. 2.3d). Transposase, insertional sequences *ISCR* and *integrase* were among the abundant MGE types detected in all the samples across the 3 mice groups (Fig. 2.3e). Multivariate analysis of the MGE type profiles showed a significant deviation and correlation pattern that was dependent on sample groups ($p = 0.0002$, PERMANOVA, $R2 = 33\%$).

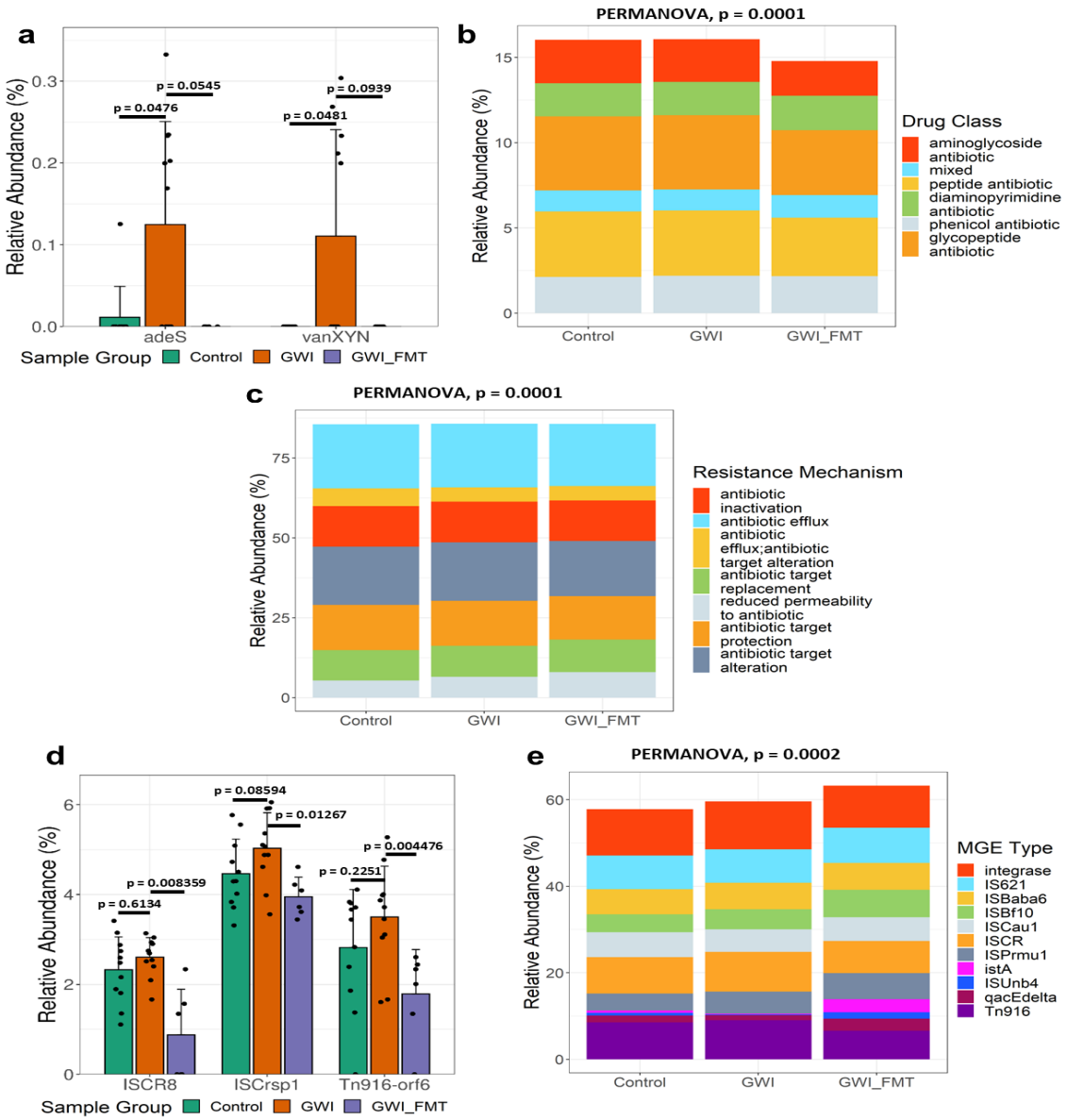

Figure 2.3. Classification of selected ARGs and MGEs in persistence GWI mouse model. a. Grouped bar graph showing relative abundance (%) of selected ARGs in Control (adult C57BL/6 J mice administered with vehicle, n = 11 biologically independent samples), GWI (adult C57BL/6 J mice administered with GW chemicals, n = 11 biologically independent samples), and GWI_FMT (adult C57BL/6 J mice group exposed to GW chemicals followed by FMT treatment, n = 6 biologically independent samples) groups. Stacked bar analysis of relative abundance (%) of b drug classes resistances and c mechanisms of resistance. d Grouped bar graph showing relative abundance (%) of selected MGEs in Control, GWI and GWI_FMT groups. e Stacked bar analysis of relative abundance (%) of MGE types. Data represented as Mean±SD (SD: Standard deviation) for the bar graphs. p-values were determined using Wald's test or PERMANOVA where $p < 0.05$ was considered statistically significant.

Demographic Information of GW Veterans

In this study, we obtained samples from 33 GW Veterans. Out of these 33 participants, 28 met the required Kansas GWI Criteria and were categorized into the Hum_GWI group. The remaining 5 participants did not meet the criteria and were considered as the Hum_Control group. There were no major differences based on age, height, weight, or body mass index of the participants in both groups (Table 2.1). In the Hum_GWI group, 61% of the participants reported diarrhea and nausea, 57% reported abdominal pain or cramping, 46% reported irritable bowel syndrome (IBS). In the Hum_Control group, there were no reports of diarrhea or IBS, but 40% of participants reported nausea and 20% reported abdominal pain or cramping.

	Hum_Control	**Hum_GWI**
N	5	28
Age (years), mean (SD)	55.5 (4.8)	53.9 (5.7)
Height (In), mean (SD)	69.8 (4.6)	68.0 (3.0)
Weight (Lbs), mean (SD)	243.0 (35.3)	214.9 (45.4)
BMI, mean (SD)	35.3 (5.7)	32.7 (6.4)
Average Number of GI symptoms, mean	0.6	2.9
Diarrhea, n (%)	0 (0)	17 (61)
Nausea or Upset Stomach, n (%)	2 (40)	17 (61)
Diarrhea, n (%)	1 (20)	16 (57)
Nausea or Upset Stomach, n (%)	0 (0)	13 (46)
Other Gastrointestinal Disorder, n (%)	0 (0)	15 (54)

Table. 2.1. Demographic Information of GWI Veterans

Characterization of antimicrobial resistance gene in Veteran samples

We studied the gut resistome pattern in GW Veterans. We performed whole-genome shotgun sequencing, metagenomic assembly, and functional gene annotation as with the mouse samples. We detected 604 unique ARGs with 224 ± 11 and 238 ± 6 total occurrences in the Hum_Control group and Hum_GWI groups respectively. Comparing the ARG profiles of the

two groups, we observed only minor and insignificant deviation in the resistome profiles between the two groups ($p = 0.2826$, PERMANOVA, $R2 = 3.4\%$). When investigating relative abundance of significantly changed ARGs (DESeq2, negative binomial GLMs, Wald's test, $p < 0.05$), we observed that the sum relative abundance of selected ARGs increased but not statistically significant in the Hum_GWI group compared to the Hum_Control group ($p = 0.08362$, Fig. 2.4a). Procrustes analysis showed a significant correlation of bacterial taxa and the ARGs ($p = 0.0001$, PROTEST, $M2 = 0.6665$, Fig. 2.4b). PCoA analysis showed clustering of the Hum_Control and Hum_GWI groups with major overlap on the first two axes accounting for only 24% of the total variance in the dataset (Fig. 2.4c). Considering the minor divergence indicated by PERMANOVA and the low proportion of explained variance, this result might have stemmed from the increased complexity of the human gut microbiome compared to that of our mouse model.

When studying the transferability, we identified 110 unique MGEs across both groups with 80 ± 5 and 86 ± 2 total MGEs in the Hum_Control group and the Hum_GWI groups respectively. We observed minor variation in the MGE profiles of the two groups which was shown to not be significantly dependent on the sample group variable ($p = 0.3757$, PERMANOVA, $R2 = 3.3\%$). The relative abundance of selected MGEs were significantly increased in Hum_GWI group compared to the Hum_Control ($p = 0.01677$, Welch two-sample t-test, Fig. 2.4d).

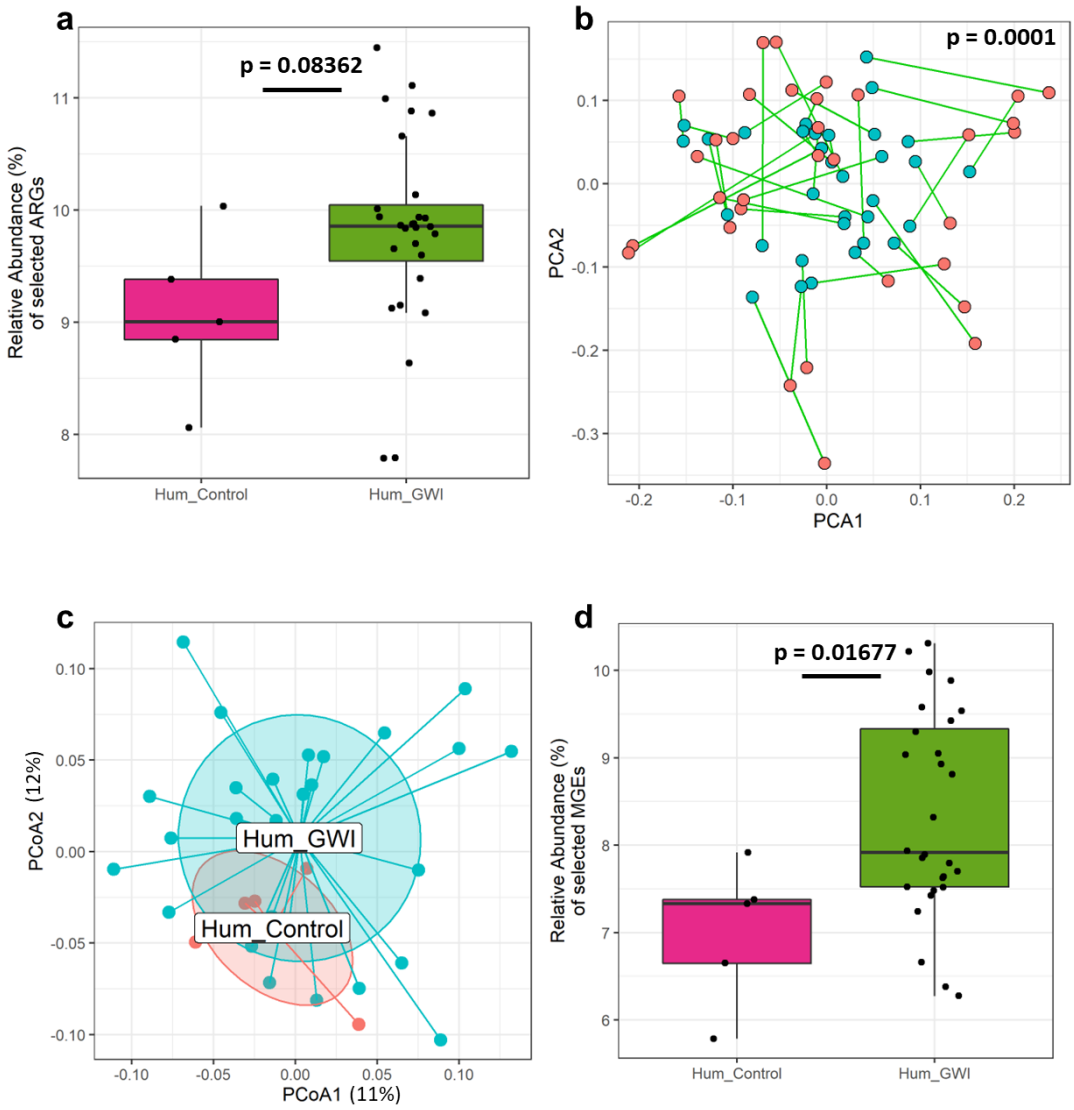

Figure 2.4. Distribution of ARGs and MGEs in GWI Veteran groups. a Box plot showing relative abundance (%) of ARGs in Hum_Control (Veteran group without GWI symptom, n = 5 biologically independent samples) and Hum_GWI (Veteran group with GWI symptom, n = 28 biologically independent samples). Median values of 9.0% in Hum_Control and 9.86% in Hum_GWI are indicated by solid black lines. b Procrustes rotation analysis comparing resistome (blue) and microbiome (red) changes using PCA ordinations, (X-axis: PCA1, Y-axis: PCA2, PROTEST, M2 = 0.6665, p = 0.0001). c PCoA of Bray-Curtis dissimilarity between ARGs and Taxa. Principal coordinate axes PCoA1(12.7%) and PCoA2 (11.5%) account for 24.2% of detected variance. d Box plot showing relative abundance (%) of selected MGEs in Hum_Control and Hum_GWI. Boxes in the box plots indicate interquartile range. Error bars in the box plots extend to the most extreme values within 1.5 times the interquartile range. Outlier data points are represented by black dots drawn outside of the box plot. p-values were determined using PROTEST or Welch's t-test where $p < 0.05$ was considered statistically significant.

Distribution of selected ARGs and MGEs in human samples

Our results showed that the relative abundance of individual ARGs was significantly higher in Hum_GWI group compared to Hum_Control group. The glycopeptide resistance gene was found to be the most abundant ARG in both groups of GW Veteran samples (not statistically significant). Based on differential abundance analysis, we found that the abundance of 3 ARGs were significantly increased in the Hum_GWI group compared to the Hum_Control group (DESeq2, negative binomial GLMs, Wald's test, $p < 0.05$, Fig. 2.5a).These ARGs were *lra-3* (ARO: 3002510), *mexD* (ARO: 3000801) and *novA* (ARO: 3002522). *Agrobacterium fabrum chloramphenicol acetyltransferase (afca)* (ARO: 3004451) increased in Hum_GWI but it was not statistically significant. These ARGs confer resistance against multiple critically important antibiotics which are used as human medicine (WHO, AGISAR 2018). Furthermore, there were 250 unique ARGs found in Hum_GWI group which were absent in Hum_Control group. Changes in the drug classes and antibiotic resistance mechanism were not statistically significant between the 2 groups (Fig. 2.5b, c).

The abundance of individual MGEs were also altered in Hum_GWI group compared to Hum_Control group. The MGE *tniB* significantly increased in the Hum_GWI group ($p = 0.021$, DESeq2, negative binomial GLMs, Wald's test, Fig. 2.5d). Although a change in the relative abundance of *istB* and *ISCre2* was observed in Hum_GWI group over the Hum_Control group, it was not statistically significant. Among the MGE types, transposons, and most importantly insertional sequence *ISCR* was increased in the Hum_GWI group (not statistically significant, Fig. 2.5e). *ISCR* has been reported to cause increased mobilization of ARGs among bacteria, presence of this type of mobilome in GW Veterans raises the concern of increased antibiotic

resistance33. According to our procrustes analysis in GW Veteran samples, changes in the resistome are correlated with the altered gut microbiome, hence increases in MGEs like *ISCR* might increase the chances of ARG mobilization which could be fatal for the GW Veteran health due to increase in resistance to antibiotics. Multivariate analysis of the MGE class profiles revealed minor deviation between sample groups which was not significant (p = 0.1422, PERMANOVA, R2 = 4.5%). Further investigations in GW Veterans are required to prove the resistance against the individual ARGs.

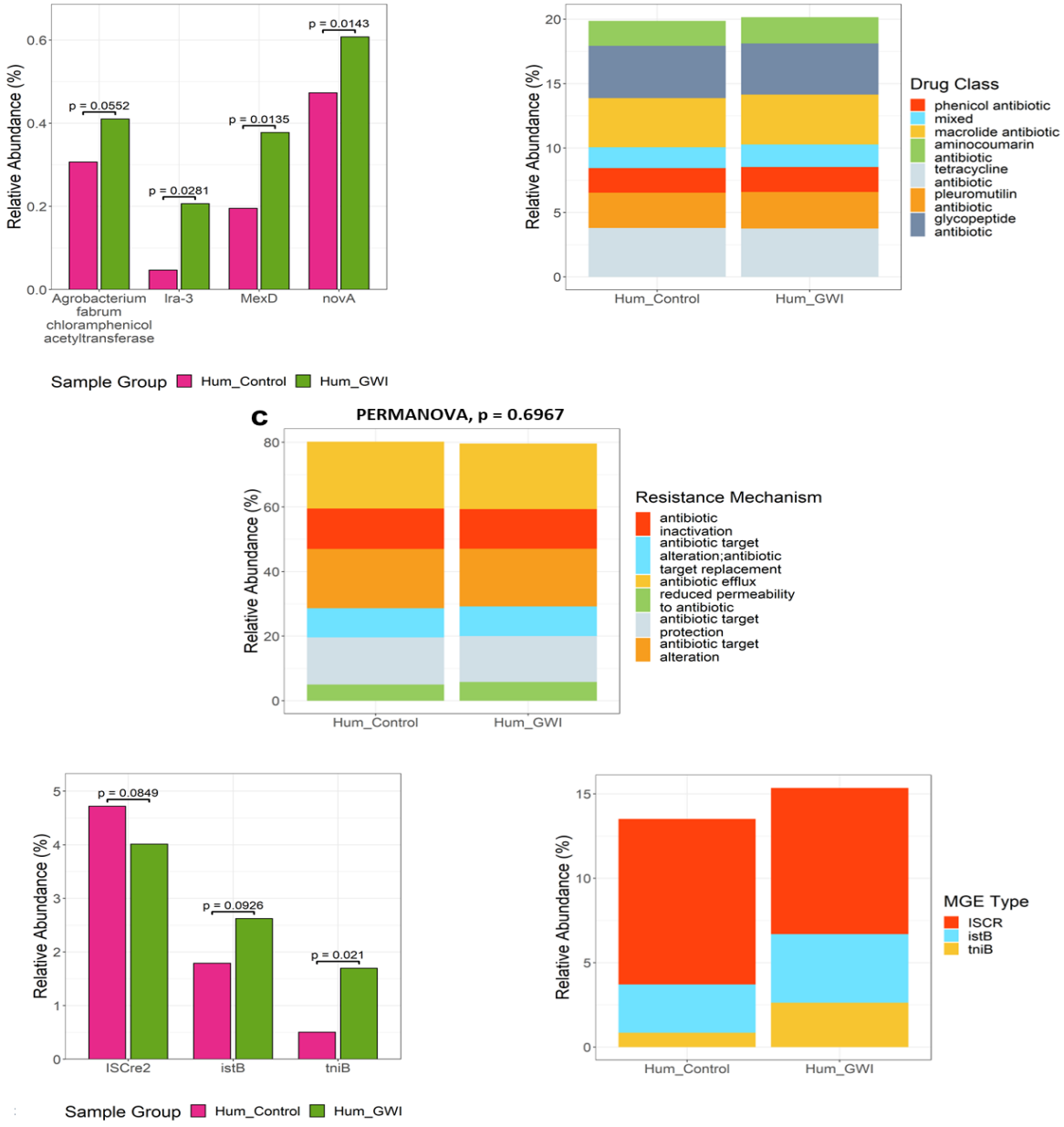

Figure 2.5. Classification of selected ARGs and MGEs in GWI Veterans groups. a Grouped bar graph showing relative abundance (%) of selected ARGs in Hum_Control (Veteran group without GWI symptom, n = 5 biologically independent samples) and Hum_GWI (Veteran group with GWI symptom, n = 28 biologically independent samples). Stacked bar analysis of relative abundance (%) of b drug classes and c mechanisms of resistance. d Grouped bar graph showing relative abundance (%) of selected MGEs in Hum_Control and Hum_GWI groups. e Stacked bar analysis of relative abundance (%) of MGE types. Data represented as Mean±SD (SD: Standard deviation) for the bar graphs. p-values were determined using Wald's test or PERMANOVA where $p < 0.05$ was considered statistically significant.

Expression study of antimicrobial resistance genes in mouse and GW Veteran samples by q-RTPCR analysis

To confirm the expression of the ARGs observed by the gene annotation studies in the previous sections (differential abundance by DESeq2), we performed q-RTPCR analysis of the same ARGs, using DNA extracted from the mouse (Fig. 2.6a) and GW Veteran fecal samples (Fig. 2.6b).

In the mouse samples, expression of *vanXYN* was significantly increased by 17.65-fold in the GWI group compared to the Control group ($p < 0.001$, two-way ANOVA with Bonferroni's post hoc test). Expression of *vanXYN* (12.87 fold compared to the Control group) significantly decreased in the GWI_FMT group compared to the GWI group ($p = 0.002$, two-way ANOVA with Bonferroni's post hoc test). Similarly, expression of *adeS* was significantly increased by 23.59-fold ($p < 0.001$, two-way ANOVA with Bonferroni's post hoc test) in the GWI group compared to the Control group. The expression of *adeS* (12.63 fold compared to the Control group) significantly decreased ($p < 0.001$, two-way ANOVA with Bonferroni's post hoc test) in the GWI_FMT group compared to the GWI group. Although q-RTPCR analysis results showed similar trend like the gene annotation study, i.e., significant increase in expression of the respective ARGs in the mice GWI group and a decrease (statistically significant by q-RTPCR) in GWI_FMT group, further experimental proof would be required to confirm that FMT administration indeed was successful in decreasing the individual ARG expressions.

In the GW Veteran samples, expression of *mexD, novA, and afca* was significantly increased by 3.68, 5.59, and 2.81-fold respectively in the Hum_GWI group compared to the Hum_Control group (for *mexD* p, for <0.001 *novA* $p < 0.001$, for *afca* $p < 0.001$ between Hum_Control and Hum_GWI group, two-way ANOVA with Bonferroni's post hoc test, Fig. 2.6b).

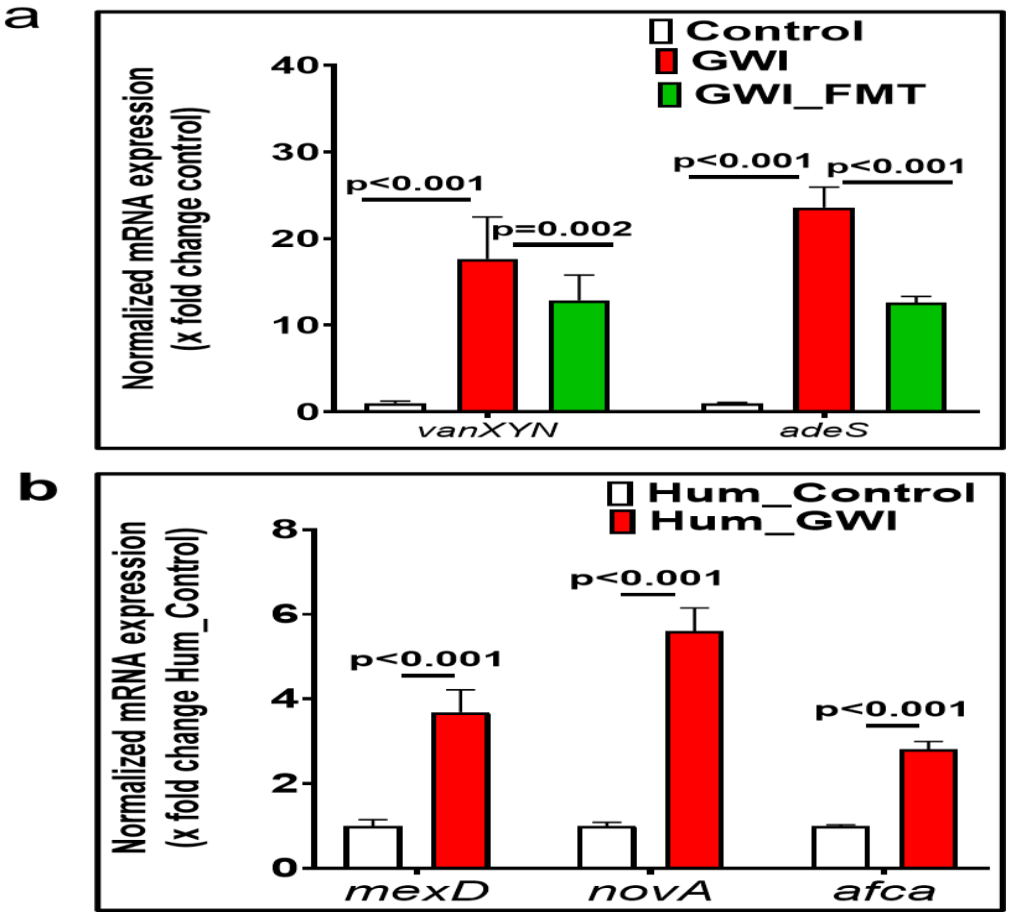

Figure 2.6. Relative expression levels of antimicrobial resistance genes. Relative mRNA expression of ARGs. a Between mouse experimental groups Control (n = 11 biologically independent samples), GWI (n = 11 biologically independent samples) and GWI_FMT (n = 6 biologically independent samples). b Between GW Veteran groups Hum_Control (n = 5 biologically independent samples) and Hum_GWI (n = 28 biologically independent samples). The mRNA expression was calculated as fold change against control (in Fig. 5a) and against Hum_Control (in Fig. 5b) Data are represented as mean ± SEM (SEM: Standard Error Mean). p-values were determined using by two-way ANOVA with Bonferroni's post hoc test for GWI mice groups and GW Veteran groups where $p < 0.05$ was considered statistically significant.

Gastrointestinal, systemic, and neuronal inflammation and its association with ARGs and Drug Classes in mouse GWI model samples and GW Veteran samples

Gastrointestinal and neuronal inflammation is reported in GW Veterans and in preclinical GWI mice models due to the influence of GW chemicals [39]. Increases in systemic inflammatory markers were also reported in GW Veterans and mouse models [28]. Following our study of the abundance and expression of ARGs and MGEs, we sought to identify a link between ARGs and biomarkers of GWI pathology which would aid in establishing a role of gut resistome in influencing host health. The purpose of this study was also to show whether a predictive insight can be made regarding future susceptibility to infectious diseases related to hospital acquired infections in GW Veterans, elderly, and immunocompromised individuals. Results in mice showed that the expression of IL-1β in the small intestine significantly increased in GWI group ($p < 0.001$, one-way ANOVA with Tukey's post hoc test) compared to the Control group, as shown through immunoreactivity of the cytokine in the villi (Fig. 2.7a, c). Treatment with FMT significantly decreased the expression of IL-1β in the GWI_FMT mice group compared to the GWI group ($p < 0.001$, one-way ANOVA with Tukey's post hoc test, Fig. 2.7a, c). To study the association between IL-1β expression and ARG diversity, we performed a correlation analysis. Results showed a positive correlation ($r = 0.9849$, $p < 0.001$ and $r = 0.9414$, $p < 0.001$ respectively, Pearson regression analysis) between α-diversity of ARGs, resistant drug classes and increased IL-1β in GWI mice group, suggesting that alteration of the gut resistome profile had a significant association with gastrointestinal inflammation (Fig. 2.7f).

We observed a significant increase in serum IL-6 level in the GWI mice group when compared to the Control. Further, there was a significant decrease in serum IL-6 levels in

GWI_FMT groups when compared to GWI group ($p < 0.001$ between GWI and Control, $p = 0.009$ between GWI and GWI_FMT, one-way ANOVA with Tukey's post hoc test, Fig. 2.7d). We also observed that α-diversity of ARGs and resistant drug classes were positively correlated ($r = 0.9546$, $p < 0.001$ and $r = 0.8732$, $p < 0.001$, Pearson regression analysis) with increased systemic IL-6 level in the GWI mice group (Fig. 2.7g).

Our previous studies have shown that a decrease in synaptic plasticity marker brain derived neurotrophic factor (BDNF) played a key role in brain pathology in GW chemical exposed mice [70]. Results showed that the expression of BDNF significantly decreased in GWI group when compared to Control. Further, the levels of BDNF as determined by morphometry from immunohistochemical analysis showed that there was a significant increase in the BDNF levels in the GWI_FMT mice groups when compared to GWI group ($p < 0.001$ between Control vs GWI; $p < 0.001$ between GWI vs GWI_FMT respectively, one-way ANOVA with Tukey's post hoc test, Fig. 2.7b, e). Interestingly, a negative correlation was observed between BDNF and ARGs and resistant drug classes ($r = -0.9668$, $p < 0.001$ and $r = -0.9146$, $p < 0.001$ respectively, Pearson regression analysis) suggesting that increased ARG-α-diversity may have a strong influence on observed neuroinflammation in the GWI mice group (Fig. 2.7h).

Furthermore, we studied the level of systemic IL-6 in the serum collected from the respective GW Veterans in this study. Results showed a significantly increased level of serum IL-6 in the Hum_GWI group compared to the Hum_Control group ($p = 0.046$, Welch's t-test; Fig. 2.8a). Correlation analysis between serum IL-6 level and the α-diversity of ARGs and resistant drug classes ($r = 0.9173$, $p < 0.001$ and $r = 0.4840$, $p = 0.042$ respectively, Pearson regression

analysis) in GW Veterans showed a positive correlation (Fig. 2.8b, c). This results may be suggestive of a link between altered gut resistome and increased systemic IL-6 in the human samples. However, further experimentation is required to confirm this hypothesis.

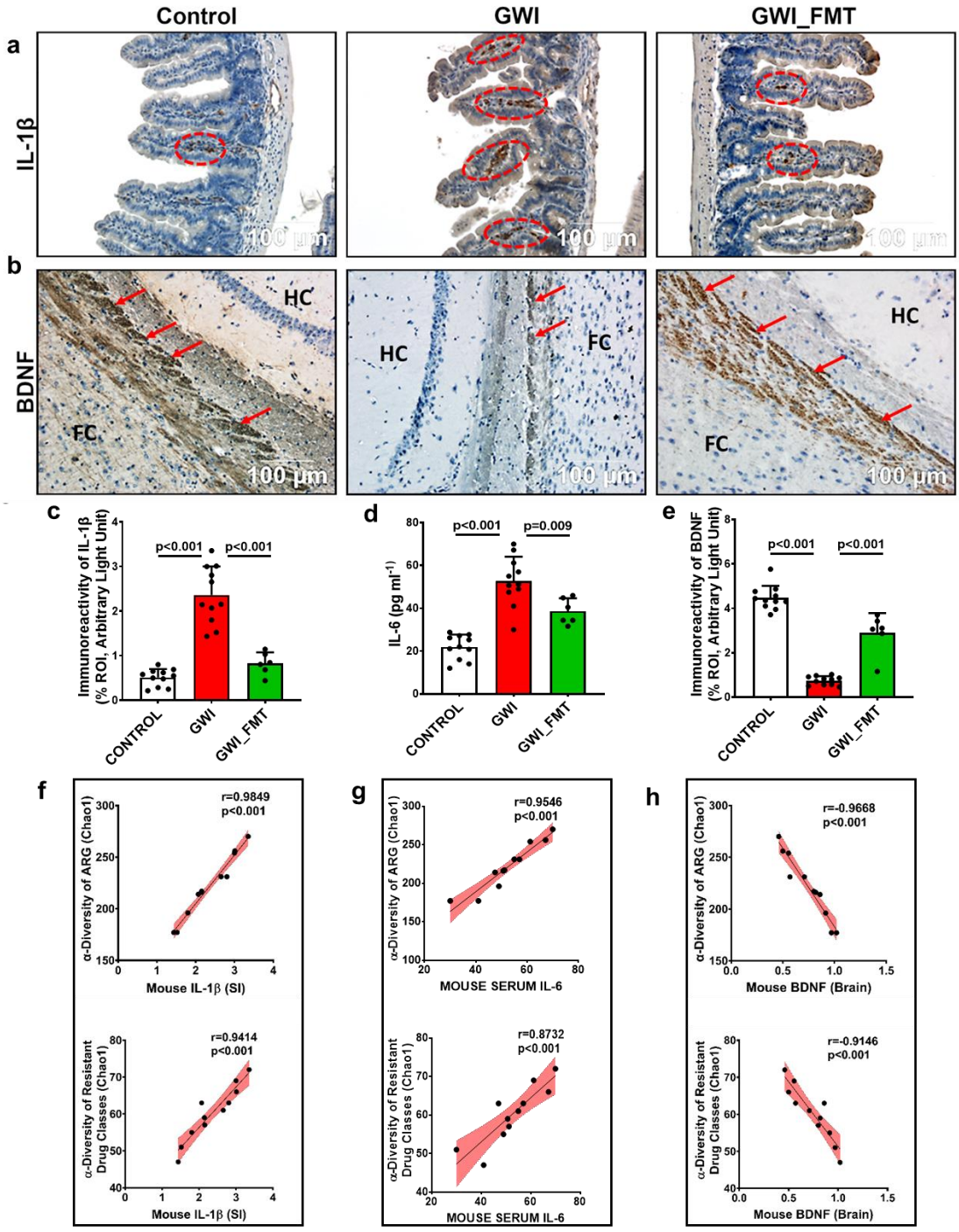

Figure 2.7. Gastrointestinal, systemic, brain inflammation and its correlation with antibiotic resistance genes and the resistant drug classes in GWI mice model. a Representative immunohistochemistry image showing immunoreactivity of proinflammatory cytokine IL-1β (marked by red circle) in mouse experimental groups Control (n = 11 biologically independent samples), GWI (n = 11 biologically independent samples) and GWI_FMT (n = 6 biologically independent samples). Images were taken at 20X

magnification. Scale bar = 100 μm b Representative immunohistochemistry image showing immunoreactivity of synaptic plasticity marker BDNF (marked by red arrows) in Control (n = 11 biologically independent samples), GWI (n = 11 biologically independent samples), GWI_FMT (n = 6 biologically independent samples) mice groups. Images were taken at 20X magnification. Scale bar = 100 μm. FC Frontal Cortex, HC Hippocampus. c Bar graph depicting immunoreactivity of IL-1β. Data are represented as mean ± SD (SD: Standard deviation) of %ROI (mean value calculated from two different fields in each sample). d Bar graph depicting the serum IL-6 level at pg/ml in Control, GWI, GWI_FMT mice groups. Data represented as mean ± SD. e Bar graph depicting immunoreactivity of BDNF. Results are represented as mean ± SD of %ROI (mean value calculated from 2 different fields in each sample). f Correlation plot between α-diversity (Chao1) of resistant ARGs and drug classes and immunoreactivity of IL-1β in mouse GW group in small intestine section. g Correlation plot between α-diversity (Chao1) of resistant ARGs and drug classes and serum IL-6 level in mouse GW group. h Correlation plot between α-diversity (Chao1) of resistant ARGs and drug classes and immunoreactivity of BDNF in mouse GW group in brain section. r-value was determined by Pearson's Regression analysis. Pearson's linear regression is shown in red with 95% confidence bands. Statistical significance was analyzed by one-way ANOVA (Tukey's post hoc test) where $p < 0.05$ was considered statistically significant.

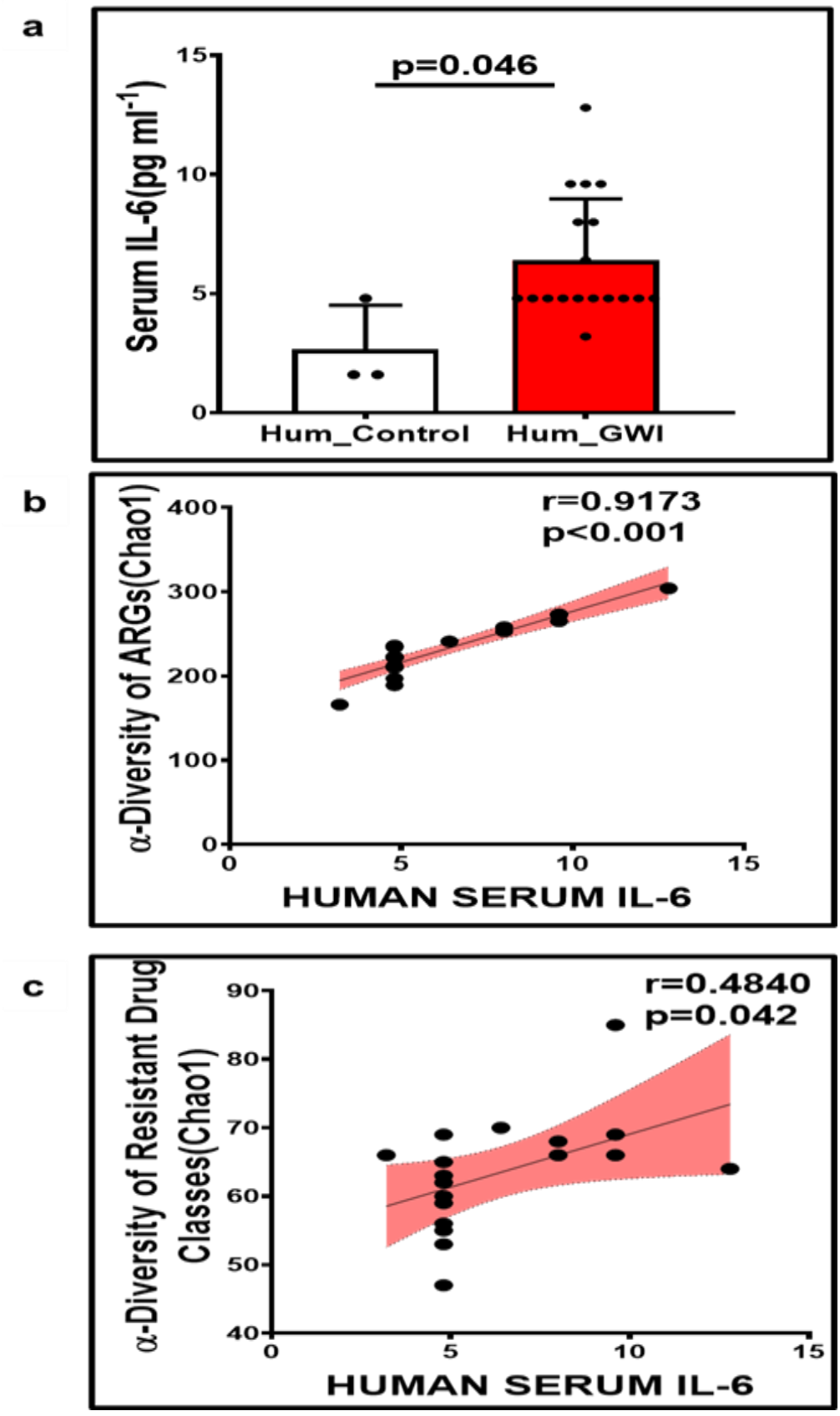
a
p=0.046
Serum IL-6(pg ml-1)
15
10
5
0
Hum_Control
Hum_GWI
b
r=0.9173
p<0.001
α-Diversity of ARGs(Chao1)
400
300
200
100
0
0
5
10
15
HUMAN SERUM IL-6
c
r=0.4840
p=0.042
α-Diversity of Resistant Drug Classes(Chao1)
90
80
70
60
50
40
0
5
10
15
HUMAN SERUM IL-6

Figure 2.8. Systemic IL-6 level and its correlation with antibiotic resistance genes and the resistant drug classes in GW Veteran samples. a Bar graph depicting the serum IL-6 level at pg/ml in Veteran control group Hum_Control (n = 3 biologically independent samples) and Hum_GWI (n = 18 biologically independent samples) groups. Correlation plot between α-diversity (Chao1) of b resistant ARGs and c resistant drug classes and serum IL-6 in Hum_GW group. Data are represented as mean ± SD (SD standard deviation). r-value was determined by Pearson's regression analysis. Pearson's linear regression is shown in red with 95% confidence bands. Statistical significance was analyzed by Welch's two-tailed t-test where $p < 0.05$ was considered statistically significant.

DISCUSSION

In the present study, we report an alteration of host gut resistome in chronic multisymptom illness as observed in a subsection of Gulf War Veterans. We also report the association of systemic inflammation with an altered gut resistome that in turn is further correlated with increased circulating proinflammatory cytokine IL-6, intestinal pathology and neurotrophic factor BDNF in preclinical GWI mice model. Most importantly, we have shown that increased systemic IL-6 had strong association with altered human gut resistome in GW Veterans. IL-6 has been shown to be a pleiotropic cytokine and is key to gastrointestinal disturbances, and cognitive deficits [71]. Recent advances in understanding the host resistome improved our knowledge about evolution, origins and emergence of antibiotic resistance though the field is continuously evolving [72]. Previously, our knowledge of resistome included proto-resistance and silent-resistance genes [72]. Silent-resistance genes do not cause phenotypic resistance until they are transferred via MGEs, or a mutation occurs in the associated regulatory elements. Gut microbiome is usually associated with a silent resistome, as they have the potential to contribute in clinical resistance through mobilization. Our study supports the existing evidence that the resistome is highly dependent on the gut microbiome and indicates to a possible association between changes in the bacteriome and the gut

resistome, particularly in GWI groups, both in the case of mouse models and Veterans with GWI as studied by PERMANOVA and procrustes analysis (Figs. 2.2b and and2.4b).

Exposure to environmental chemicals like pesticides, biocides, aerosols have been reported to the increase in antimicrobial resistance via HGT which have long-lasting changes and increase in these resistant bacterial population in human due to selection pressure leads to treatment failure with available antibiotic [73]. This led us to our hypothesis that exposure to a mixture of environmental hazards (war theater) in GW Veterans as well as representative GW chemical exposure in GWI mice model may affect the gut resistome. Our results suggested that representative GW chemicals PB and permethrin (Per) may change the ARGs significantly, but the changes observed in individual MGE profiles in GWI group of the mouse model when compared to the control group were not significant. One of the limitations in this study includes our inability to experimentally confirm that the GW chemical-treated mice were indeed resistant to the classes of antibiotics or the individual ARGs that has been found in this study. However, we would also like to state that to the best of our knowledge no GWI mice model could exactly mimic the health condition of the GW Veterans. Different combinations of GW chemicals along with different routes of administration needs to be included during the various GWI mice model studies to further elucidate the mechanisms proposed. Future studies need to overcome these limitations for in-depth mechanistic links to gut resistome in GWI mice models.

Previous reports stated that elderly individuals and Veterans had increased resistance to sulfonamide, macrolide, β-lactam antibiotics followed by tetracycline as well as fluoroquinolones especially found in Acinetobacter baumannii isolates [74]. Reports also

stated that fluoroquinolones and cephalosporin usage should be prescribed in a limited manner among the elderly and Veterans as they have higher susceptibility in developing resistances upon treatment with such high generation antibiotics [75]. However, there is very little evidence about the ARGs in Veterans, especially GW Veterans suffering from CMI or collectively referred as GWI who were deployed 30 years back and are presently in the age range of 50–60 years. The present study attempted to report the alteration of ARG and MGE signature in GW Veterans belonging to the aforementioned age group. Another limitation of the present study includes the inability to confirm whether the gut resistome alteration is a result of GW chemical exposures alone. GW Veterans may have been exposed to multiple courses of antibiotics at different points in their lifetime, along with this factors like diet, metabolic conditions like obesity that might prompt an increase in the altered gut resistome. A further limitation in our analysis of gut resistome in GW Veterans may be whether the GW Veterans recruited in our study were actually resistant to the ARGs and antibiotics reported. The limitation is also confounded by the small sample size of Veterans that may have caused low significance of our ARG and MGE results. To overcome these limitations, future studies with a large cohorts with sufficient power would help to obtain more in-depth knowledge about the antibiotic resistance in GWI Veterans. We identified that glycopeptide resistance was high in GWI compared to other mouse groups as well as in GW Veterans (not statistically significant). Glycopeptide group of antibiotics especially Vancomycin is used to treat bacterial infections like *methicillin-resistant Staphylococcus aureus* (MRSA), *Clostridium difficle*, and *Enterococcus spp.* 25118105 [76]. Recently it has been reported that administration of Vancomycin in patients at Veterans Affair Hospitals have been ineffective against these clinically important bacteria and causing nephrotoxicity

[77]. Increased glycopeptide resistance as detected in our GW Veteran samples might be suggestive of the reason behind the ineffectiveness of Vancomycin antibiotic used to treat a section of Veterans. A further study of the resistant drug classes as well as mechanisms of resistance could be helpful to confirm this result.

FMT has been reported to restore the beneficial microbiome in pathological conditions like inflammatory bowel disease (IBD), type 2 diabetes, nonalcoholic steatohepatitis and neurological disorders where gut microbial dysbiosis plays a direct role in the disease progression [78]. Studies have also reported that FMT administration have decreased the ARGs in patients with cirrhosis and *Clostridium difficile* infection [79]. In the present study, we aimed to study if FMT could be a therapeutic by decreasing antimicrobial resistance in GWI condition in preclinical GWI mice model. We observed a decrease in relative individual ARGs and MGEs in GWI_FMT group compared to GWI group in the GWI mice model (Fig. 2.3a, d). FMT treatment was able to significantly ameliorate GW chemical induced gastrointestinal inflammation and systemic inflammation and significantly increase synaptic plasticity marker expression. Moreover, future dosing considerations are required in FMT treatment since prolonged FMT treatment may cause stress alteration of gut microbiome and resistome. This also emphasizes the need for screening the fecal samples of healthy donors for FMT which has been a limitation63. Hence, these criteria should be considered in using FMT as a therapeutic measure to ameliorate gut resistome alteration and systemic inflammation in GW Veterans through carefully designed clinical trials.

Interestingly, we observed the accumulation of ARGs that are highly mobile and transferable. The mice in the preclinical GWI model were never exposed to any classes of antibiotics

during the entire course of the study, but they showed a spontaneous acquisition of unique ARGs in GW chemical exposed group but not in Control and GWI_FMT groups. This transfer may occur due to intrinsic or extrinsic transfer by HGT method based on MGE patterns. This study also suggested that GW chemical exposure may be responsible for the alteration and appearance of ARGs and MGEs in mice since they have been maintained in a controlled environment with very limited risk of exposure to a multifaceted environment, though the presence of these ARGs needs to be further elucidated.

We were able to identify diverse types of MGEs in which transposons were majorly observed in both mouse and GW Veteran samples. A study by Parnanen et al. stated that transposase constitutes the most abundant MGE class [64]. This study completely is consistent with our observations about MGEs. Higher abundance of MGEs belonging to transposon group along with integrons, insertional sequence might indicate a probability for inter-bacterial ARG transfer which might increase the adverse consequences due to increase in antimicrobial resistance in GWI pathology 23550063 [80]. To track the ARG transfer through MGE, further detailed investigation is needed to identify the ARGs associated with the MGEs.

Studies have also reported that low dose antibiotics have increased the abundance of a single pathogenic bacteria, however, difference in ARGs were not significant compared to control groups [81]. This study also showed change in immunological markers but association between ARGs and immunological markers have not been established [81]. Also, IBD phenotype is known to be associated with microbiome dysbiosis which led to upregulation of antibiotic resistance [82] a condition also observed in GW Veterans. We have shown an association between gastrointestinal, systemic, and neuronal inflammation observed in GWI

pathology and diversity of ARGs and resistant drug classes in a GWI mice model. Our results also indicated an association between systemic inflammation reflected by increased serum IL-6 and ARG diversity in GW Veterans. Interestingly, association between diversity of ARGs and systemic proinflammatory marker IL-6 will be an important benchmark in future studies of chronic multisymptom illness and other related pathology. Future mechanistic studies are needed to establish the exact role of ARGs in GWI pathophysiology by using germ free and gnotobiotic models combined with the use of short chain fatty acid treatment regimens such as butyrate therapy.

Limitations of the study

Modeling the chronic multisyptomatic condition of GWI in rodent models to mimic the health condition of the present-day GW Veterans has been challenging. Due to the complex environmental chemical exposures during the Persian Gulf War, it is imperative that incorporation of other chemicals like organophosphates, N,N-diethyl-meta-toluamide (DEET), depleted uranium exposure, vaccines, oil smoke along with Per and PB would strengthen the translatability of the results in GWI. The research in GWI should consider the differences in the routes of exposure of these environmental mixtures such as the dermal route for administration of Per, a widely used insecticide. Small sample size of the GWI persistence mouse model as well as GWI Veteran cohorts may have affected the resistome analysis, hence an incorporation of a larger sample size along with studies with significant statistical power in future mechanistic analyses of the gut resistome will help us in better understanding the changes ARGs and MGEs. This is especially important in detecting the minute changes related to the resistant drug classes, antibiotic resistance mechanisms and

MGE types. In the GWI mice model, inclusion of an FMT-only control would help us to clearly distinguish the effects of the above treatment regimen on gut resistome. A modification of the treatment plan of FMT in the murine model that takes into account the additional stress-induced changes in the gut resistome that might have occurred, would be pertinent to the present line of investigation. Future studies would also need to screen the fecal samples from the healthy mice-Control groups to minimize the transfer of ARGs to the recipient group. The present study should not be conceived as an attempt to integrate the mouse data with that of the data from the human cohorts as there are remarkable differences in the exposure patterns as underlined in our previous sections. The human cohort was included to investigate if resistome alteration occurred in GWI conditions as an effect of microbiome dysbiosis, as reported in earlier studies. The GW Veterans have been exposed to multiple environmental chemical exposures singly or in combination. In addition, diet, sedentary lifestyle after deployment, metabolic conditions like obesity and exposure to multiple courses of antibiotics and treatment regimens may have contributed to higher resistome diversity. Another significant limitation might be the inability to confirm experimentally if the GWI Veterans or the mice exposed to representative GWI chemicals were actually resistant to the antibiotics observed from the gene annotation studies. These limitations could have been overcome by exposing GWI mice to representative antibiotics following a bacterial infection or an acute challenge with bacteria that cause pathogenesis. Inclusion of these set of experiments might have supported our hypothesis that a resistome signature can predict phenotypic disease susceptibility later in life. Also, inclusion of the previously stated factors like diet and obesity in the future GWI mouse model study along with use of humanized and germ-free mice might improve the translatability of the results obtained

from the animal studies. We were also limited in linking the MGEs with the ARGs as well as identifying the mechanism that connected the GWI pathology with altered gut resistome which we plan to study in the immediate future. The present study is a preliminary report. The observations can help build a stronger hypothesis that points to the role of the host gut resistome in GWI disease pathology. Further studies with larger sample sizes may establish causality and help in determining risk of GWI Veterans to antibiotics and other co-morbidities.

In conclusion, to the best of our knowledge the present study is the first to investigate gut resistome alterations in GWI. Further, a preliminary association was established between an altered resistome and systemic IL-6 levels in a translatable mouse model that has broad implications in the general population suffering from similar ailments though the actual causality is yet to be established. It is expected that 78 million of the US population is expected to be in the elderly category by 2030. Most of them have a history of prolonged antibiotic use, a case similar with our aging Veterans. The elderly population belonging to the age group of 50–60 years have increased risk of acquiring antibiotic resistance due to several factors like impaired immune functioning, immunosenescence, and exposure to muti-drug resistant bacteria due to multiple visits to clinics and hospitals [83]. In the present study, the GW Veterans were of the same age group (53–56 years) and studies have reported that the present day GW Veterans have a maladaptive immune system primarily due to GW chemical exposure and aging [84]. The scenario is also significant owing to old age associated hospitalizations and increased chances of hospital acquired infections. Based on the above facts and our study results, we can predict that GW Veterans may have a very high chance of acquiring antimicrobial resistance. In addition, FMT can be used as a therapeutic strategy

against the increased antibiotic resistance in Veterans and elderly to attenuate a possible altered resistome. Knowledge gained from the microbiome and resistome profiles from GW Veterans can be very helpful for treating a variety of bacterial diseases or hospital acquired infections (following surgery) that may require antibiotic treatment in the Veterans and can be a useful tool for a personalized medicine approach.

Supplementary Table 2.1. List of primers for q-RTPCR analysis of mouse and GW veteran ARGs:

a. Mouse Primers:

SL no.	Gene name	ARO Number	Forward	Reverse
1	***vanXYN***	ARO:3002969	TGATGGTCATCGAACGGTTG	CAGCCAGGAGATGCTACATAAC
2	***adeS***	ARO:3000549	CCGAGTTTCGGGACGATTTA	CCCATCTCTTCATGACCCATAG

b. Human Primers:

SL no.	Gene name	ARO Number	Forward	Reverse
1	***mexD***	ARO:3000801	GTCAAGTCCGTGCACAGTATAA	GTTCACACGAGCAACCAATTC
2	***novA***	ARO:3002522	TCACGTTGGACAAAGCGTATC	GGTCATCTGCACCAGCATATAG
3	**Agrobacterium fabrum chloramphenicol acetyltransferase (*afca*)**	ARO:3004451	AACTCGCCGCGTCAATATAA	GGCCAGGTTTCCTGTATCAA

c. 16S Primer:

SL no.	Gene name	Sequence
1	***16S_1237 F***	GGGCTACACACGYGCWAC
2	***16S_1391 R***	GACGGGCGGTGTGTRCA

CHAPTER 3

A Double Humanized Mouse Model for Studying Host Gut-Microbiome-Immune Interactions in Gulf War Illness

Funding: This study was supported by VA Merit Award I01CX001923-01 awarded to Dr. Saurabh Chatterjee. Disclaimer: The contents do not represent the views of the U.S. Department of Veterans Affairs or the United States Government.

Dipro Bose, Punnag Saha, Subhajit Roy, Ayushi Trivedi, Madhura More, Nancy G. Klimas, Ashok Tuteja, Saurabh Chatterjee (2024). A Double Humanized Mouse Model for Studying Host Gut-Microbiome-Immune Interactions in Gulf War Illness. International Journal of Molecular Sciences (Under Review)

UNDERSTANDING THE GUT MICROBIOME-IMMUNE CROSSTALK IN GULF WAR ILLNESS USING A NOVEL DOUBLE HUMANIZED MOUSE MODEL

ABSTRACT

Unraveling the multisymptomatic Gulf War Illness (GWI) pathology and finding an effective cure has eluded researchers for decades. The chronic symptom persistence and limitations of studying the etiologies in mouse models that differ significantly in humans pose a challenge for drug discovery and finding effective therapeutic regimens. The GWI exposome differs significantly in the study cohorts, and the above makes it difficult to recreate a model closely resembling the GWI symptom pathology. We have used a double engraftment strategy of reconstituting a human immune system coupled with human microbiome transfer to create a humanized mouse model for GWI. Using whole genome shotgun sequencing and blood immune cytokine enzyme-linked immunosorbent assay (ELISA), we show that our double humanized mice treated with Gulf War (GW) chemicals show significantly altered gut microbiome, similar to those reported in a Veterans cohort of GWI. The results also showed similar cytokine profiles such as increased levels of IL-1β, IL-6, and TNF R-1 in the double humanized model as found previously in a human cohort. Further, a novel GWI Veteran fecal microbiota transfer was used to create a second alternative model that closely resembled the microbiome and immune system-associated pathology of a GW-Veteran. GWI-Veteran microbiota transplant in humanized mice showed human microbiome reconstitution and systemic inflammatory pathology as reflected by an increase in IL-1β, IL-6, IL-8, TNF R-1, and endotoxemia. In conclusion, though preliminary, we report a novel in vivo model with human microbiome reconstitution and engrafted human immune phenotype that may help better understand gut-immune interactions in GWI.

Keywords: Humanized mice; NSG, Bacteriome, IL-6, TNF-R1, Gut-Immune Axis

INTRODUCTION

Significant research has been conducted, including clinical and pre-clinical studies, for the past 30 years on Gulf War Illness (GWI), advancing our understanding of complex multisymptomatic pathology. Studies have reported the prevalence of GWI symptoms to be significantly higher among the Veterans who were deployed in the 1990-91 Gulf War (GW) compared to the non-deployed population [1]. It is important to note that the aging GW Veterans in the present day, continue to experience the persistence of the GWI symptoms 36612580 [85].

GWI has been reported to be the result of the exposure to multiple chemical and environmental toxicants by the Veterans during the war [3]. Several research groups including ours have attempted to administer two or more such reported toxicants as a mixture in pre-clinical murine models to understand the pathophysiology and exposome profile of GWI. However, most of the studies have used experimental mouse or rat strains to design their respective chronic or sub-chronic GWI models [86].

Recent approaches have focused on substituting the experimental murine models with humanized mouse models. The advantage of the humanized mouse model lies in its ability to possess human immune cells, gut microbiome, specific tissues, and, tumor growth [87]. Further modification of existing humanized mouse model such as the bone-marrow, liver, thymus-humanized (hu-BLT) mice by engrafting with human gut microbiome via fecal microbiota transfer (FMT) has led to the development of a “double humanized-mouse model” [88]. This model has the advantage of being more translatable for mimicking the

human gut microbiome-induced host immune response as opposed to immune responses due to altered murine microbiome which is different [89].

GWI pathology has been identified to be associated with altered gut microbiome due to GW chemical exposures [23], [70]. Hence, it will be more advantageous to utilize a double humanized mice model to study the GWI pathology as the immunological response could be more translatable to the clinical data available from the GWI Veterans. In the present study, we have used CD34+ hu-NSG (NOD.Cg-Prkdcscid Il2rgtm1Wjl/SzJ), mostly termed as NSGTM mice strains which have been engrafted with human hematopoietic stem cells (hu-CD34+). The CD34+ hu-NSG mice have been further engrafted with human gut microbiome from a healthy human subject after antibiotic-induced gut depletion via FMT following the protocol reported by Daharsh et al., with modifications [88]. We have studied the gut microbiome and systemic immune responses by administering GW-representative chemicals. Further, we report the altered gut microbiome and immunological signature post-engrafting the CD34+ hu-NSG mice with a GWI Veteran microbiome by performing FMT using a stool sample from GWI Veteran.

MATERIALS AND METHODS

Animals

We purchased pathogen-free, adult (21 weeks old), CD34+ hu-NSG mice from Jackson Laboratories (Bar Harbor, ME, USA). Upon arrival, all the mice were accommodated in a room with controlled temperature (22–24°C), having 12 hours light/12 hours dark cycle and with ad-libitum access to food and water. Mice were housed under SPF conditions with air exchange, prefilters, and HEPA filters (0.22 μm) in a room with controlled temperature,

humidity, and pressure. The mice were maintained in autoclaved individual microisolator cages in a rack system capable of managing air exchange with prefilters and HEPA filters (0.22 μm). All the experiments with mice were approved by the University of California Irvine and carried out by following the local Institutional Animal Care and Use Committee standards (protocol number AUP-23-015 approved on 04/14/2023).

Mouse model of Gulf War Illness

The mice were acclimatized for one week and followed by random distribution into five experimental groups where each group comprised of 6 mice per group. The NSG_Control mice group was administered with a phosphate-buffered saline solution via oral gavage for 30 days. NSG_ABX Treatment group was administered with an antibiotic cocktail solution (metronidazole 1g/kg, neomycin 1 g/kg, vancomycin 0.5 g/kg, and ampicillin 1g/kg) via oral gavage for 12 days and allowed to persist for the remaining 18 days period. NSG_Hu-FMT group was administered with the antibiotics cocktail via oral gavage for the initial 12 days for native gut bacteriome depletion, after which FMT via oral gavage was performed for the next 2 days to establish the gut bacteriome of a healthy human. Healthy human fecal samples were purchased from Creative Biomart Inc (Shirley, NY, USA) dissolved in sterile phosphate-buffered saline solution and centrifuged at 3000 x g for 5 minutes. 100μl of the supernatant was administered in the mice. After the FMT procedure, the mice were allowed to persist for the remaining 15 days. In the NSG_Hu-FMT+GWI group, gut depletion was done by antibiotic cocktail administration via oral gavage for 12 days, and human bacteriome establishment was done by performing FMT like the NSG_Hu-FMT group. After the FMT process, representative GW chemicals pyridostigmine bromide (2mg/kg diluted in phosphate-

buffered saline) and permethrin (200mg/kg diluted in 0.6% dimethyl sulfoxide) were administered via oral gavage on a triweekly basis for 15 days. The NSG_GWIV mice group were administered with antibiotics cocktail via oral gavage for 12 days for gut bacteriome depletion followed by an FMT process with a GWI Veteran stool sample for 2 days. The stool sample was homogenized in 1ml of phosphate-buffered solution, and centrifugation was performed at 3000 x g for 5 minutes. 100µl of the supernatant was immediately administered in the NSG_GWIV mice group. The deidentified GWI Veteran stool samples was kindly provided by Dr. Tuteja from his recently conducted study [90]. The human cohort study from where the human stool sample was collected, was approved by the Salt Lake City Veterans Affairs Medical Center and the University of Utah Institutional Review Board. The study was registered in ClinicalTrials.gov (NCT03078530). These mice were allowed to persist for the remaining 15 days for effective repopulation of the gut bacteriome. All the mice were sacrificed after the experimental period, fecal pellets were collected for bacteriome analysis and serum was collected from freshly collected blood by the process of cardiac puncture.

Bacteriome Analysis

Fecal pellets were collected from all the experimental mice groups for bacteriome analysis by the vendor CosmosID Inc. (Germantown, MD, USA). Briefly, total DNA from the fecal pellets were isolated following the manufacturer's protocol using QIAGEN DNeasy PowerSoil Pro Kit (Germantown, MD, USA). Quantification of the extracted DNA was performed using Qubit Flex fluorometer and Qubit dsDNA HS Assay Kit (Thermofisher Scientific, Waltham, MA, USA). The DNA library was prepared using the xGen DNA Library Prep Kit (IDT,

Coralville, IA, USA) and xGen Normalase UDI Primers with a total DNA input of 1.5ng. DNA fragmentation was performed using a specified amount of IDT xGEN fragmentation enzyme (Coralville, IA, USA). The library was constructed by adding unique dual indexes to each sample followed by 10 cycles of PCR. Purification of DNA libraries was done using AMpure magnetic Beads (Beckman Coulter, Indianapolis, IA, USA) and eluted in QIAGEN EB buffer (Germantown, MD, USA). DNA libraries were quantified using a Qubit fluorometer and Qubit dsDNA HS Assay Kit. The libraries were sequenced on the Illumina NovaSeq X Plus (San Diego, CA, USA) platform at 2x150bp. The data upon arrival was run through fastqc. The multiqc report was reviewed to ensure that the read depths met the thresholds and there were no errors with duplication rates, read quality, and adaptor content. Results for the taxonomic analysis was viewed on the vendor's CosmosID-Hub Microbiome platform to ensure there were no barcoding or contamination issues.

ELISA

ELISA was performed using serum collected from the mice using commercially available kits for human interleukin-1β (IL-1β) (Proteintech, Rosemont, IL, USA), human interleukin-6 (IL-6) (Proteintech, Rosemont, IL, USA), human interleukin-8 (IL-8) (Proteintech, Rosemont, IL, USA) and human tumor necrosis factor receptor-1 (TNF R-1) (R&D Systems Inc., Minneapolis, MN, USA). The procedure was carried out following the manufacturer's protocol.

Limulus Lysate Test (LAL) Assay

The serum endotoxin levels were quantified using Pierce LAL Chromogenic Endotoxin Quantitation Kit from Thermo Fisher Scientific (Waltham, MA, USA). The procedure was carried out following the manufacturer's protocol.

Statistical Analysis

The statistical analyses were done using GraphPad Prism software version 10.2.2 (San Diego, CA, USA). One-way ANOVA and unpaired two-tailed t-tests were done with Bonferroni-Dunn post-hoc corrections. The data is represented as Mean±SEM. $p \leq 0.05$ was considered to be statistically significant for all the analyses.

RESULTS

Establishment of healthy human gut bacteriome in CD34+ hu-NSG mice.

We wanted to establish the gut bacteriome of a healthy human donor in the CD34+ hu-NSGTM mouse strain. Gut depletion was performed by administering an antibiotic cocktail via oral gavage for 12 days, followed by FMT with a healthy human fecal sample for 2 days. To study the efficacy of the antibiotic cocktail-induced gut depletion and the subsequent human gut bacteriome establishment, we performed a whole genome sequencing study using fecal samples from the three groups. Results showed that the alpha diversity (Chao1) of the gut bacteriome was significantly decreased in the NSG_ABX Treatment group compared to the NSG_Control group ($p<0.001$) (Figure 1A). Administration of human FMT after the initial gut depletion by antibiotic treatment in the NSG_Hu-FMT group resulted in a significant increase in the α-diversity (Chao1) compared to the NSG_ABX Treatment group which indicated the establishment of human gut bacteria ($p<0.001$) (Figure 3.1A). The Bray-Curtis β-diversity analysis showed a significant difference in the gut bacteriome profile

between the NSG_Control and NSG_ABX Treatment groups ($p<0.002$) and between NSG_ABX Treatment and NSG_Hu-FMT groups ($p<0.005$) (Figure 3.1B). At, the phylum level, an increase in the relative abundance of *Firmicutes* and a decrease in *Verrucomicrobia* was observed in the NSG_ABX Treatment group as compared to the NSG_Control group (Figure 3.1C). Moreover, human FMT treatment increased the relative abundance of *Verrucomicrobia* and decreased *Firmicutes* in the NSG_Hu-FMT group compared to the NSG_ABX Treatment group (Figure 3.1C). Further investigating the colonized bacterial population in CD34+ hu-NSG mouse strain by comparing the bacterial profile of the donor at the genus level, we observed that the relative abundance of *Bifidobacterium* and *Roseburia* were significantly increased in NSG_Hu-FMT groups compared to the NSG_ABX Treatment group (Figure 3.1D). We also observed a significant increase in the relative abundance of beneficial gut commensal bacteria *Akkermansia*, *Lachnospiraceae*, and *Schaedlerella* in NSG_Hu-FMT groups compared to the NSG_ABX Treatment group (Figure 3.1D). Further, we wanted to study the expression of systemic inflammation in the three groups by performing serum Enzyme-linked immunosorbent assay (ELISA). We observed a significantly increased expression of human proinflammatory cytokines IL-1β, IL-6, IL-8 and human soluble receptor TNF R-1 at serum level in the NSG_ABX Treatment group compared to the NSG_Control group which was significantly decreased in NSG_Hu-FMT group (Figure 3.2A-D) There was no statistical significance in the endotoxin levels between NSG_ABX Treatment versus NSG_Hu-FMT groups (Figure 3.2E). The results suggested that the gut bacteriome depletion and subsequent microbiome repopulation from a healthy human donor restored the gut bacteriome diversity typical of a healthy human donor with no significant systemic inflammation.

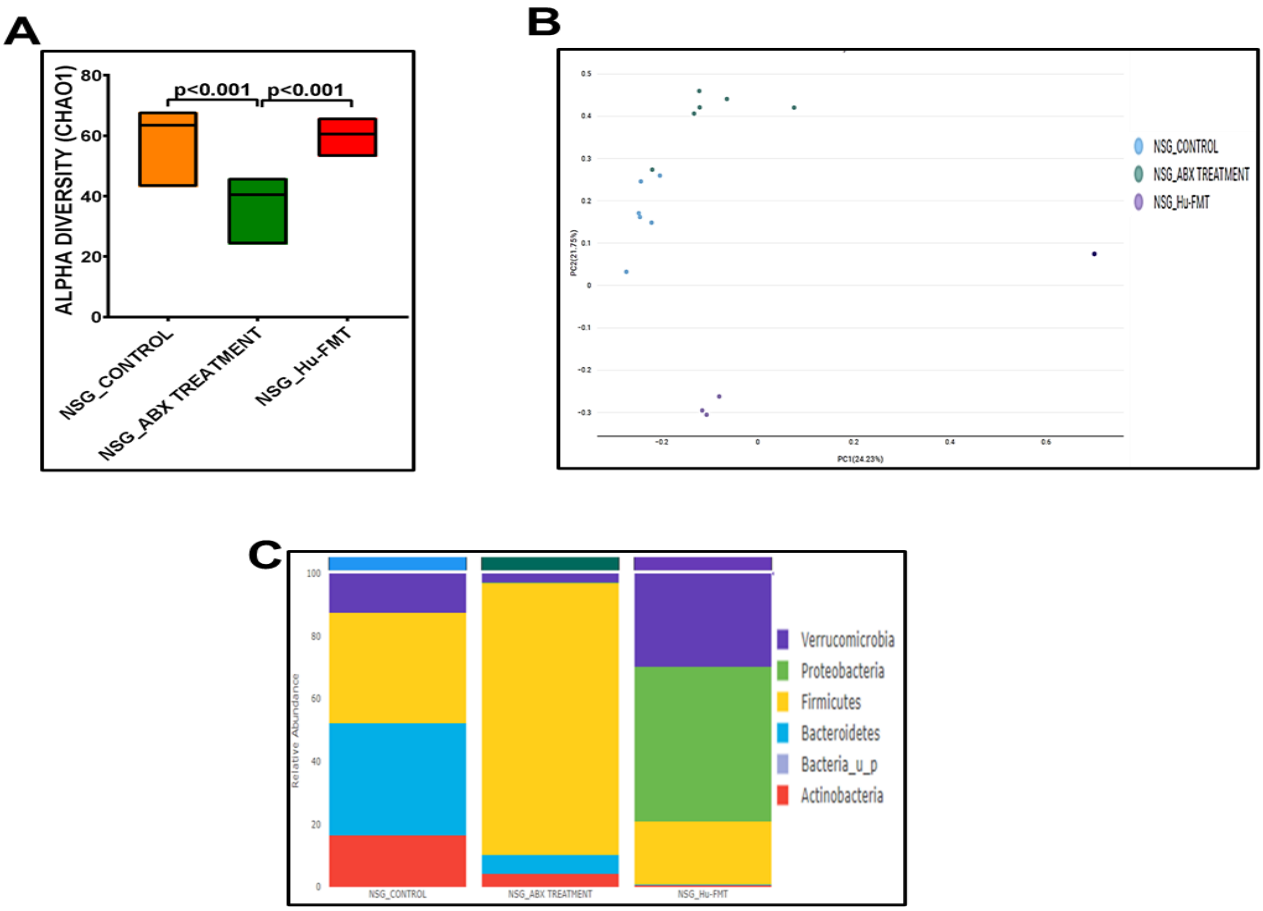
A
ALPHA DIVERSITY (CHAO1)
p<0.001
p<0.001
NSG_CONTROL
NSG_ABX TREATMENT
NSG_Hu-FMT
B
NSG_CONTROL
NSG_ABX TREATMENT
NSG_Hu-FMT
PC1(24.23%)
PC2(21.75%)
C
Relative Abundance
Verrucomicrobia
Proteobacteria
Firmicutes
Bacteroidetes
Bacteria_u_p
Actinobacteria
D
Akkermansia
Bifidobacterium
Lachnospiraceae
Roseburia
Schaedlerella
Relative Abundance (%)
p<0.001
p=0.001

Figure 3.1. Establishment of human gut bacteria in NSG-CD34+ mice (A). Box plots showing α-diversity (Chao1) of gut bacteriome in NSG_Control group (mice administered with the vehicle), NSG_ABX Treatment (mice administered with antibiotics cocktail via oral gavage for 12 days), and NSG_Hu-FMT (mice administered with human fecal microbiota transfer after gut bacteriome depletion with antibiotics cocktail). (B) β-diversity analysis (Bray Curtis) of NSG_Control, NSG_ABX Treatment and NSG_Hu-FMT groups. (C) Stacked bar representation of relative abundance of gut bacteriome at the phylum level of NSG_Control, NSG_ABX Treatment, and NSG_Hu-FMT groups. (D) Bar graph representation of relative abundance of gut bacteriome at the genus level of NSG_Control, NSG_ABX Treatment, and NSG_Hu-FMT groups. $p<0.05$ was considered statistically significant.

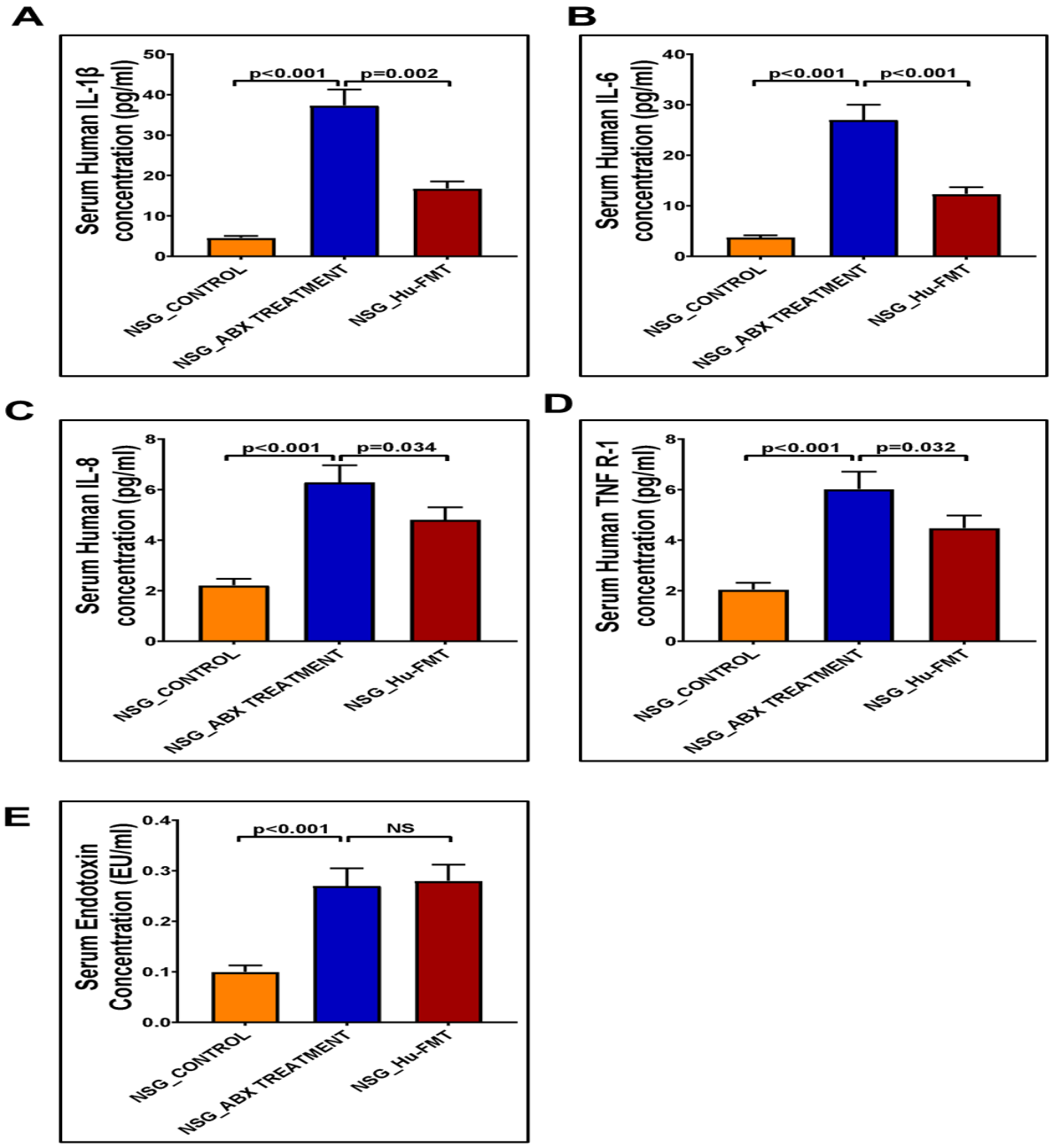

Figure 3.2. Altered expression of systemic pro-inflammation biomarkers during establishment of human gut bacteria in NSG-CD34+ mice. Bar graph representation of systemic cytokines (A) IL-1β, (B) IL-6, (C)IL-8, (D) TNF-R1 in NSG_Control, NSG_ABX Treatment and NSG_Hu-FMT groups. (E) Bar graph representation of serum endotoxemia by LAL Assay in NSG_Control, NSG_ABX Treatment, and NSG_Hu-FMT groups. $p<0.05$ was considered statistically significant.

Effect of representative GW chemical treatment on the gut bacteriome, resistome profiles, and systemic inflammation in CD34+ hu-NSG mice with established human gut bacteriome.

The current aim for the below-reported experiments was to use the humanized gut bacteriome model to study the possible alteration in gut microbial diversity following GW-chemical exposure. We studied the alteration of gut bacteriome and resistome profile after the administration of representative GW chemicals pyridostigmine bromide and permethrin in CD34+ hu-NSG mice having established human gut bacteriome. The α-diversity (Chao1) was significantly decreased in the NSG_Hu-FMT+GWI group when compared to the NSG_Hu-FMT group ($p<0.05$) (Figure 3.3A). Bray-Curtis β-diversity analysis, a representation of richness and unique niches between groups, showed that the observed difference in the gut bacteriome profile between the NSG_Hu-FMT and NSG_Hu-FMT+GWI groups was non-significant ($p=0.131$) (Figure 3.3B). At the phylum level, we observed an increase in the relative abundance of Firmicutes and a decrease in *Verrucomicrobia* in NSG_Hu-FMT+GWI compared to the NSG_Hu-FMT group (Figure 3.3C). At genus level, a significant decrease in the relative abundances of *Akkermansia* ($p=0.001$), *Bifidobacterium* ($p<0.001$), *Lachnospiraceae* ($p<0.05$), *Roseburia* ($p<0.001$), and *Schaedlerella* ($p<0.001$) in NSG_Hu-FMT+GWI group compared to the NSG_Hu-FMT group (Figure 3.3D). Further, we studied the gut resistome profile between these two experimental mice groups since our previous study reported the association of gut resistome alteration in underlying GWI condition [91]. A significant increase in the α-diversity of antibiotic resistance genes was observed in NSG_Hu-

FMT+GWI compared to the NSG_Hu-FMT group (p=0.006) (Figure 3.4A). Bray-Curtis β-diversity analysis showed that although there was a distinct separation in gut resistome profile between the two groups, however, the difference was statistically non-significant (p=0.141) (Figure 3.4B). We also observed a significant increase in the relative abundances of antibiotic resistance genes *aminoglycoside gene aadE 1 KF864551* (p<0.001), *macrolide 29 1724 Branch* (p<0.01), *macrolide 57 1774 Branch* (p<0.001) and *tetracycline 7 2471 Branch* (p<0.001) in NSG_Hu-FMT+GWI compared to NSG_Hu-FMT group (Figure 4C). Further, we observed a significant increase in the expression of serum proinflammatory markers IL-1β (p<0.001), IL-6 (p<0.001), IL-8 (p<0.001) and soluble receptor TNF R-1 (p<0.001) in NSG_Hu-FMT+GWI compared to NSG_Hu-FMT group (Figure 3.5A-D). Further, we observed a significant increase in the endotoxin levels (p<0.001) in NSG_Hu-FMT+GWI compared to the NSG_Hu-FMT group (Figure 3.5E), suggesting a distinct gut leaching phenomenon often associated with profound gut dysbiosis in GWI and other metabolic and environment-linked disease phenotypes.

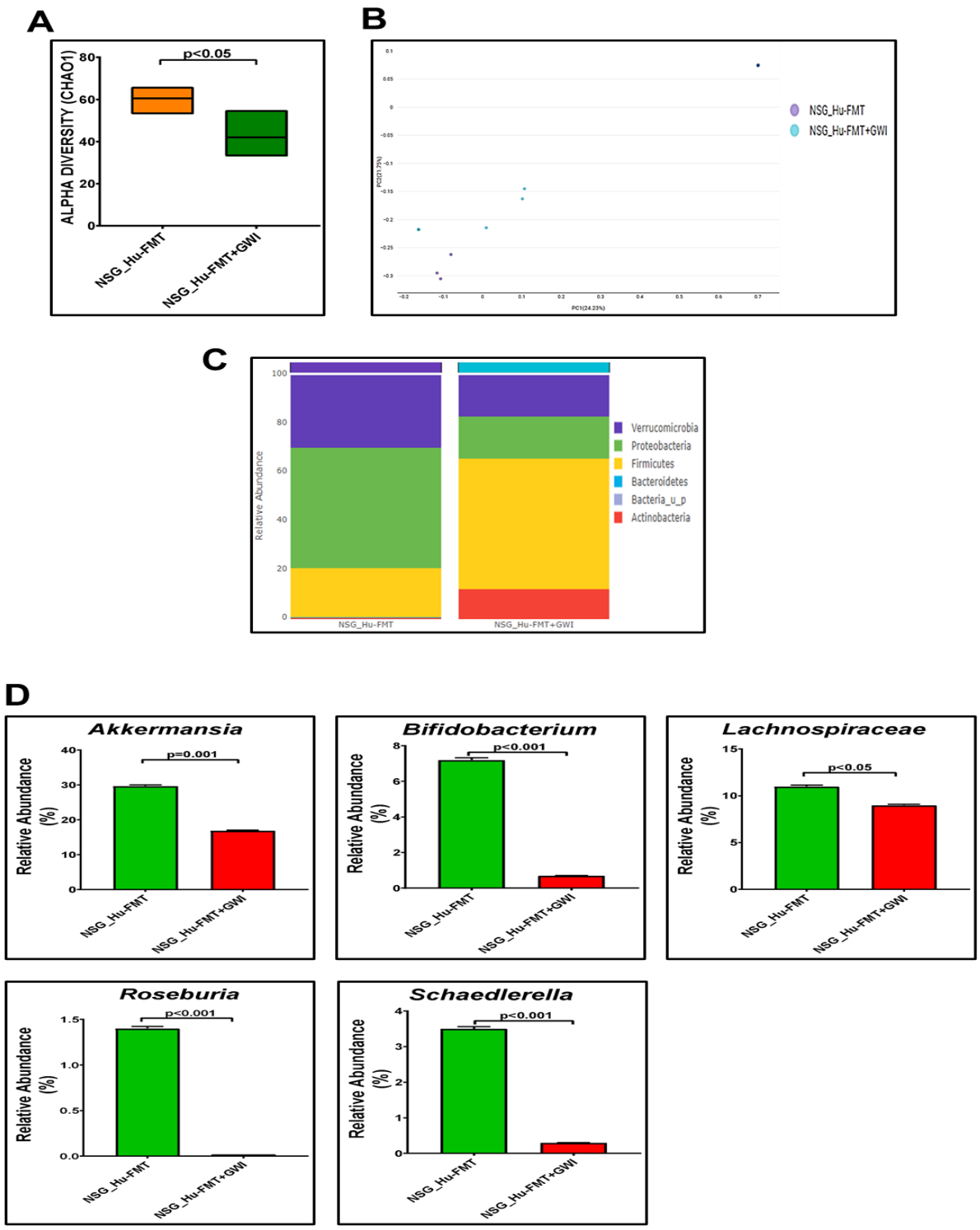

Figure 3.3. Exposure to representative GW chemicals altered gut bacteriome profile in NSG-CD34+ mice with established human gut bacteria. (A). Box plots showing α-diversity of gut bacteriome (Chao1) in NSG_Hu-FMT (mice administered with human fecal microbiota transfer after gut bacteriome depletion with antibiotics cocktail) and NSG_Hu-

FMT+GWI (mice administered with representative GW chemicals pyridostigmine bromide and permethrin for 15 days after gut bacteriome depletion with antibiotics cocktail and human fecal microbiota transfer). (B) β-diversity analysis (Bray Curtis) of NSG_Hu-FMT and NSG_Hu-FMT+GWI groups. (C) Stacked bar representation of relative abundance of gut bacteriome at the phylum level of NSG_Hu-FMT and NSG_Hu-FMT+GWI groups. (D) Bar graph representation of relative abundance of gut bacteriome at the genus level of NSG_Hu-FMT and NSG_Hu-FMT+GWI groups. $p<0.05$ was considered statistically significant.

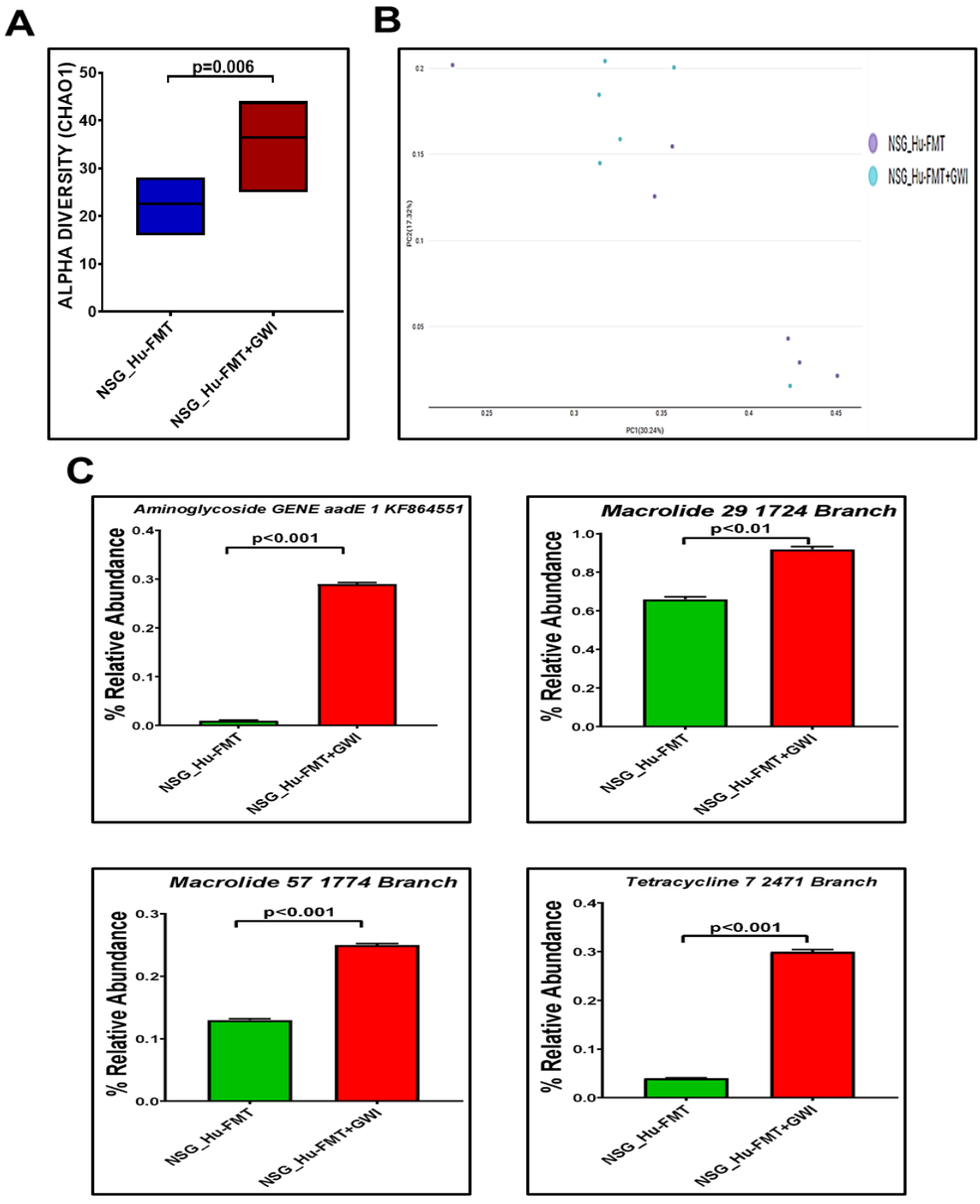

Figure 3.4. Exposure to representative GW chemicals altered gut resistome profile in NSG-CD34+ mice with established human gut bacteria. (A). Box plots showing α-diversity (Chao1) of gut resistome in NSG_Hu-FMT (mice administered with human fecal microbiota transfer after gut bacteriome depletion with antibiotics cocktail) and NSG_Hu-FMT+GWI (mice administered with representative GW chemicals pyridostigmine bromide and permethrin for 15 days after gut bacteriome depletion with antibiotics cocktail and human fecal microbiota transfer). (B) β-diversity analysis (Bray Curtis) of NSG_Hu-FMT and NSG_Hu-FMT+GWI groups. (C) Bar graph representation of relative abundance of altered antibiotic resistance gene of NSG_Hu-FMT and NSG_Hu-FMT+GWI groups. $p<0.05$ was considered statistically significant.

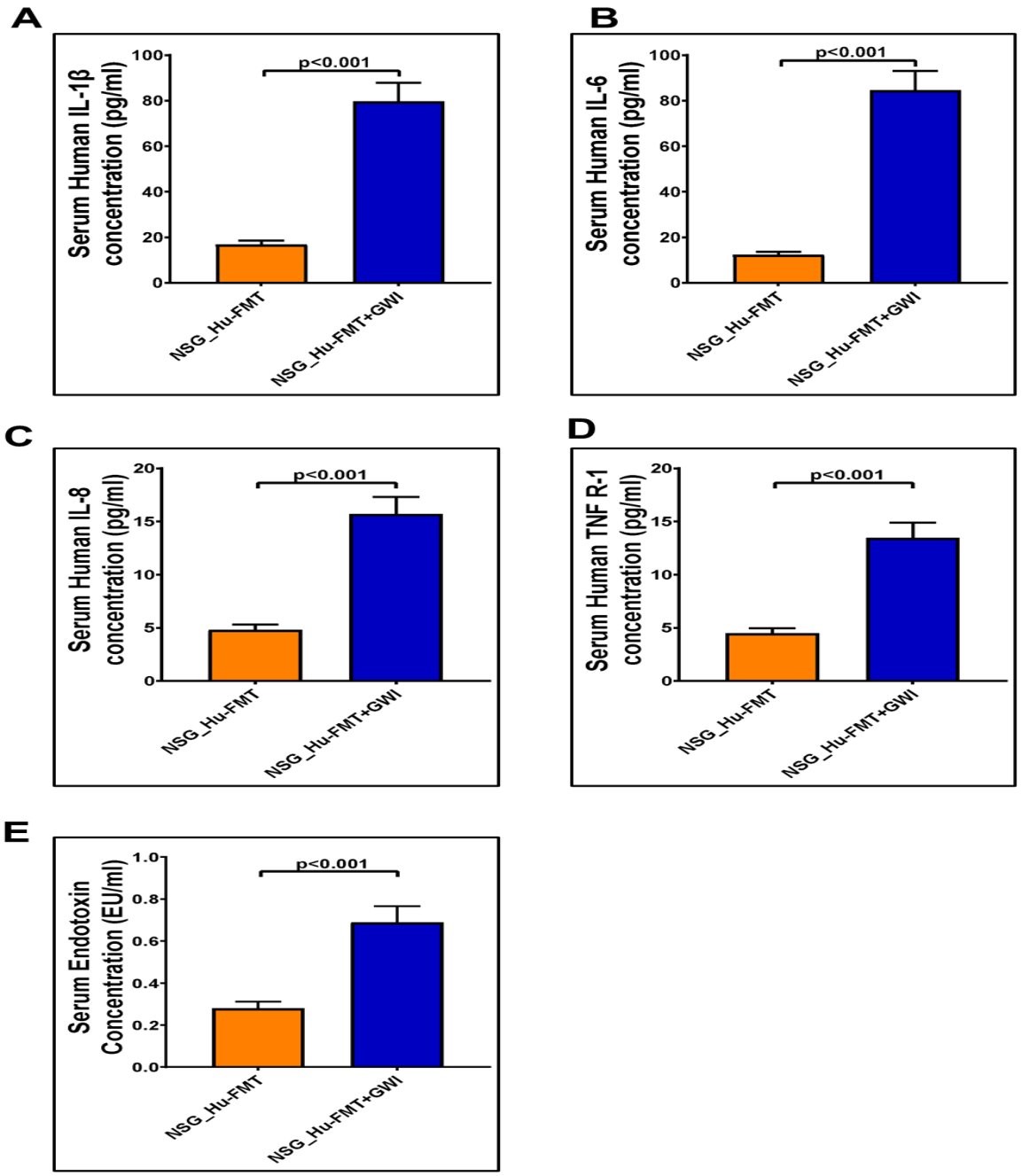

Figure 3.5. Altered expression of systemic pro-inflammation biomarkers after administration with representative GW chemicals in NSG-CD34+ mice with established human gut bacteria. Bar graph representation of systemic cytokines (A) IL-1β, (B) IL-6, (C)IL-8, (D) TNF-R1 in NSG_Hu-FMT and NSG_Hu-FMT+GWI groups groups. (E) Bar graph representation of serum endotoxemia by LAL Assay in NSG_Hu-FMT and NSG_Hu-FMT+GWI groups. $p<0.05$ was considered statistically significant.

Effect of fecal microbiota transfer from GWI Veteran stool sample on the gut bacteriome, resistome profiles, and systemic inflammation in CD34+ hu-NSG mice.

Further, we wanted to study whether establishing the gut bacteriome from GWI Veterans by FMT would result in similar alterations in the gut bacteriome, resistome, and systemic inflammatory patterns as the new GWI mouse model discussed in the previous section. The aim was to recreate a unique gut microbiome specific to a deployed Gulf War Veteran. We compared the results of this GWI-humanized mouse group with the results of the NSG_Hu-FMT, which mimics the health condition of a healthy human supposedly representing a non-deployed individual. Results showed that the α-diversity (Chao1) of the NSG_GWIV group was significantly increased ($p<0.001$) compared to the NSG_Hu-FMT group (Figure 3.6A). We observed that the gut bacteriome profiles of the two groups were significantly distinct ($p=0.004$) from each other by the Bray-Curtis β-diversity analysis (Figure 3.6B). At the phylum level, the relative abundance of *Verrucomicrobia* was decreased in the NSG_GWIV group compared to the NSG_Hu-FMT group (Figure 3.6C). However, there was no change observed in the relative abundance of *Firmicutes* (Figure 3.6C). At genus level, we observed a significant decrease in the relative abundances of *Akkermansia* ($p=0.001$), *Bifidobacterium* ($p<0.001$), *Lachnospiraceae* ($p<0.001$), *Roseburia* ($p<0.001$), and *Schaedlerella* ($p<0.001$) in NSG_GWIV group compared to the NSG_Hu-FMT group (Figure 3.6D). We observed that the α-diversity (Chao1) of the antibiotic resistance gene profile in the NSG_GWIV group was significantly altered as compared to the NSG_Hu-FMT group ($p=0.025$) (Figure 3.7A). The Bray-Curtis β-diversity analysis showed a significant difference ($p<0.003$) between the gut resistome profile of the two groups (Figure 3.7B). At the individual gene level, we observed a significant increase in the relative abundances of *aminoglycoside gene aadE 1 KF864551* ($p=0.001$), *macrolide 29 1724 Branch* ($p<0.001$), *macrolide 57 1774 Branch* ($p<0.001$) and

tetracycline 7 2471 Branch ($p<0.001$) in NSG_GWIV compared to NSG_Hu-FMT group (Figure 3.7C). Finally, we studied whether the colonized bacteriome from the GWI Veteran resulted in the expression of systemic proinflammatory biomarkers. A significant increase in expressions of IL-1β ($p<0.001$), IL-6 ($p<0.001$), IL-8 ($p=0.025$), and soluble receptor TNF R-1 ($p=0.007$) was observed in NSG_GWIV group compared to NSG_Hu-FMT group (Figure 3.8A-D). A significant increase in the endotoxin levels ($p=0.042$) in NSG_GWIV was observed when compared to the NSG_Hu-FMT group (Figure 3.8E) suggesting that our novel approach to recreate the GWI microbiome in a humanized mouse model bore similarities with the average GW-Veteran having systemic inflammation as reported in several human studies 31 [92], [93].

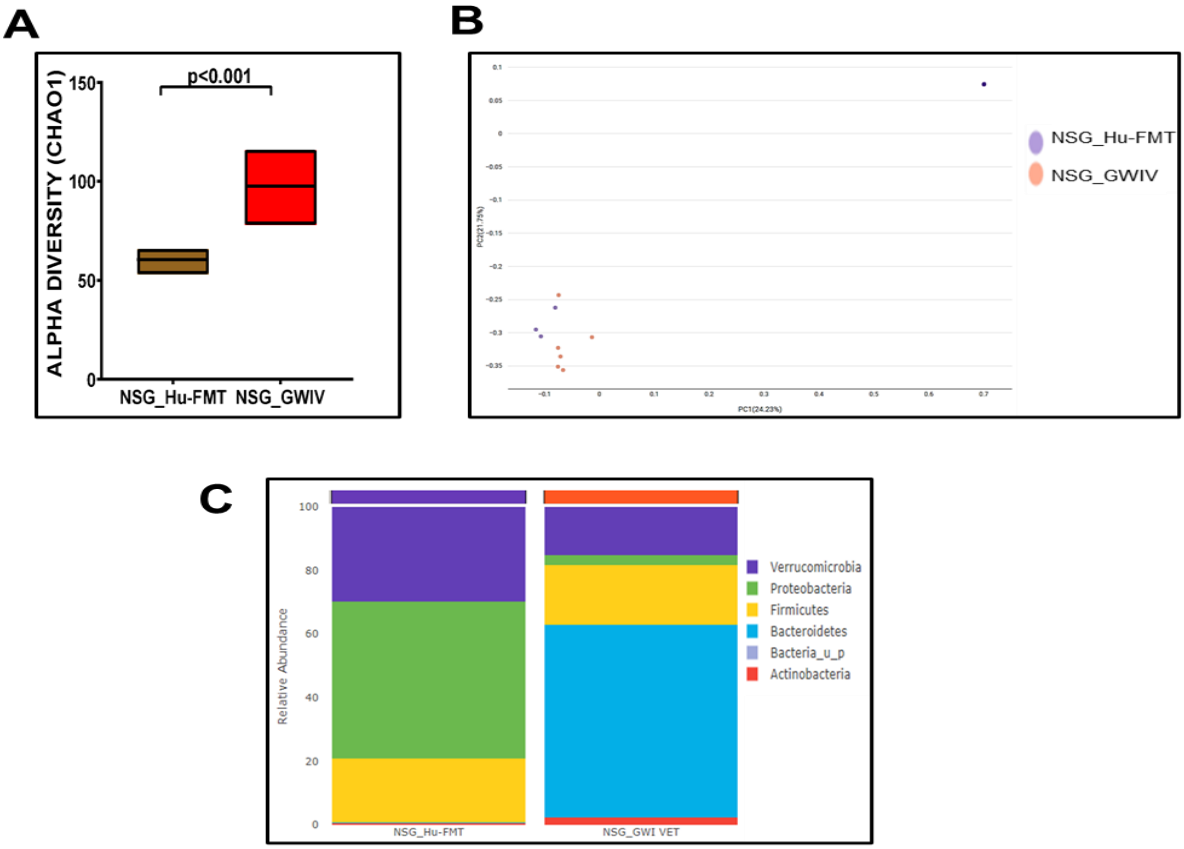
A
ALPHA DIVERSITY (CHAO1)
p<0.001
150
100
50
0
NSG_Hu-FMT
NSG_GWIV
B
NSG_Hu-FMT
NSG_GWIV
C
Relative Abundance
100
80
60
40
20
0
NSG_Hu-FMT
NSG_GWI VET
Verrucomicrobia
Proteobacteria
Firmicutes
Bacteroidetes
Bacteria_u_p
Actinobacteria
D
Akkermansia
p=0.001
Relative Abundance (%)
40
30
20
10
0
NSG_Hu-FMT
NSG_GWIV
Bifidobacterium
p<0.001
8
6
4
2
0
Lachnospiraceae
p<0.001
15
10
5
0
Roseburia
p<0.001
1.5
1.0
0.5
0.0
Schaedlerella
p<0.001
5
4
3
2
1
0

Figure 3.6. Administration with human fecal microbiota transfer from GWI Veteran stool sample altered gut bacteriome profile in NSG-CD34+ mice. (A). Box plots showing α-diversity of gut bacteriome (Chao1) in NSG_Hu-FMT (mice administered with human fecal microbiota transfer after gut bacteriome depletion with antibiotics cocktail) and NSG_GWIV (mice administered with human fecal microbiota transfer from GWI Veteran stool sample after gut bacteriome depletion with antibiotics cocktail). (B) β-diversity analysis (Bray Curtis) of NSG_Hu-FMT and NSG_GWIV groups. (C) Stacked bar representation of relative abundance of gut bacteriome at the phylum level of NSG_Hu-FMT and NSG_GWIV groups. (D) Bar graph representation of relative abundance of gut bacteriome at the genus level of NSG_Hu-FMT and NSG_GWIV groups. $p<0.05$ was considered statistically significant.

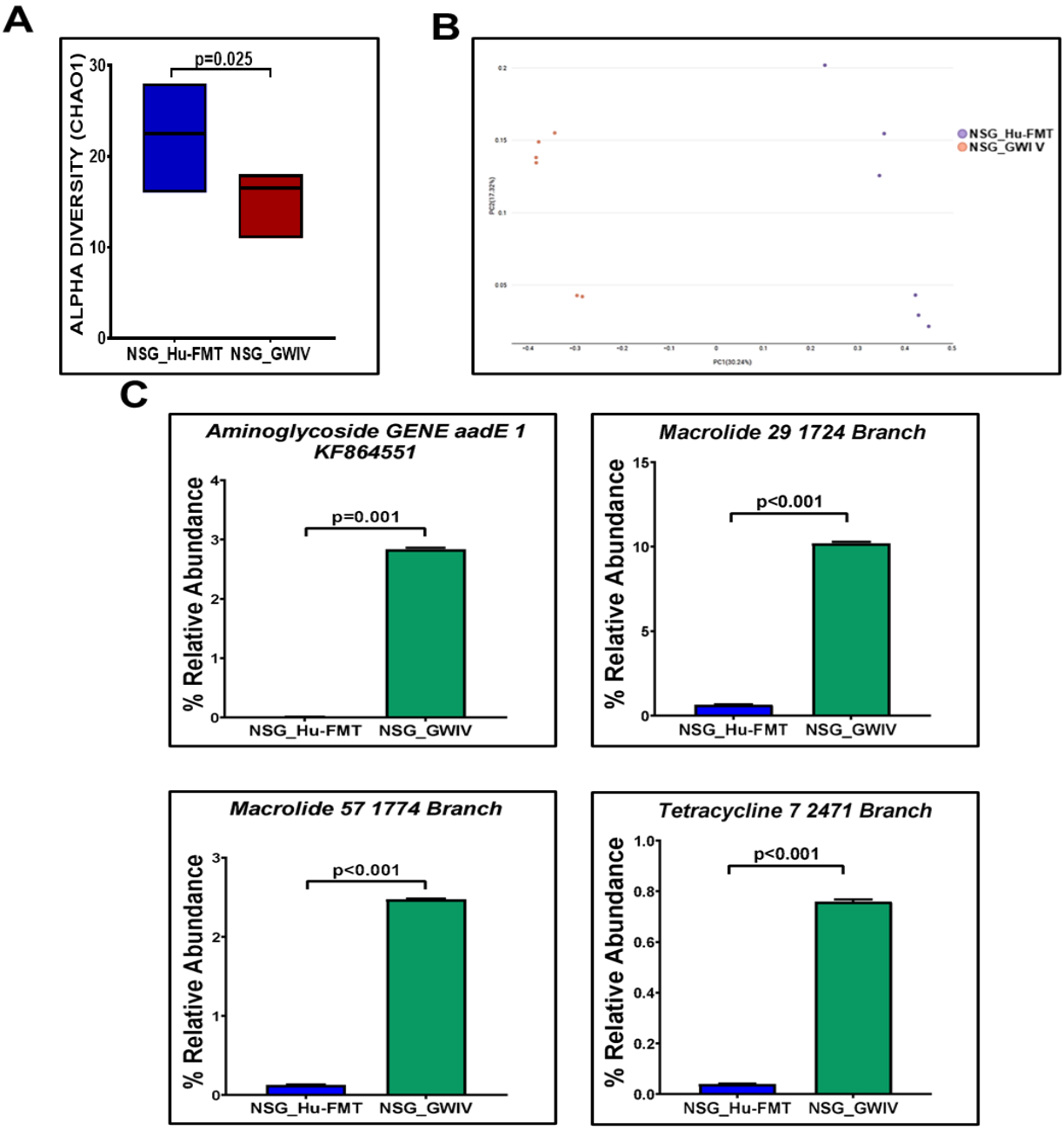

Figure 3.7. Administration with human fecal microbiota transfer from GWI Veteran stool sample altered gut resistome profile in NSG-CD34+ mice. (A). Box plots showing α-diversity (Chao1) of gut resistome in NSG_Hu-FMT (mice administered with human fecal microbiota transfer after gut bacteriome depletion with antibiotics cocktail) and NSG_GWIV (mice administered with human fecal microbiota transfer from GWI Veteran stool sample after gut bacteriome depletion with antibiotics cocktail. (B) β-diversity analysis (Bray Curtis) of NSG_Hu-FMT and NSG_GWIV groups. (C) Bar graph representation of relative abundance of altered antibiotic resistance gene of NSG_Hu-FMT and NSG_GWIV groups. $p<0.05$ was considered statistically significant.

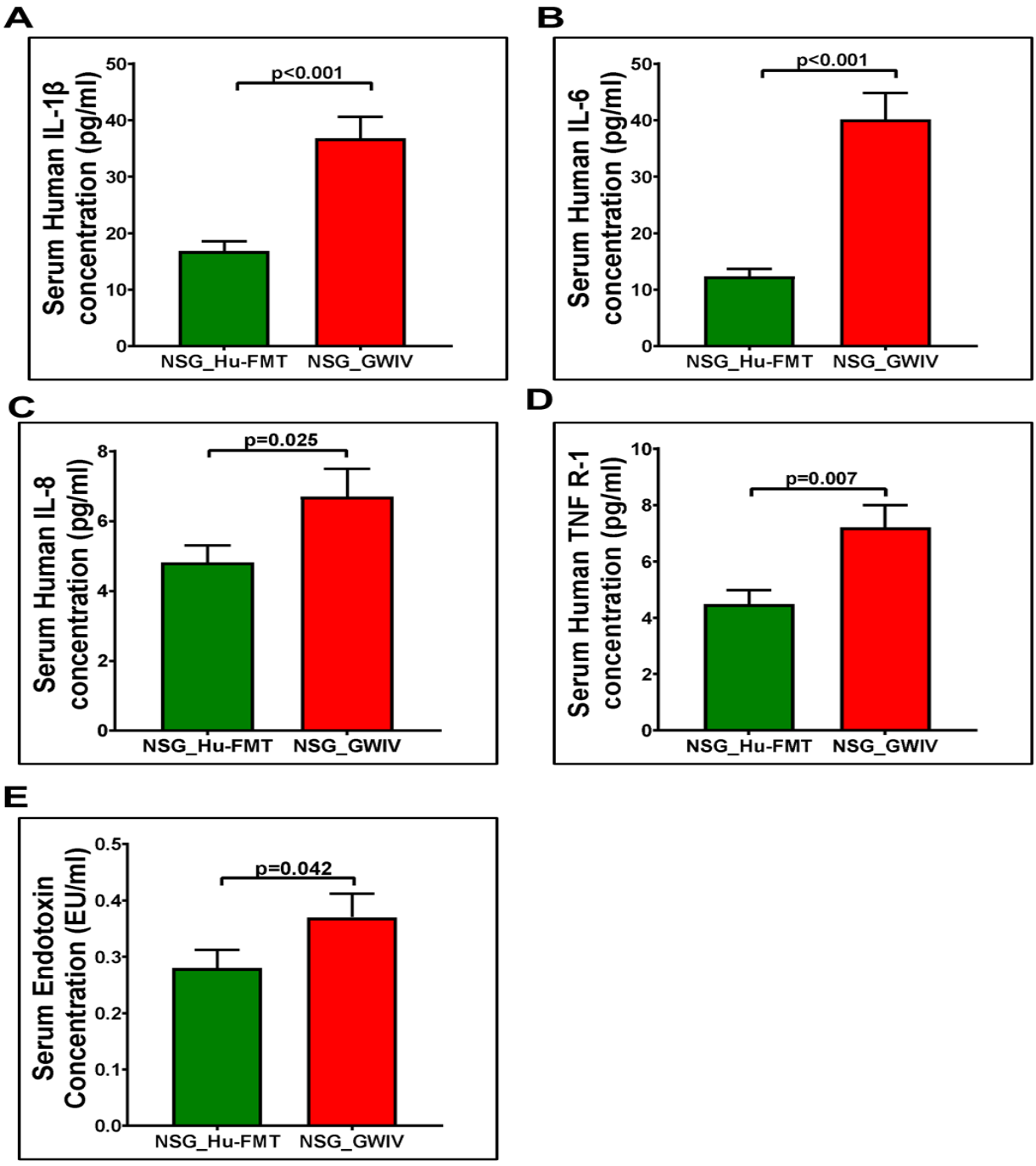

Figure 3.8. Altered expression of systemic pro-inflammation biomarkers after human fecal microbiota transfer from GWI Veteran stool sample in NSG-CD34+ mice. Bar graph representation of systemic cytokines (A) IL-1β, (B) IL-6, (C)IL-8, (D) TNF-R1 in NSG_Hu-FMT and NSG_GWIV groups groups. (E) Bar graph representation of serum endotoxemia by LAL Assay in NSG_Hu-FMT and NSG_GWIV groups. $p<0.05$ was considered statistically significant.

DISCUSSION

Our study is the first attempt to recreate a mouse model of GWI that reflects a human immune system and a human gut microbiome. Owing to many research studies primarily conducted on mouse or rat models, several mechanistic pathways related to the pathology of GWI have been identified [94]. These studies helped us understand the possible therapeutic targets ranging from systemic inflammation, neuroinflammation, and gut microbiome alterations. However, many such studies differed in the endpoints when related to human cohorts and patient outcomes, thus underscoring the limitations of the animal models. For example, our own studies in mouse models that reported gut bacteriome alterations showed a marked difference in cytokine profiles and microbiome diversity when compared to a pilot study in humans [23]. It is not unknown that mouse microbiome profiles are distinctly different when compared to human microbiota and it is difficult to correlate the mouse pathology arising from such a diverse microbiome to a possible human disease interface [95]. Further, mouse gut associated lymphoid tissue and its interactions with the specific mouse immune phenotype may have subtle differences with a human immunophenotype [96]. The above challenges have led investigators wishing to study gut-microbiome immune interactions to switch to mouse models that effectively have a human microbiome coupled with a human immune system [97]. Though such a hypothesis is easily said than done, novel methodologies implemented may have challenges. For example, the use of immunocompromised mice, their resistance or the absence of it to overcome a series of surgical interventions, exposure to repeated drugs/handling stress can have profound implications on the health of the mice [88]. Moreover, the costs and sophistication involved in conducting such experiments have limited their use. We have attempted to use an

established mouse strain commercially available from Jackson laboratories (NSGTM, engrafted with bone marrow-derived CD34+) to supplant a human microbiome following a modified protocol previously used by Daharsh et al [88]. We also used two distinct approaches to recreate a GW Veteran phenotype in the mouse. Firstly, we recreated a more established model, widely used in the GWI pathology field, that uses GW chemicals permethrin and pyridostigmine bromide as routine exposure coupled with transplantation of healthy human microbiome to facilitate the human-gut-immune interaction, and the other novel concept to repopulate the GW Veteran microbiome in the mice that already had a human immunophenotype.

The procedure to create a double humanized engraftment comes with numerous challenges. The one who had to be dealt with relied on the successful engraftment of a healthy human microbiome after the depletion of a mouse microbiome. Results showed that mouse microbiome deletion with a cocktail of antibiotics significantly decreased the α-diversity of the host gut microbiota but was restored to a higher diversity upon human microbiome engraftment (Fig 3.1A). Notably, our whole genome sequencing approach allowed us to deep dive into the species diversity and results showed that healthy human microbiome engraftment significantly restored several probiotic species which were otherwise decreased upon antibiotic treatment (Fig 3.1D). The above approach and data confirmed that, though complex, we were successful in repopulating the human microbiota after depleting the mouse microbiota in these mice. Further, the increased systemic inflammation that followed antibiotic treatment, a natural occurrence due to the severe stress involved, was also restored to normal levels upon human healthy microbiota engraftment, another evidence that mice recovered fully after human microbiota engrafted. There was no residual

inflammation that could skew our results if and when these same mice were to be exposed to disease mechanisms (Fig. 3.2).

Having successfully engrafted the human microbiota, we tested whether the gut-immune axis in a double humanized microenvironment withstood the test of GW chemical exposure and bore a resemblance to the present-day GW veteran. Results showed that a GW chemical exposure showed an altered microbiota and increased systemic inflammatory profile in this model when compared to non-exposed mice (Figs. 3.3,3.4 and 3.5). Notably, the resistome profile also showed a similar altered signature to human cohorts from our previously published study [23]. We should emphasize, however, that the β-diversity in the GW chemical exposed mice had a non-significant difference when compared to the humanized controls. Still, this result opened up a new avenue to explore a deeper approach to study the induvial species abundance, not explored in human exposure. Results showed that probiotic bacteria and principal short-chain fatty acid (SCFA) producing bacteria were significantly decreased in the GW chemical-exposed humanized mice when compared to controls. The result also confirmed the need to use SCFA supplementation as an effective therapeutic modality as the one being tested now by our group [98]. Notably, a previous pilot study from our group found a significant increase in TNF R-1 levels in GW Veterans, a result that was similar to our humanized mouse model thus confirming that the present model may be a viable alternative to a murine drug discovery platform confined to using only mouse immune system and/or mouse immune phenotypes [23].

There are various limitations in using the GW chemical-induced model for studying pathology and though several mouse models have been used to study symptoms of GWI, no

one model represents a true exposome of GWI. Often, studies in mouse models do not reflect the true exposure of either chemicals or mixtures that may been present in the war theater. This causes a number of variabilities in data interpretation. We, therefore, used another novel approach to mimic exposure or recreate a true GW exposome using microbiome engraftment as an option. In this aim, we engrafted human microbiota derived from a deployed GW Veteran who had persistent GWI with most of the prominent symptoms, as noted from a list of veterans with GWI from the George E. Wahlen Veterans Affairs (VA) Medical Center (GEWVAMC) Gulf War registry [90]. The control group received the microbiota transplant from a healthy non, non-deployed volunteer. Results showed that the engrafted human microbiota group from the deployed individual had significantly decreased probiotic species abundance similar to what was found in the GW-chemical exposure group (Fig. 3.6-3.7). The group also had a similar resistome profile and a significant elevation in TNF R-1, IL-1β, and IL-6, a profile that matched our earlier pilot study with the GWI human cohort (Fig. 3.8).

In the study, several breakthroughs were achieved. The study is the very first to create a model that closely resembles a GWI exposome, albeit that mimics the human exposure and its immune phenotype more closely than a typical mouse model. Secondly, the study takes into account a more controlled human microbiota behavior and its interactions with the immune system as more studies confirm the important role of the host gut microbiome in the pathology of multisymptom illnesses. The model can be used for a variety of exposures more often associated with GWI, such as oil well smoke and side effects of vaccines, apart from the regular and more common exposures, such as insecticides and pyridostigmine bromide. Further, the present model can serve to be used in studying more systemic

pathology, such as chronic fatigue, as fatigue is known to influence gut microbiome-immune system interactions. Interestingly, our model can also have a broader role in pathological studies involving chronic fatigue syndrome. Though the results of our study provide a viable alternative to existing pathology and drug discovery models in GWI that exist currently, we have identified several limitations and alternative approaches that need to be resolved.

Though NSG-CD34+ mice are a viable humanized model for human microbiota engraftment, a bone marrow, thymus and liver graft engrafted mice in an NSG background or BLT engraftment in triple knock out (TKO) mice (CD47-/-RAG1−/−IL15Ra−/−) immunodeficient mice on the C57BL/6 background) might have better results since gut-associated lymphoid tissues (GALT) structures are better defined in these models15. Further, humanized mouse models often have severe graft versus host disease, which can have either an earlier or late onset depending on the model. NSG mice supplanted with CD34+ cells as used in our model may suffer from insufficient engraftment [99], [100]. Our model did not have an early onset of graft versus host (GVH), but we were severely limited in extending our studies for more than 15 weeks post-exposure. Interestingly, many GWI studies using mouse models and chemical exposures used a 20-week resting period before study termination to prove symptom persistence. In these models, it would be advantageous to use a BLT-TKO Humanized model with a very late GVH onset (> 45-week onset).

GWI pathology has been studied related to its manifestation in the brain, especially in areas of neuroinflammation, pain, and cognitive dysfunction [101], [102]. We have shown that gut microbiome dysbiosis may have a role in neuroinflammation [70]. A double humanized mouse model such as that discussed in the present study may not be suitable for studying

organ manifestations distant to the gut as brain tissue in these mice is not humanized. This will be true for secondary organ targets like the liver and kidney. Another possible limitation is the use of GW Veteran microbiota transfer for recreating/mimicking the typical GW Veteran. Interestingly, the human microbiome is diverse, and several differences exist between individuals. Not one Veteran stool sample may be a true representative of a cohort. To ideally represent the GWI cohort in a humanized model, each mouse transplanted with the Veteran stool microbiota should represent a single Veteran rather than generalize the entire cohort by pooling the stool samples or using just 2-3 representative microbiome engraftments from stool samples. The process may be extensively rigorous, but engrafting and recreating a humanized microbiome in a mouse from each individual Veteran will create a true cohort accurately representing each Veteran as is done in a clinical study. The above approach and a humanized immune system similar to what has been described in this study may serve as an ideal humanized model for GWI.

CONCLUSION

In conclusion, I would like to state that although the pathophysiology behind the symptom persistence remains elusive, however, the three studies reported in this dissertation significantly advance the present understanding of GWI, further providing explanations for the symptom persistence for three decades after the initial exposure. From the results of the preclinical studies, it is important to note that the altered gut microbiome due to exposure to the representative GW chemicals plays a significant role in worsening the health condition in GWI. The experimental murine models used in the studies have been designed to mimic the health condition of the present-day GW Veteran with GWI. The three studies have their strengths and limitations which are further discussed here.

In the first study, the adoption of an established GWI murine model to use a Western diet as compared to the high-fat diet, makes it more relevant to study the health condition of the present-day GW Veterans who are in a non-combat role and suffering from metabolic conditions. The use of shotgun metagenomics has provided a deeper understanding of gut bacteriome alteration at the species level associated with metabolic diseases like obesity with underlying GWI conditions. This analysis further led us to identify gut bacteriome-targeted future therapeutic targets. The suggestion of using a combination of probiotic bacterial species *Akkermansia muciniphila* and *Lactococcus lactis* could help ameliorate the obesity-induced worsening of GWI symptoms. The study also provides valuable insights into the possible mechanisms associated with gut dysbiosis and subsequent gastrointestinal, hepatic, and neurological pathologies. Certain limitations could be addressed in future studies. These include the inclusion of a larger sample size for the mice groups and

investigating alternative routes of exposure such as the dermal route for permethrin. There is further scope to prove the mechanistic associations between obesity, GWI and gut dysbiosis using germ-free or humanized mice models.

The second study is an important effort to understand a previously unexplored aspect associated with GWI pathology. Results from the experimental murine GWI provided insights about novel therapeutic targets associated with altered host gut resistome profile under GWI conditions. The observation of similar changes in the resistome profile between the GW Veterans with GWI and the GWI murine model provides a translatability of the approach. Further, the results have shown a novel association of altered gut resistome with systemic inflammation, which needs to be further investigated through mechanistic studies. The limitations of this study include the increase in sample number to have a higher statistical power and the addition of other GW chemicals in combination with the present representative GW chemicals permethrin and pyridostigmine bromide. Further studies need to be done to confirm the antibiotic resistance in the Veterans and mouse model. The therapeutic potential of FMT against the gut dysbiosis associated with GWI condition and the related systemic inflammation underscores the potential of personalized or targeted therapeutic approaches in the treatment of complex GWI symptoms.

The third study was instrumental in addressing the limitation of the absence of a translatable mouse model. This model could be helpful in carrying out mechanistic studies, which could be translatable for treating symptom persistence among GW Veterans. The results of the double humanized mouse model specifically the altered gut bacteriome and resistome pattern and systemic biomarker expression showed similarities between the experimental

mice data and GW Veteran data reported in an earlier study by our group. This proves the efficacy of this novel model. It can also provide new therapeutic targets to design appropriate drug candidates. However, this model is limited in the ability to not being able to replicate the human pathology of GWI, thereby decreasing the generalizability of the results to a diverse GW Veteran population. There may be certain confounding factors due to the antibiotic cocktail administration in the process of gut depletion that might increase the expression of systemic inflammatory markers. Further, increasing the sample size of GW Veterans across a large population could be beneficial for the targeted FMT process in humanized mice enabling us to have more accurate and translatable results.

List of References

1. White, R.F., et al., *Recent research on Gulf War illness and other health problems in veterans of the 1991 Gulf War: Effects of toxicant exposures during deployment.* Cortex, 2016. **74**: p. 449-75.
2. Iversen, A., T. Chalder, and S. Wessely, *Gulf War Illness: lessons from medically unexplained symptoms.* Clin Psychol Rev, 2007. **27**(7): p. 842-54.
3. Chatterjee, S., D. Bose, and R. Seth, *Host gut microbiome and potential therapeutics in Gulf War Illness: A short review.* Life Sci, 2021. **280**: p. 119717.
4. Haley, R.W., T.L. Kurt, and J. Hom, *Is there a Gulf War Syndrome? Searching for syndromes by factor analysis of symptoms.* JAMA, 1997. **277**(3): p. 215-22.
5. Fukuda, K., et al., *Chronic multisymptom illness affecting Air Force veterans of the Gulf War.* JAMA, 1998. **280**(11): p. 981-8.
6. Steele, L., *Prevalence and patterns of Gulf War illness in Kansas veterans: association of symptoms with characteristics of person, place, and time of military service.* Am J Epidemiol, 2000. **152**(10): p. 992-1002.
7. Elhaj, R. and J.M. Reynolds, *Chemical exposures and suspected impact on Gulf War Veterans.* Mil Med Res, 2023. **10**(1): p. 11.
8. Nettleman, M., *Gulf War Illness: Challenges Persist.* Trans Am Clin Climatol Assoc, 2015. **126**: p. 237-47.
9. Moradi, F., *The Gulf War Illness and the Iraqi Population's Forgotten Pain and Suffering.* Mil Med, 2023. **188**(9-10): p. 241-243.
10. Haley, R.W. and T.L. Kurt, *Self-reported exposure to neurotoxic chemical combinations in the Gulf War. A cross-sectional epidemiologic study.* JAMA, 1997. **277**(3): p. 231-7.
11. Steele, L., et al., *Complex factors in the etiology of Gulf War illness: wartime exposures and risk factors in veteran subgroups.* Environ Health Perspect, 2012. **120**(1): p. 112-8.
12. Bem, H. and F. Bou-Rabee, *Environmental and health consequences of depleted uranium use in the 1991 Gulf War.* Environ Int, 2004. **30**(1): p. 123-34.
13. Peakman, M., A. Skowera, and M. Hotopf, *Immunological dysfunction, vaccination and Gulf War illness.* Philos Trans R Soc Lond B Biol Sci, 2006. **361**(1468): p. 681-7.
14. De Palma, G., S.M. Collins, and P. Bercik, *The microbiota-gut-brain axis in functional gastrointestinal disorders.* Gut Microbes, 2014. **5**(3): p. 419-29.
15. Frazier, T.H., J.K. DiBaise, and C.J. McClain, *Gut microbiota, intestinal permeability, obesity-induced inflammation, and liver injury.* JPEN J Parenter Enteral Nutr, 2011. **35**(5 Suppl): p. 14S-20S.
16. Round, J.L. and S.K. Mazmanian, *The gut microbiota shapes intestinal immune responses during health and disease.* Nat Rev Immunol, 2009. **9**(5): p. 313-23.
17. Tremlett, H., et al., *The gut microbiome in human neurological disease: A review.* Ann Neurol, 2017. **81**(3): p. 369-382.
18. Mu, C., Y. Yang, and W. Zhu, *Gut Microbiota: The Brain Peacekeeper.* Front Microbiol, 2016. **7**: p. 345.
19. Appleton, J., *The Gut-Brain Axis: Influence of Microbiota on Mood and Mental Health.* Integr Med (Encinitas), 2018. **17**(4): p. 28-32.
20. McVey Neufeld, K.A., et al., *The microbiome is essential for normal gut intrinsic primary afferent neuron excitability in the mouse.* Neurogastroenterol Motil, 2013. **25**(2): p. 183-e88.
21. Rogers, G.B., et al., *From gut dysbiosis to altered brain function and mental illness: mechanisms and pathways.* Mol Psychiatry, 2016. **21**(6): p. 738-48.

22. Koloski, N.A., et al., *The brain--gut pathway in functional gastrointestinal disorders is bidirectional: a 12-year prospective population-based study.* Gut, 2012. **61**(9): p. 1284-90.
23. Janulewicz, P.A., et al., *The Gut-Microbiome in Gulf War Veterans: A Preliminary Report.* Int J Environ Res Public Health, 2019. **16**(19).
24. Alhasson, F., et al., *Altered gut microbiome in a mouse model of Gulf War Illness causes neuroinflammation and intestinal injury via leaky gut and TLR4 activation.* PLoS One, 2017. **12**(3): p. e0172914.
25. Kimono, D., et al., *Dysbiosis-Associated Enteric Glial Cell Immune-Activation and Redox Imbalance Modulate Tight Junction Protein Expression in Gulf War Illness Pathology.* Front Physiol, 2019. **10**: p. 1229.
26. Seth, R.K., et al., *Gut DNA Virome Diversity and Its Association with Host Bacteria Regulate Inflammatory Phenotype and Neuronal Immunotoxicity in Experimental Gulf War Illness.* Viruses, 2019. **11**(10).
27. Ritz, N.L., et al., *The gut virome is associated with stress-induced changes in behaviour and immune responses in mice.* Nat Microbiol, 2024. **9**(2): p. 359-376.
28. Kimono, D., et al., *Host Akkermansia muciniphila Abundance Correlates With Gulf War Illness Symptom Persistence via NLRP3-Mediated Neuroinflammation and Decreased Brain-Derived Neurotrophic Factor.* Neurosci Insights, 2020. **15**: p. 2633105520942480.
29. Seth, R.K., et al., *Increased butyrate priming in the gut stalls microbiome associated-gastrointestinal inflammation and hepatic metabolic reprogramming in a mouse model of Gulf War Illness.* Toxicol Appl Pharmacol, 2018. **350**: p. 64-77.
30. Bose, D., et al., *TLR Antagonism by Sparstolonin B Alters Microbial Signature and Modulates Gastrointestinal and Neuronal Inflammation in Gulf War Illness Preclinical Model.* Brain Sci, 2020. **10**(8).
31. Saha, P., et al., *Andrographolide Attenuates Gut-Brain-Axis Associated Pathology in Gulf War Illness by Modulating Bacteriome-Virome Associated Inflammation and Microglia-Neuron Proinflammatory Crosstalk.* Brain Sci, 2021. **11**(7).
32. Gwini, S.M., et al., *Increased symptom reporting persists in 1990-1991 Gulf War veterans 20 years post deployment.* Am J Ind Med, 2015. **58**(12): p. 1246-54.
33. Coughlin, S.S., *Physical Activity and Chronic Illnesses among Gulf War Veterans.* Ann Transl Med Epidemiol, 2016. **3**(1).
34. Coughlin, S.S., H.K. Kang, and C.M. Mahan, *Selected Health Conditions Among Overweight, Obese, and Non-Obese Veterans of the 1991 Gulf War: Results from a Survey Conducted in 2003-2005.* Open Epidemiol J, 2011. **4**: p. 140-146.
35. Angoa-Perez, M., et al., *Effects of a high fat diet on gut microbiome dysbiosis in a mouse model of Gulf War Illness.* Sci Rep, 2020. **10**(1): p. 9529.
36. Zakirova, Z., et al., *A Chronic Longitudinal Characterization of Neurobehavioral and Neuropathological Cognitive Impairment in a Mouse Model of Gulf War Agent Exposure.* Front Integr Neurosci, 2015. **9**: p. 71.
37. Kim, J., et al., *Permethrin alters adipogenesis in 3T3-L1 adipocytes and causes insulin resistance in C2C12 myotubes.* J Biochem Mol Toxicol, 2014. **28**(9): p. 418-24.
38. Cenit, M.C., et al., *Rapidly expanding knowledge on the role of the gut microbiome in health and disease.* Biochim Biophys Acta, 2014. **1842**(10): p. 1981-1992.
39. Broderick, G., et al., *A pilot study of immune network remodeling under challenge in Gulf War Illness.* Brain Behav Immun, 2011. **25**(2): p. 302-13.
40. Catanzaro, R., et al., *The gut microbiota and its correlations with the central nervous system disorders.* Panminerva Med, 2015. **57**(3): p. 127-43.

41. Rogero, M.M. and P.C. Calder, *Obesity, Inflammation, Toll-Like Receptor 4 and Fatty Acids.* Nutrients, 2018. **10**(4).
42. Bertiaux-Vandaele, N., et al., *The expression and the cellular distribution of the tight junction proteins are altered in irritable bowel syndrome patients with differences according to the disease subtype.* Am J Gastroenterol, 2011. **106**(12): p. 2165-73.
43. Totsch, S.K., et al., *Effects of a Standard American Diet and an anti-inflammatory diet in male and female mice.* Eur J Pain, 2018. **22**(7): p. 1203-1213.
44. Kelsall, H.L., et al., *Physical, psychological, and functional comorbidities of multisymptom illness in Australian male veterans of the 1991 Gulf War.* Am J Epidemiol, 2009. **170**(8): p. 1048-56.
45. Zakirova, Z., et al., *Gulf War agent exposure causes impairment of long-term memory formation and neuropathological changes in a mouse model of Gulf War Illness.* PLoS One, 2015. **10**(3): p. e0119579.
46. Christ, A. and E. Latz, *The Western lifestyle has lasting effects on metaflammation.* Nat Rev Immunol, 2019. **19**(5): p. 267-268.
47. Martinez, K.B., V. Leone, and E.B. Chang, *Western diets, gut dysbiosis, and metabolic diseases: Are they linked?* Gut Microbes, 2017. **8**(2): p. 130-142.
48. Wilson, C.R., et al., *Western diet, but not high fat diet, causes derangements of fatty acid metabolism and contractile dysfunction in the heart of Wistar rats.* Biochem J, 2007. **406**(3): p. 457-67.
49. Dutta, S. and P. Sengupta, *Men and mice: Relating their ages.* Life Sci, 2016. **152**: p. 244-8.
50. Janda, J.M. and S.L. Abbott, *16S rRNA gene sequencing for bacterial identification in the diagnostic laboratory: pluses, perils, and pitfalls.* J Clin Microbiol, 2007. **45**(9): p. 2761-4.
51. Ballal, S.A., et al., *Host lysozyme-mediated lysis of Lactococcus lactis facilitates delivery of colitis-attenuating superoxide dismutase to inflamed colons.* Proc Natl Acad Sci U S A, 2015. **112**(25): p. 7803-8.
52. Singh, N., et al., *Activation of Gpr109a, receptor for niacin and the commensal metabolite butyrate, suppresses colonic inflammation and carcinogenesis.* Immunity, 2014. **40**(1): p. 128-39.
53. Engelhart, M.J., et al., *Inflammatory proteins in plasma and the risk of dementia: the rotterdam study.* Arch Neurol, 2004. **61**(5): p. 668-72.
54. Petra, A.I., et al., *Gut-Microbiota-Brain Axis and Its Effect on Neuropsychiatric Disorders With Suspected Immune Dysregulation.* Clin Ther, 2015. **37**(5): p. 984-95.
55. Lai, S.W., et al., *Regulatory Effects of Neuroinflammatory Responses Through Brain-Derived Neurotrophic Factor Signaling in Microglial Cells.* Mol Neurobiol, 2018. **55**(9): p. 7487-7499.
56. Goedert, M., D.S. Eisenberg, and R.A. Crowther, *Propagation of Tau Aggregates and Neurodegeneration.* Annu Rev Neurosci, 2017. **40**: p. 189-210.
57. Lull, M.E. and M.L. Block, *Microglial activation and chronic neurodegeneration.* Neurotherapeutics, 2010. **7**(4): p. 354-65.
58. Wang, W.Y., et al., *Role of pro-inflammatory cytokines released from microglia in Alzheimer's disease.* Ann Transl Med, 2015. **3**(10): p. 136.
59. Sabtu, N., D.A. Enoch, and N.M. Brown, *Antibiotic resistance: what, why, where, when and how?* Br Med Bull, 2015. **116**: p. 105-13.
60. Singh, S., N. Verma, and N. Taneja, *The human gut resistome: Current concepts & future prospects.* Indian J Med Res, 2019. **150**(4): p. 345-358.
61. McInnes, R.S., et al., *Horizontal transfer of antibiotic resistance genes in the human gut microbiome.* Curr Opin Microbiol, 2020. **53**: p. 35-43.
62. Sun, J., et al., *Environmental remodeling of human gut microbiota and antibiotic resistome in livestock farms.* Nat Commun, 2020. **11**(1): p. 1427.

63. Phillips, M.L., *Gut reaction: environmental effects on the human microbiota.* Environ Health Perspect, 2009. **117**(5): p. A198-205.
64. Parnanen, K., et al., *Maternal gut and breast milk microbiota affect infant gut antibiotic resistome and mobile genetic elements.* Nat Commun, 2018. **9**(1): p. 3891.
65. Fitzpatrick, M.A., et al., *Changes in bacterial epidemiology and antibiotic resistance among veterans with spinal cord injury/disorder over the past 9 years.* J Spinal Cord Med, 2018. **41**(2): p. 199-207.
66. Fitzpatrick, M.A., et al., *Epidemiology and clinical outcomes associated with extensively drug-resistant (XDR) Acinetobacter in US Veterans' Affairs (VA) medical centers.* Infect Control Hosp Epidemiol, 2021. **42**(3): p. 305-310.
67. Lai, Z.L., et al., *Fecal microbiota transplantation confers beneficial metabolic effects of diet and exercise on diet-induced obese mice.* Sci Rep, 2018. **8**(1): p. 15625.
68. Smets, E.M., et al., *The Multidimensional Fatigue Inventory (MFI) psychometric qualities of an instrument to assess fatigue.* J Psychosom Res, 1995. **39**(3): p. 315-25.
69. Proctor, S.P., et al., *Health status of Persian Gulf War veterans: self-reported symptoms, environmental exposures and the effect of stress.* Int J Epidemiol, 1998. **27**(6): p. 1000-10.
70. Bose, D., et al., *Obesity Worsens Gulf War Illness Symptom Persistence Pathology by Linking Altered Gut Microbiome Species to Long-Term Gastrointestinal, Hepatic, and Neuronal Inflammation in a Mouse Model.* Nutrients, 2020. **12**(9).
71. Wright, C.B., et al., *Interleukin-6 is associated with cognitive function: the Northern Manhattan Study.* J Stroke Cerebrovasc Dis, 2006. **15**(1): p. 34-8.
72. Perry, J.A., E.L. Westman, and G.D. Wright, *The antibiotic resistome: what's new?* Curr Opin Microbiol, 2014. **21**: p. 45-50.
73. Levy, S.B. and B. Marshall, *Antibacterial resistance worldwide: causes, challenges and responses.* Nat Med, 2004. **10**(12 Suppl): p. S122-9.
74. Modak, R., D. Ross, and V.L. Kan, *Macrolide and clindamycin resistance in Staphylococcus aureus isolates and antibiotic use in a Veterans Affairs Medical Center.* Infect Control Hosp Epidemiol, 2008. **29**(2): p. 180-2.
75. Livorsi, D.J., et al., *The feasibility of implementing antibiotic restrictions for fluoroquinolones and cephalosporins: a mixed-methods study across 15 Veterans Health Administration hospitals.* J Antimicrob Chemother, 2021. **76**(8): p. 2195-2203.
76. Butler, M.S., et al., *Glycopeptide antibiotics: back to the future.* J Antibiot (Tokyo), 2014. **67**(9): p. 631-44.
77. Tokars, J.I., et al., *The prevalence of colonization with vancomycin-resistant Enterococcus at a Veterans' Affairs institution.* Infect Control Hosp Epidemiol, 1999. **20**(3): p. 171-5.
78. Wang, H., et al., *Promising Treatment for Type 2 Diabetes: Fecal Microbiota Transplantation Reverses Insulin Resistance and Impaired Islets.* Front Cell Infect Microbiol, 2019. **9**: p. 455.
79. Vindigni, S.M. and C.M. Surawicz, *Fecal Microbiota Transplantation.* Gastroenterol Clin North Am, 2017. **46**(1): p. 171-185.
80. Domingues, S., G.J. da Silva, and K.M. Nielsen, *Integrons: Vehicles and pathways for horizontal dissemination in bacteria.* Mob Genet Elements, 2012. **2**(5): p. 211-223.
81. Hu, Q., et al., *Effects of Low-Dose Antibiotics on Gut Immunity and Antibiotic Resistomes in Weaned Piglets.* Front Immunol, 2020. **11**: p. 903.
82. Xia, Y., et al., *Combined analysis of metagenomic data revealed consistent changes of gut microbiome structure and function in inflammatory bowel disease.* J Appl Microbiol, 2021. **131**(6): p. 3018-3031.
83. Denkinger, C.M., et al., *Increased multi-drug resistance among the elderly on admission to the hospital--a 12-year surveillance study.* Arch Gerontol Geriatr, 2013. **56**(1): p. 227-30.

84. Nkiliza, A., et al., *Adaptive Immune Responses Associated with the Central Nervous System Pathology of Gulf War Illness.* Neurosci Insights, 2021. **16**: p. 26331055211018458.
85. Duong, L.M., et al., *Association of Gulf War Illness with Characteristics in Deployed vs. Non-Deployed Gulf War Era Veterans in the Cooperative Studies Program 2006/Million Veteran Program 029 Cohort: A Cross-Sectional Analysis.* Int J Environ Res Public Health, 2022. **20**(1).
86. Ribeiro, A.C.R. and L.S. Deshpande, *A review of pre-clinical models for Gulf War Illness.* Pharmacol Ther, 2021. **228**: p. 107936.
87. Walsh, N.C., et al., *Humanized Mouse Models of Clinical Disease.* Annu Rev Pathol, 2017. **12**: p. 187-215.
88. Daharsh, L., et al., *A Double Humanized BLT-mice Model Featuring a Stable Human-Like Gut Microbiome and Human Immune System.* J Vis Exp, 2019(150).
89. Hansen, C.H., et al., *Patterns of early gut colonization shape future immune responses of the host.* PLoS One, 2012. **7**(3): p. e34043.
90. Tuteja, A.K., et al., *Randomized, Double-Blind Placebo-Controlled Trial to Assess the Effect of Probiotics on Irritable Bowel Syndrome in Veterans With Gulf War Illness.* Fed Pract, 2022. **39**(10): p. 410-417.
91. Bose, D., et al., *Host gut resistome in Gulf War chronic multisymptom illness correlates with persistent inflammation.* Commun Biol, 2022. **5**(1): p. 552.
92. Butterick, T.A., et al., *Gulf War Illness-associated increases in blood levels of interleukin 6 and C-reactive protein: biomarker evidence of inflammation.* BMC Res Notes, 2019. **12**(1): p. 816.
93. Parkitny, L., et al., *Evidence for abnormal cytokine expression in Gulf War Illness: A preliminary analysis of daily immune monitoring data.* BMC Immunol, 2015. **16**: p. 57.
94. Slevin, E., et al., *Dysbiosis in gastrointestinal pathophysiology: Role of the gut microbiome in Gulf War Illness.* J Cell Mol Med, 2023. **27**(7): p. 891-905.
95. Mestas, J. and C.C. Hughes, *Of mice and not men: differences between mouse and human immunology.* J Immunol, 2004. **172**(5): p. 2731-8.
96. Morbe, U.M., et al., *Human gut-associated lymphoid tissues (GALT); diversity, structure, and function.* Mucosal Immunol, 2021. **14**(4): p. 793-802.
97. Chuprin, J., et al., *Humanized mouse models for immuno-oncology research.* Nat Rev Clin Oncol, 2023. **20**(3): p. 192-206.
98. Ikeda, T., et al., *Short-chain fatty acid receptors and gut microbiota as therapeutic targets in metabolic, immune, and neurological diseases.* Pharmacol Ther, 2022. **239**: p. 108273.
99. Yu, C.I., et al., *Engraftment of adult hematopoietic stem and progenitor cells in a novel model of humanized mice.* iScience, 2024. **27**(3): p. 109238.
100. Sonntag, K., et al., *Chronic graft-versus-host-disease in CD34(+)-humanized NSG mice is associated with human susceptibility HLA haplotypes for autoimmune disease.* J Autoimmun, 2015. **62**: p. 55-66.
101. Michalovicz, L.T., et al., *Corticosterone and pyridostigmine/DEET exposure attenuate peripheral cytokine expression: Supporting a dominant role for neuroinflammation in a mouse model of Gulf War Illness.* Neurotoxicology, 2019. **70**: p. 26-32.
102. O'Callaghan, J.P. and D.B. Miller, *Neuroinflammation disorders exacerbated by environmental stressors.* Metabolism, 2019. **100S**: p. 153951.